Generation of recombinant antibodies against the β-(1,6)-branched β-(1,3)-D-glucan Schizophyllan

Von der Fakultät für Lebenswissenschaften
der Technischen Universität Carolo-Wilhelmina zu Braunschweig
zur Erlangung des Grades eines
Doktors der Naturwissenschaften
(Dr. rer. nat.)
genehmigte
D i s s e r t a t i o n

von Jörn Nils Henrick Josewski
aus Cloppenburg.

1. Referent apl. Professor Dr. Udo Rau
2. Referent Professor Dr. Stefan Dübel
eingereicht am: 24.10.2018
mündliche Prüfung (Disputation) am: 19.12.2018

Druckjahr 2019

Veröffentlichungen der Dissertation

Teilergebnisse aus dieser Arbeit wurden mit Genehmigung der Fakultät für Lebenswissenschaften, vertreten durch den Mentor der Arbeit, in folgenden Beiträgen vorab veröffentlicht:

Publikationen

Josewski, J., Buchmeier, S., Frenzel, A., Dübel, S., Tinnefeld, P., and Rau, U. (2017). Generation of recombinant antibodies against the beta-(1,6)-branched beta-(1,3)-D-glucan Schizophyllan from immunized mice via phage display. *Biotechnol Res Int* 2016, 8791359.

Sung, K. H., Josewski, J., Dübel, S., Blankenfeldt, W., and Rau, U. (2018). Structural insights into antigen recognition of an anti-β-(1,6)-β-(1,3)-D-glucan antibody. *Scientific Reports* 2018, 13652.

Posterbeiträge

Josewski, J, Buchmeier, S., Frenzel, A., Hust, M. and Rau, U. Generation of antibodies against fungal beta-(1,6) branched beta-(1,3)-D-glucans via antibody phage display. PEGS Europe 2016, 8th annual Protein & Antibody Engineering Summit, Lissabon, Portugal.

Table of Contents

Abbreviations and Units

Abbreviations

A_X	Absorption of radiation with λ = X
BSA	Bovine serum albumine
cDNA	Complementary DNA
CDR	Complementary determining region
C_H	Constant Ig domain of HC
CIP	Calve intestinal phosphatase
C_L	Constant Ig domain of LC
DMF	N.N-dimethylformamide
DNA	Deoxyribonucleic acid
DNS	3,5-Dinitrosalicylic acid
EC50	Half maximal effective concentration
ELISA	Enzyme-linked immunosorbent assay
Fab	Ig fragment antigen binding
Fc	Ig fragment crystallizable
Fv	Ig fragment variable
HC	Ig heavy chain
HRP	Horseradish peroxidase
Ig	Immunoglobulin
LC	Ig light chain
mRNA	Messenger RNA

OD_X	Optical density at radiation with λ = X
ori	Origin of replication
PAGE	Polyacrylamide gel electrophoresis
PCR	Polymerase chain reaction
PEI	Polyethyleneimine
rAb(s)	Recombinant Antibody (/-bodies)
RBS	Ribosome binding site
RNA	Ribonucleic acid
RU	Repeating unit
RT	Room temperature
scFv	Single-chain Fv
scFv-Fc	ScFv-Fc fusion protein
SCH	Schizophyllan
SCH-PK	Proteinase K treated SCH
SDS	Sodium dodecyl sulfate
ssDNA	Single stranded DNA
UV	Ultraviolet radiation
V_H	Variable Ig domain of HC
V_L	Variable Ig domain of LC
λ	Wavelength

OD_X	Optical density at radiation with λ = X
ori	Origin of replication
PAGE	Polyacrylamide gel electrophoresis

Units

Å	Ångström(s)
% (v/v)	Volume per mixture volume in percent
% (w/v)	Mass per mixture volume in percent
% (w/w)	Mass per mixture mass in percent
bp, kbp	Base pair(s), Kilobase pair(s)
°C	Degree Celsius
cfu	Colony forming unit(s)
Da, kDa	Dalton(s), kilodalton(s)
g, mg, µg, ng	Gram(s), milligram(s), microgram(s), nanogram(s)
h, min, s	Hour(s), minute(s), second(s)
kb	Kilobase(s)
L, mL, µL, nL	Liter(s), milliliter(s), microliter(s), nanoliter(s)
m, cm, mm, µm, nm	Meter(s), centimeter(s), millimeter(s), micrometer(s), nanometer(s)
M, mM, µM, nM, pM, fM	Molar, millimolar, micromolar, nanomolar, picomolar, femtomolar
mol, mmol	Mole, millimole
rpm	Revolutions per minute
U	Enzyme unit(s)
V	Volt(s)
xg	Relative centrifugal force

1 Introduction

1.1 Schizophyllan

Schizophyllan (SCH) is a neutral and water soluble homopolysaccharide, that consists of a β-(1,3)-D-glucan main chain with additional single β-(1,6)-bound D-glucose at every third glucose moiety of the backbone [1]. Reports of the average molecular weight range from 5.7×10^6 to 1.3×10^7 g mol^{-1} [2, 3]. It is produced as extracellular polysaccharide by the wood rotting basidiomycete *Schizophyllum commune* also commonly known as Split Gill [4].

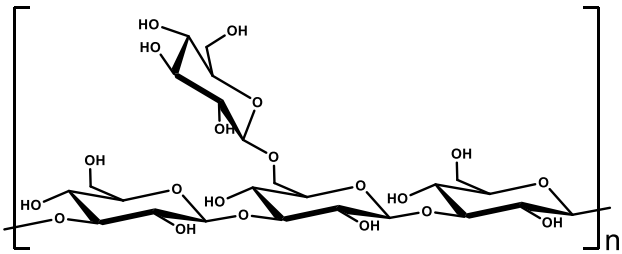

Figure 1-1 Smallest repeating unit (RU) of Schizophyllan, three β-(1,3)-linked D-glucose with a single β-(1,6)-bound D-glucose as branch with n = 8,810 to 20,093.

In aqueous solution SCH forms a triple helical structure composed of three twisted SCH chains with the β-(1,6)-bound

glucose residues directed to the outside [3, 5–7]. The height of one helix turn and the average helix diameter were determined as 1.8 nm and 2.6 nm, respectively [6, 7]. The triplex is understood to be stabilized by hydrogen bonds, especially between the C-2 hydroxyl groups of the glucose molecules at the glucan backbones [8]. Due to the high stability of the triplex, dissociation into single strands occurs only at temperatures above 135 °C, at pH above 12 or by supplementation with at least 87 % (w/w) or higher of dimethyl sulfoxide [3, 7, 9]. The denaturation of the structure is particular possible and recovery of initial conditions leads to formation of random coiled structures [3, 7, 9, 10].

Solutions of triple helical SCH show high viscosity with pseudoplastic flow behavior [4, 11]. The triplex conformation is considered to be primarily responsible for this property since the breakup into single strands leads to strong reduction of viscosity [3, 7, 9]. Because of the stability of the viscosity at high temperatures and high salt concentrations, SCH is tested as agent for polymer flooding in enhanced oil recovery [12, 13]. Due to its biophysical properties, the glucan has further potential applications e.g. as component of lubricants, thickening agent and moisturizing cosmetic.

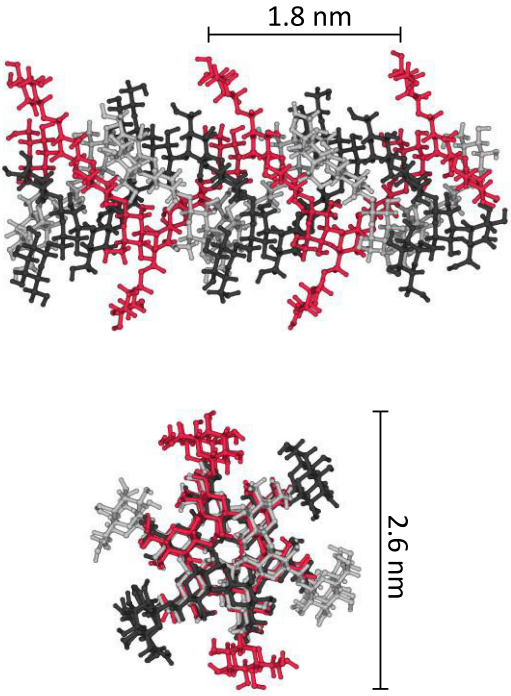

Figure 1-2 Model of the Schizophyllan triple helix structure (SCH chain 1 in red; SCH chain 2 in black; SCH chain 3 in grey)**.** One helix turn with 1.8 nm height consists of six β-(1,3)-linked main chain D-glucose monomers and an average helix diameter of 2.6 nm with the protruding β-(1,6)-bound D-glucose (modeled by Dr. Kwang Hoon Sung, Helmholtz Centre for Infection research, Braunschweig, Germany).

Like a variety of other fungal β-(1,3)-D-glucans, SCH shows antitumoral and immunomodulating effects [14]. It is reported to be effective in mice against solid forms of sarcoma

37, sarcoma 180, Ehrlich carcinoma and Yoshida sarcoma, as well as 7,12-diemthylbenz(α)anthracene induced hepatic and mammary carcinoma [15, 16]. From clinical trials of radiation and chemotherapy with SCH as assistant agent, a prolonged survival time of patients could be observed explained by aiding against radiation damage and accelerated recovery of bone marrow function [17–19]. Results of studies *in vivo* in mice and *in vitro* suggest that its bioactivity is based on the enhancement of cell-mediated immune response with stimulation of T-lymphocytes as well as macrophages and improving cytokine production [20–25].

1.2 Theoretical basics on antibody generation

1.2.1 Antibodies

Antibodies are proteins of the immunoglobulin (Ig) family and an essential part of the humoral adaptive immune system in *Gnathostomes* (higher vertebrates with jaws). They are produced and secreted by B-lymphocytes as consequence of an immune response [26]. The primary function of antibodies is the specific binding to pathogens and their toxic products as well as other extracellular immunogenic particles. By binding they induce three protective mechanisms: Neutralization through blocking of the interaction with cells, opsonization to prompt recognition by

phagocytes for elimination and activation of the complementary system that eliminates directly and improves recognition by phagocytes [27]. The recognition of antibodies as therapeutic agent in medicine and as analytic tool in diagnostic and research, drove to the development of a research area specialized on the generation of antibodies.

The general antibody structure consists of four polypeptide chains connected by disulfide-bonds and non-covalent interactions. One pair of identical chains with a size of ≈50 kDa or higher (heavy chain, HC) is bound to each other in their C-terminal region. While two identical chains of ≈25 kDa (light chain, LC) are attached to the N-terminal region of the heavy chains. This results in a Y-shaped molecule, with two N-terminal regions involved in antigen binding (Fab, fragment antigen binding) and one C-terminal region responsible for the effector mechanism (Fc, fragment crystallizable). Different structural und functional properties of the heavy chain divide antibodies into different classes (isotypes) for example, in human exist 5 classes: IgA (IgA1 & IgA2), IgD, IgE, IgG (IgG1-IgG4) and IgM [27–29]. Antibodies of the IgG class are the most abundant isotypes of human blood and are further described in the following paragraph.

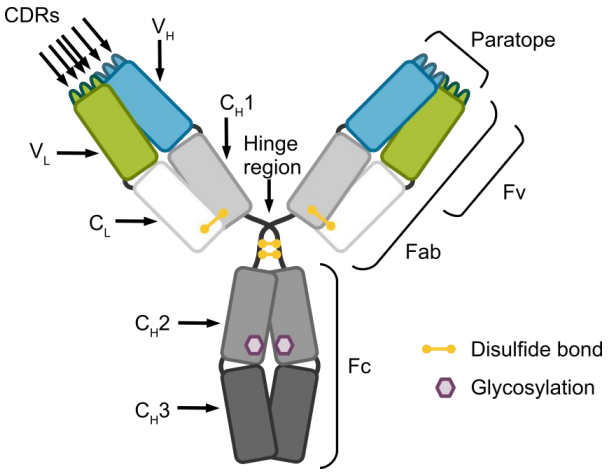

Figure 1-3 Schematic structure of an immunoglobulin G, IgG. Antibodies are composed of two identical heavy protein chains (HC) and two identical light chains (LC). The HC of the IgG isotype consists of three IgG specific constant domains (C_H1, C_H2 & C_H3) and one variable domain (V_H). Both HCs are connected by disulfide bonds at their hinge region. The LC consists of two domains, one constant domain (C_L) and one variable domain (V_H). Each LC is bound to one of the heavy chains by a disulfide bond between C_H1 and C_L domains. The resulting Y-shaped molecule can be subdivided into three fragments, two identical fragments needed for antigen binding (fragment antigen binding, Fab) and one fragment responsible for the effector activity (fragment crystallizable, Fc). The Fc is formed by the N-glycosylated C_H2 and the C_H3 domains of both HCs. While each Fab is formed by C_H1 and V_H of one HC as well as the respective LC. VH and VL in a Fab represent the smallest functional antigen binding unit called Fv (fragment variable). Both domains contain three hyper variable sequence regions

(complementarity determining regions, CDRs) which are the components of the antibody paratope and determine its antigen complementarity.

The IgG heavy chain has a size of ≈50 kDa and possess four structural domains (β-barrels) V_H, C_H1, C_H2, C_H3, a flexible peptide linker (hinge region) between C_H1 and C_H2 as well as a N-glycosylation in C_H2. The N-terminal V_H is a domain with variable sequence while C_H1 to C_H3 are domains with a constant sequence specific for the Ig class. As for every Ig isotype, the light chain is either of the kappa or the lambda type, depending from which of the two chromosomal LC gene loci they originated. They have two structural domains: the variable domain V_L and the constant domain C_L. Disulfide bonds between the C_H1 and C_L domain and between the hinge regions of the heavy chains connect the polypeptides. Together the N-terminal domains V_H and V_L form the smallest unit of the antibody that leads to antigen binding, the Fv (Fragment variable). Each of the variable domains has three hypervariable sequence regions, which are located in the loop-structures of the beta barrels. They form the region of the domains that non-covalently interacts with the antigen, the paratope. Since their sequence determines the specificity for an antigen epitope, they are also called CDRs

(complementary determining regions). The residual parts of the V-domains are the framework regions which are involved in stabilization of the paratope structure [27–29].

Some applications for antibodies are based only on antigen binding and do not depend on the effector mechanism or even need novel Ig-unlike properties. Therefore, different recombinant antibody formats have been developed and studied. Here, the formats used in this work are described: Single chain Fv (scFv), single chain Fv fused to Fc (scFv-Fc) and Fab.

The scFv format is an analog to the Fv region of antibodies with a size of 25 - 30 kDa. It consists of a V_L and V_H domain connected to each other by a peptide linker, which promotes the formation and stabilization of the paratope [30, 31]. In the scFv-Fc format, a scFv is fused to the C_H2 and C_H3 domains via the hinge region. Through the connections of the hinge regions of two scFv-Fc chains, it forms an IgG-like structure of approx. 110 kDa size with scFvs instead of Fabs and shows IgG-like functional effects [32]. The Fab format (approx. 50 kDa) equals the Fab part of immunoglobulins and can be derived recombinant but also non-recombinant by treatment of IgG with the protease pepsin [28].

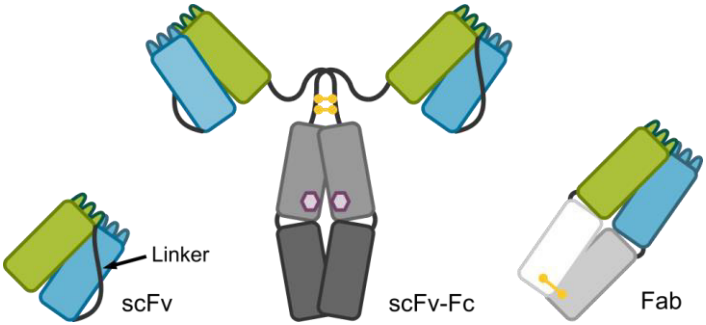

Figure 1-4 Schematic structures of the antibody format scFv, scFv-Fc and Fab. The recombinant antibody format scFv (single chain Fv, on the left) is derived from connecting the VH and VL with a short linker peptide. Another recombinant format is the scFv-Fc (in the middle) with a scFv connected to the IgG domains C_H2 and C_H3 via the hinge region. Through the interchain disulfide bonds of the hinge region it mimics an IgG with its two antigen binding sites and a functional Fc. The Fab of an IgG (right) can be produced as recombinant molecule or by pepsin treatment of an IgG.

1.2.2 Antibody generation

The first developed method for antibody generation is the isolation of sera from animals which were immunized with the antigen of interest. The purified anti sera hold an enriched mixture of different antibodies (polyclonal antibodies) against the pathogen. Later in 1975 Köhler and Milstein developed a technology for fusing B-lymphocytes from the spleen of an immunized mice with myeloma cells, the

hybridoma technology [33]. The resulting hybridoma cells obtain the properties of both cells: antigen specificity, antibody secretion and immortality. This technology enabled the selection of one specific antibody (monoclonal antibody) with desired antigen binding properties and the unlimited availability for production of this antibody.

Today - in consequence of the ongoing development of the recombinant DNA technology - it is also possible to generate monoclonal antibodies *in vitro* directly from a library of antibody genes and to produce them in different expression systems. Antibody gene libraries are derived from humans or other *Gnathostomes* by isolating the antibody genes from a repertoire of B-lymphocytes in a defined sample [34]. An immune antibody gene library is constructed by isolation of the antibody genes from IgG secreting B-lymphocytes after immunization [35]. Due to the immunization with the antigen of interest, the library contains maturated antibodies with high affinity for the antigen. Whereas an universal antibody gene library is generated by isolation of antibody genes from IgM presenting B-lymphocytes and presents a repertoire of naive antibodies against a high number of antigens [36]. The high diversity allows the isolation of antibodies against different antigens from one library but the antibodies show lower affinities. The diversity of universal libraries

can be further increased by additional randomization of the CDR3 regions (semi-synthetic gene library) or of all CDR regions in the variable domains (synthetic gene library) [37, 38].

Selection of the desired antibody from those libraries is possible by using display technologies. All display technologies have in common that a protein or peptide is expressed and physically coupled to its genetic information. This allows the selection of desired antibodies for their specificity and the direct isolation of their genetic information. Examples are the ribosome display with covalent fixation of the mRNA-ribosome-protein complex, the phage display with packaging of the gene into phage particles presenting its product fused to a phage coat protein and the yeast display with transformation of a gene into yeast cells and its expression as cell surface protein fusion [39–41]. The antibody phage display with the bacteriophage M13 used in this work is further described in the next chapter.

1.2.3 Antibody phage display

The *E. coli* specific bacteriophage M13 is a filamentous phage (length 930 nm & diameter 6.5 nm) with a circular and single stranded DNA genome (6.5 kb). Its genome consists of the M13 origin and eleven additional genes: g2, g5 and g10

are coding proteins responsible for replication of the phage DNA; g1, g4 and g11 are coding proteins responsible for the assembly of the phage particles; g3, g6, g7, g8 and g9 coding for the phage coat proteins. The product of g8 is the main coat protein p8 with some thousand copies (≈2700) per phage. Five copies of the other coat proteins are assembled on the tail end (p7 & p9) and on the head end (p3 & p6).

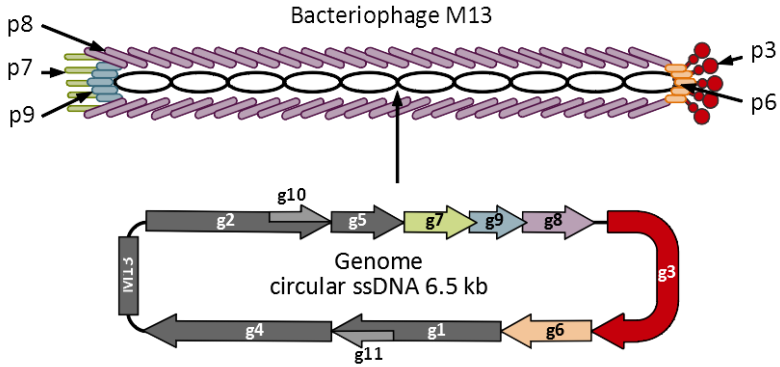

Figure 1-5 Schematic of bacteriophage M13 and its genome. The circular ssDNA (single stranded DNA) genome of bacteriophage M13 is packed in a filamentous particle that consists mainly of the coat protein p8 (≈2700 copies). At the head end of the particle are five copies of the coat proteins p6 and p3 and at the tail end five copies of p7 and p9. Next to the genes for the coat proteins (g3, g6, g7, g8 & g9) the genome contains genes for genome replication in *E. coli* (g2, g5 & g10) and for the assembly new phage particles at the cell membrane (g1, g4 & g11) as well as the M13ori sequence.

Infection of *E. coli* is induced by binding of p3 to the F-pili and to the surface protein TolA. The phage replication does not kill the cells but leads to a reduced growth rate. New phage particles emerge from the cell by adding of the inner membrane located coat proteins to the genome while it is passing through the periplasm to the outside [42].The most commonly used method for antibody phage display is the fusion of the antibodies in the scFv format to the coat protein p3. Variants with the fusion to the other coat proteins and with the usage of different antibody formats are also tested and described [43–46]. For construction of phage displayed antibody libraries special vectors were developed that can be packed into phage particles. They consist of an expression cassette for the scFv-p3 fusion protein, an antibiotic resistance gene, an *E. coli* origin of replication for non-phage mediated replication and a M13 origin of replication for packaging into phage particles. The expression cassette contains a LacZ promotor, the pelB leader for translocation of the scFv into the periplasm, cloning sites for the integration of the V domain genes, a linker sequence with myc-tag and amber stop codon as well as the g3 sequence [47, 48].

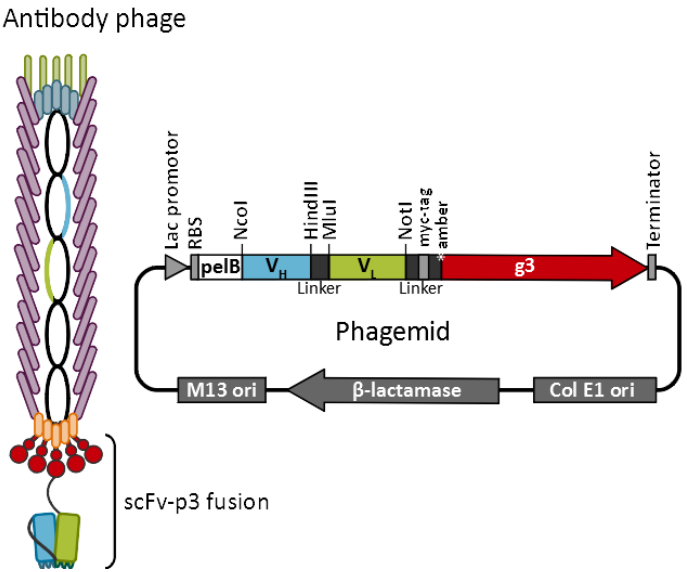

Figure 1-6 Schematic of a bacteriophage M13 based antibody phage particle and the respective phagemid. The antibody phage (left) contains a phagemid packed with the coat proteins of the bacteriophage M13. Depending on the helper phage used for packaging, the antibody phage presents on its surface one to five copies of a scFv as scFv-p3 fusion protein. The phagemid consists of an expression cassette coding for the scFv-p3 fusion protein, the bacterial origin of replication Col E1 (Col E1 ori) for phagemid amplification, the origin of replication from bacteriophage M13 as phage packaging signal and the β-lactamase gene as antibiotic resistance for selection. The expression cassette is framed by an inducible lac promotor and a terminator sequence for transcription. It also possesses the ribosome binding site sequence (RBS) for the translation of the scFv-p3 fusion protein. The sequence for the expressed fusion protein contains the pelB leader for translocation of the

scFv into the periplasm, the scFv (V_H, Linker & V_L) and the fused p3 (Linker & g3). For cloning, the V_H and V_L sequences are framed by the recognition sites of the endonucleases NcoI, HindIII, MluI and NotI. Furthermore, the linker sequence between scFv and g3 includes the sequence for a myc-tag and contains an amber stop codon.

After transformation of the phage display vector into the host, an infection with helper phage is necessary to produce the antibody displaying phage particles. The helper phage delivers the genetic information to produce the phage proteins needed for phage formation. It is repressed in its own replication and depending on the helper phage strain leads to different amount of presented scFv-p3 fusion proteins on the phage particle. Helper phage M13K07 results in antibody phage particles with an average of one presented scFv-p3 fusion protein per 10 particles [49, 50]. Infection with the strain hyperphage results in the maximal presentation of five scFv-p3 fusion proteins per particle [51].

Isolation of the desired antibodies from a phage displayed antibody library is conducted by two or three rounds of selection and amplification, also called panning [52, 53]. The phage displayed antibody library is incubated with an immobilized antigen of interest, through extensive washing the non-binding and weak binding antibody phage are removed.

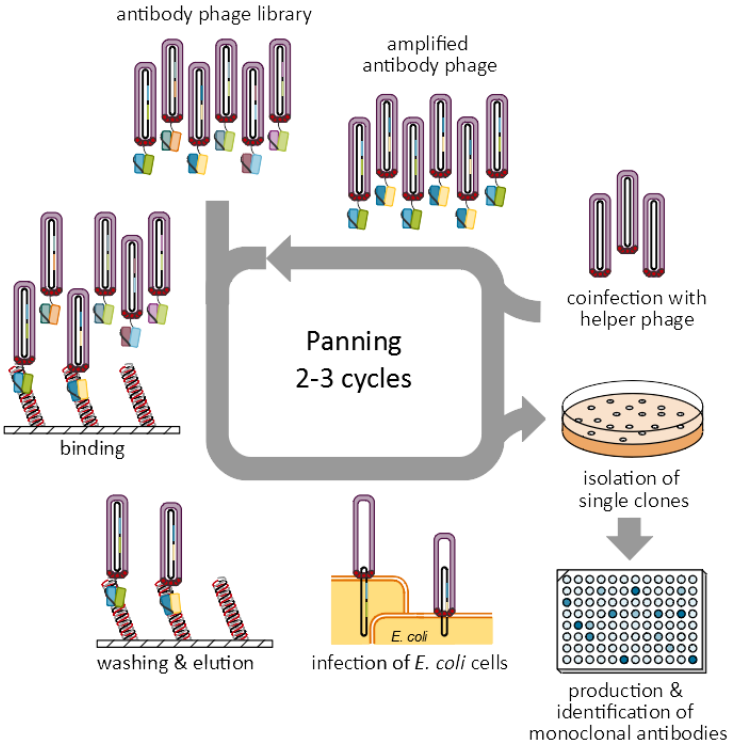

Figure 1-7 Schematic of the procedure for the selection of monoclonal antibodies from an antibody phage library via panning. The antibody phage library is incubated with the immobilized antigen. Weak and not bound antibody phage are washed away. The bound antibody phage are eluted with trypsin or via pH-shift and used for the infection of *E. coli* cells. Infected cells are co infected with helper phage for production of new antibody phage. The derived antibody phage preparation enriched by antigen binding antibody phage is used for another round of selection. After 2 to 3 rounds of selection, single clones of the infected E. coli are isolated and used for

production of the monoclonal antibodies. Produced and antigen-specific antibodies are identified via immunoassay.

The bound phage are eluted from the immobilized antigen by trypsin treatment or pH shift and used for infection of *E. coli* cells [54]. After production of new antibody phage particles, the enriched library is used for one or two further rounds of selection. Single clones of the *E. coli* cells infected with the selected phages from the last round are isolated. Through the weak amber stop codon and induction by IPTG, the isolated clones are able to produce the scFvs as solved proteins in a sufficient amount for detection [55]. The culture supernatants of the clones are screened by antigen ELISA for specific scFvs. Now, the scFv sequence of a positive tested clone can be isolated and used for further characterization of the selected monoclonal antibody.

1.3 Objective of this study

Due to the various properties of SCH which make it interesting for different applications, anti-SCH antibodies would be of great value as tool for quantitative analysis and for the investigation of glucan bioactivity. The objective of this study was the generation of such recombinant monoclonal antibodies against the β-D-glucan Schizophyllan from an

immune library as well as from a naive library. Isolation of the respective antibodies should be performed via phage display. Therefore, a suitable immobilization method of SCH to a solid carrier matrix had to be established. At last the antigen specificity of the isolated antibodies should be characterized.

2 Materials and Methods

2.1 Materials

2.1.1 Equipment

The equipment used in this project is listed in the following table:

Table 2-1 List of equipment used in this project

Device	Model	Manufacturer
Balances	Sartorius analytic	Sartorius, Göttingen, Germany
	Sartorius excellence	Sartorius, Göttingen, Germany
Blotting machine	Trans-Plot® Turbo™	Bio-Rad Laboratories, München, Germany
Centrifuges	5810 R	Eppendorf, Hamburg, Germany
	5415 D	Eppendorf, Hamburg, Germany
	Multifuge® 3 S-R	Heraeus, Hanau, Germany
	Multifuge® 1 S-R	Thermo Scientific, Dreieich, Germany
	Sorvall™ RC6 Plus	Thermo Scientific, Dreieich, Germany

	Sprout®	Heathrow Scientific, Illinois, USA
Chromatography system	ÄKTApurifier™	GE Healthcare, München, Germany
Desiccator	SICCO Star-Vitrum	Bohlender, Grünsfeld, Germany
Electrophoresis chamber	Mini-Protean® 3	Bio-Rad Laboratories, München, Germany
	Model 40-0708/ 40-1410	Peqlab, Erlangen, Germany
Electroporation device	MicroPulser™	Bio-Rad Laboratories, München, Germany
ELISA readers	Epoch™	BioTek Instruments, Winooski, USA
	Sunrise™	Tecan, Crailsheim, Germany
ELISA washer	HydroFlex™	Tecan, Crailsheim, Germany
Gel documentation system	Gel Jet Imager	Intas, Göttingen, Germany
Incubators	Certomat® BS-1	Braun, Melsungen, Germany
	HERAcell™	Thermo Scientific, Dreieich, Germany
	Minitron	Infors HT, Bottmingen, Switzerland

	Multitron	Infors HT, Bottmingen, Switzerland
	Typ BE400	Memmert, Schwabach, Germany
	VorTemp™ 56	Labnet, Woodbridge, USA
Laminar flow benches	Hera safe™	Heraeus, Hanau, Germany
	HLB 2472	Heraeus, Hanau, Germany
	MSC-Advantage™	Thermo Scientific, Dreieich, Germany
Liquid handling system	EL406	BioTek Instruments, Winooski, USA
Multiwell plate stackers	Biostack™ 3	BioTek Instruments, Winooski, USA
	Biostack™ 4	BioTek Instruments, Winooski, USA
Orbital shakers	Celltron	Infors HT, Bottmingen, Switzerland
	Titramax 101	Heidolph, Schwabach, Germany
Oven	Heratherm®	Thermo Scientific, Dreieich, Germany
pH meter	CG810	Schott, Mainz, Germany

Photometers	NanoDrop™ ND1000	Peqlab, Erlangen, Germany
	Libra S11	Biochrom, Holliston, USA
Pipettes	e1200	BIOHIT, Helsinki, Finland
	Multipette® Plus	Eppendorf, Hamburg, Germany
	Eppendorf Research®	Eppendorf, Hamburg, Germany
	VIAFLO 96	INTEGRA Biosciences, Zizers, Switzerland
Power supply	EPS 301	Amersham Bioscience, Freiburg, Germany
Protein purification system	Profinia™	Bio-Rad Laboratories, München, Germany
Peristaltic pump	MasterFlex® L/S™	Cole-Palmer, Wertheim, Germany
Rotors	A-4-81	Eppendorf, Hamburg, Germany
	BIOShield™ 1000A	Heraeus, Hanau, Germany
	F12S-6x500y	FIBERLite, Santa Clara, USA
	HIGHConic™	Thermo Scientific, Dreieich, Germany

	Microlitre rotor AL	Heraeus, Hanau, Germany
	SS-34 (Sorvall)	Thermo Scientific, Dreieich, Germany
Sterilizer	FVA/A1	Fedegari Autoclavi, Albuzzano, Italy
Thermocycler	PTC-200 DNA Engine®	MJ Research, Waltham, USA
Thermomixers	Thermomixer® Comfort	Eppendorf, Hamburg, Germany
	Thermomixer® Compact	Eppendorf, Hamburg, Germany
Vacuum oven	Vacutherm™	Thermo Scientific, Dreieich, Germany
Vacuum manifold	NucleoVac 96	Macherey-Nagel, Düren, Germany
Vacuum pumps	MZ 2C NT	VACUUBRAND, Wertheim, Germany
	N 035.1.2 AT.18	KNF Neuberger, Freiburg, Germany
Water baths	1002/1003	GFL, Burgwedel, Germany
	SW20	Julapo, Seelbach, Germany
Water installation	Arium® 611	Sartorius, Göttingen, Germany

2.1.2 Consumables

The consumables used in this project are listed in the following table:

Table 2-2 List of consumables used in this project

Material	Manufacturer
AeraSeal™, multiwell plate cover seal	Excel Scientific, Victorville, USA
Air-o-Seal – hydrophobic gas permeable seal	4titude, Dorking, UK
Amicon® Ultra – 0.5 mL Centrifugal Filters, 30 kDa cut-off	Merck Millipore, Darmstadt, Germany
CentriStar™, Centrifugation tubes	Corning, New York, USA
Chelating Sepharose® Fast Flow	GE Healthcare, München, Germany
Combitips™ plus	Eppendorf, Hamburg, Germany
Costar® disposable serelogical pipettes	Corning, New York, USA
Costar® Carbo-BIND™ 96-well multiwell plate	Corning, New York, USA
Deep well plates	Thermo Scientific, Dreieich, Germany
Disposable cuvettes	Brand, Wertheim, Germany

Dynabeads™ M-270 Amine	Thermo Scientific, Dreieich, Germany
Dynabeads™ M-270 Epoxy	Thermo Scientific, Dreieich, Germany
Electroporation cuvettes, Gene Pulser® 0.1 cm	Bio-Rad Laboratories, München, Germany
Inoculation loops	VWR, Darmstadt, Germany
MabSelect™ SuRe™ (protein A resin)	GE Healthcare, München, Germany
Multiwell plate seal	4titude, Dorking, UK
Multiply®-µStrip Pro 8-strip	Sarstedt, Nümbrecht, Germany
Petri dishes	Greiner Bio-One, Frickenhausen, Germany
Pipette tips	Sarstedt, Nümbrecht, Germany
Pipette tips	INTEGRA Biosciences, Zizers, Switzerland
Pipette tips, filtered	Greiner-Bio-One, Frickenhausen, Germany
Pipette tips, filtered	Nerbe plus, Winsen, Germany
Polycarbonate Erlenmeyer flask with vent cap	Corning, New York, USA

Polypropylene 96-Well multiwell plate, Flat-shaped	Greiner-Bio-One, Frickenhausen, Germany
Polypropylene 96-Well multiwell plate, U-shaped	Greiner-Bio-One, Frickenhausen, Germany
Polypropylene screw cap tube, 40 mL	Sarstedt, Nümbrecht, Germany
Polystyrene lid for multiwell plate	Greiner-Bio-One, Frickenhausen, Germany
Polyvinylidene fluoride membrane	Carl Roth, Karlsruhe, Germany
Polypropylene micro tubes 1.5 mL & 2 mL	Sarstedt, Nümbrecht, Germany
SealPlate®, multiwell plate cover seal	Excel Scientific, Victorville, USA
Screw-top micro caps	Sarstedt, Nümbrecht, Germany
Spatulas	VWR, Darmstadt, Germany
Square BioAssay Dish, 245 mm	Corning, New York, USA
Sterile filters	Sartorius, Göttingen, Germany
Sterile syringes	B.Braun, Melsungen, Germany

Vivaflow® 200, crossflow module, 100 kDa cut-off, polyethersulfone	Sartorius, Göttingen, Germany

2.1.3 Commercial kits und chromatography columns

The commercial kits and chromatography columns used in this project are listed in the following table:

Table 2-3 List of commercial kits and chromatography columns used in this project

Description	Manufacturer
Bio-Scale™ Mini Bio-Gel® P-6 Desalting Cartridge	Bio-Rad Laboratories, München, Germany
Bio-Scale™ Mini UNOsphere Supra™ Cartridge	Bio-Rad Laboratories, München, Germany
Direct-zol™ RNA MiniPrep Plus	Zymo Research, Freiburg, Germany
Glucatell® Kit β-(1,3)-D-glucan detection	Assoc. Cape Cod, Mörfelden-Walld., Ger.
Hi Yield® Plasmid Mini DNA Kit	Süd-Laborbedarf, Gauting, Germany
Hi Yield® Gel/PCR DNA Fragment Extraction Kit	Süd-Laborbedarf, Gauting, Germany
NucleoBond® Xtra Midi	Marcherey-Nagel, Düren, Germany
NucleoSpin® Plasmid	Marcherey-Nagel, Düren, Germany

NucleoSpin® Plasmid EasyPure	Marcherey-Nagel, Düren, Germany
NucleoSpin® Gel and PCR Clean-Up	Marcherey-Nagel, Düren, Germany
Superdex™ 75 HiLoad™ 16/60	GE Healthcare, München, Germany
SuperScript™ IV First-Strand Synthesis System	Thermo Scientific, Dreieich, Germany
Zeba™ Desalt Spin columns	Thermo Scientific, Dreieich, Germany

2.1.4 Chemicals and water

The chemicals used in this project were purchased from the following manufacturers, if not mentioned otherwise: AppliChem (Darmstadt, Germany), BD (Sparks, USA), Carl Roth (Karlsruhe, Germany), GE Healthcare (München, Germany), MBI Fermentas (St. Leon-Rot, Germany), Merck (Darmstadt, Germany), Riedel-de Häen (Sarstedt, Germany), Roche (Mannheim, Germany), Fluka/Sigma-Aldrich (Neu-Ulm, Germany) und Serva (Heidelberg, Germany).

Ultrapure water purified with the water installation arium66 (Sartorious, Göttingen, Germany) was generally used in this project.

2.1.5 Buffers and Solutions

Buffers and solutions used in this project are listed in the following table:

Table 2-4 List and composition of buffers or solutions used in this project

Description	Composition	
TAE buffer (pH 8.0)	40 mM	Tris
	20 mM	Acetic acid
	2 mM	Ethylenediaminetetraacetic acid
Agarose gel		TAE buffer (solvent)
	1 % (w/v)	Agarose
	4.2 µg L^{-1}	Ethidium bromide
Lowry reagent A	2 % (w/v)	Na_2CO_3
	0.4 % (w/v)	NaOH
Lowry reagent B	1 % (w/v)	$CuSO_4$ x $5H_2O$
Lowry reagent C	2 % (w/v)	Sodium potassium tartrate tetrahydrate
DNS reagent	1 % (w/v)	3,5-Dinitrosalicylic acid
	30 % (w/v)	Sodium potassium tartrate tetrahydrate
	1.6 % (w/v)	NaOH

5x Laemmli buffer (reducing)	10 % (w/v)	Sodium dodecyl sulfate
	500 % (w/v)	Glycerol
	0.2 % (w/v)	Bromophenol blue
	15 % (v/v)	β-Mercaptoethanol
5x Laemmli buffer (non-reducing)	10 % (w/v)	Sodium dodecyl sulfate
	50 % (w/v)	Glycerol
	0.02 % (w/v)	Bromophenol blue
SDS-PAGE running buffer (pH 8.3)	25 mM	Tris
	192 mM	Glycin
	0.1 % (w/v)	Sodium dodecyl sulfate
Coomassie staining solution	0.5 % (w/v)	Coomassie Brilliant Blue R250
	10 % (v/v)	Acetic acid
	2.5 % (v/v)	2-Propanol
Blotting buffer (pH 8.3)	25 mM	Tris
	192 mM	Glycin
NBT	30 g L^{-1}	Nitro blue tetrazolium chloride
	70 %(v/v)	N,N-Dimethylformamide
BCIP	15 g L^{-1}	5-Bromo-4-chloro-3-indolyl phosphate (diNa-salt)
	70 %(v/v)	N,N-Dimethylformamide
AP substrate buffer	100 mM	Tris
	0.5 mM	$MgCl_2$
10 mM acetate buffer (pH 5.4)		Solutions of 10 mM acetate and 10 mM sodium acetate mixed until a pH of 5.4 was reached.

PBS (phosphate buffered saline, pH 7.4)	0.8 % (w/v)	NaCl
	0.02 % (w/v)	KCl
	0.144 % (w/v)	Na_2HPO_4 x $2H_2O$
	0.024 % (w/v)	KH_2PO_4
PBST		PBS (solvent)
	0.05 % (v/v)	Tween20
MPBST		PBST (solvent)
	2 % (w/v)	Milk powder
TMB A (pH 4.1)	30 mM	KCl
	50 mM	Citric acid
TMB B	90 % (v/v)	Ethanol
	10 % (v/v)	Acetone
	0.3 % (v/v)	H_2O_2
	1 mM	3,3',5,5'-Tetramethylbenzidine
TFB1	10 mM	$CaCl_2$
	30 mM	Potassium acetate
	100 mM	RbCl
	50 mM	$MnCl_2$
	15 % (v/v)	Glycerole
TFB2	10 mM	MOP
	50 mM	$CaCl_2$
	10 mM	RbCl
	15 % (v/v)	Glycerole
Trypan blue solution		PBS (solvent)
	0.4 % (w/v)	Trypan blue

Proteinase K buffer (pH 7.4)	500 mM 1 M	$CaCl_2$ Tris
5x Protein A binding buffer (pH 7.4)	685 mM 13.5 mM 40.5 mM 21.5 mM	NaCl KCl KH_2PO_4 Na_2HPO_4
Protein A binding buffer	137 mM 2.7 mM 8.1 mM 4.3 mM	NaCl KCl KH_2PO_4 Na_2HPO_4
His-tag binding buffer (pH 7.4)	500 mM 20 mM 20 mM 10 mM	NaCl Na_2HPO_4 NaH_2PO_4 Imidazole
His-tag elution buffer	 100 mM	PBS (solvent) Ethylenediaminetetraacetic acid
Gel filtration buffer (pH 8)	20 mM 150 mM	Tris NaCl
Phage precipitation solution	20 % (v/v) 2.5 M	Polyethylene glycol (average molecular weight 6 kDa) NaCl
Phage dilution buffer (pH 7.5)	10 mM 20 mM 2 mM	Tris NaCl Ethylenediaminetetraacetic acid

If not mentioned otherwise, water was used as solvent and the pH was adjusted with 1 M HCl and 1 M NaOH.

2.1.6 Media and Supplements

Media and supplements used in this project are listed in the following table:

Table 2-5 List and composition of media or supplements used in this project

Description	Composition	
2xYT-medium	1.6 % (w/v) 1.0 % (w/v) 0.5 % (w/v)	Bacto™ trypton Yeast extract NaCl
Ampicillin	100 mg mL^{-1}	Ampicillin
Glucose	2 M	Glucose
IPTG	1 M	Isopropyl β-D-1-thiogalacto-pyranoside
Kanamycin	10 mg mL^{-1}	Kanamycin
2xYT-A medium	100 µg mL^{-1}	Ampicillin in 2xYT medium
2xYT-AI medium	1 mM	IPTG in 2xYT-A medium
2xYT-GA medium	100 mM	Glucose in 2xYT-A medium
2xYT-KA medium	50 mg mL^{-1}	Kanamycin in 2xYT-A medium
2xYT-GA agar	1.5 % (w/v)	Bacto™ Agar in 2xYT-GA medium

SOC medium	2 % (w/v)	Bacto™ trypton
	0.5 % (w/v)	Yeast extract
	50 % (w/v)	NaCl
	10 mM	$MgCl_2$
	20 mM	Glucose
Recovery medium		Purchased from Lucigen (Middleton, USA)
FreeStyle™ F17-medium		Purchased from Invitrogen (Darmstadt, Germany)
HEK TF-medium		Purchased from Xell AG (Bielefeld, Germany)
HEK cell culture medium		Freestyle™ F17-medium (solvent)
	25 µg mL^{-1}	G418
	8 mM	L-glutamin
	0.1 % (v/v)	Pluronic® (PAA Laboratories, Cölbe, Germany)
HEK cell transfection medium		Freestyle™ F17-medium (solvent)
	8 mM	L-glutamin
	0.1 % (v/v)	Pluronic® (PAA Laboratories, Cölbe, Germany)

HEK cell feeding medium (for HEK293-6E)		Freestyle™ F17-medium (solvent)
	8 mM	L-glutamin
	0.1 % (v/v)	Pluronic® (PAA Laboratories, Cölbe, Germany)
	0.1 % (w/v)	Trypton N1 (PAA Laboratories, Cölbe, Germany)
HEK cell feeding medium (for EXPI293-F)		HEK TF-medium (solvent)
	8 mM	L-glutamin
	16 % (v/v)	HEK FS (Xell AG, Bielefeld, Germany)

All media and supplements were prepared with water as solvent. 1 M HCl and 1 M NaOH were used for adjustment of pH.

2.1.7 Glucans and other saccharides

Glucans and other saccharides used in this project are listed in the following table:

Table 2-6 List of glucans and saccharides used for the studies in this project

Glucan	Source
β-(1,6)-D-Gentiobiose	Carl Roth, Karlsruhe, Germany

Actigum CS 11 (Scleroglucan, lyophilized)	Degussa Construction Polymers, Trostberg, Germany
Cinerean from *Botrytis cinerea* (LU 14548, 2 g L^{-1} in cell free culture supernatant, 5 g L^{-1} formic acid)	U. Rau, TU Braunschweig, Braunschweig, Germany
Dextran	Pharmacia Fine chemicals, Uppsala, Sweden
Fructigan from *Monilinia fructigena* (ATCC 24976, 4 g L^{-1} in cell free culture supernatant, 5 g L^{-1} formic acid)	U. Rau, TU Braunschweig, Braunschweig, Germany
Laminarihexaose	Megazyme, Wicklow, Ireland
Laminarin	Sigma Aldrich, Neu-Ulm, Germany
Schizophyllan (lyophilized)	Contipro Biotech, Dolní Dobrouč, Czech Republik)
Schizophyllan from *Schizophyllum commune* (ATCC 38548, 5 g L^{-1} in cell free culture supernatant, 5 g L^{-1} fomic acid)	U. Rau, TU Braunschweig, Braunschweig, Germany
Scleroglucan from *Sclerotium glcanicum* (DSM 2159, lyophilized)	U. Rau, TU Braunschweig, Braunschweig, Germany

Scleroglucan from *Sclerotium rolfsii* culture (ATCC 15205, 5 g L^{-1} in cell free culture supernatant, 5 g L^{-1} formic acid)	U. Rau, TU Braunschweig, Braunschweig, Germany
Xanthan	Carl Roth, Karlsruhe, Germany

2.1.8 Commercial enzymes, buffers and molecular weight standards

Commercial enzymes, buffers and molecular weight standards used in this project are listed in the following table:

Table 2-7 List of commercial enzymes, buffers and molecular weight standards used in this project

Description	Manufacturer
5x CutSmart® buffer	New England Biolabs, Frankfurt a. M., Germany
5x Green GoTaq® Reaction Buffer	Promega, Madison, USA
5x Phusion® HF Buffer	Thermo Scientific, Dreieich, Germany
25 mM $MgCl_2$	Promega, Madison, USA
Alkaline phosphatase, calf intestinal (CIP)	New England Biolabs, Frankfurt a. M., Germany

BsiWI	New England Biolabs, Frankfurt a. M., Germany
BssHII	New England Biolabs, Frankfurt a. M., Germany
GeneRuler 1 kb Plus DNA Ladder	Thermo Scientific, Dreieich, Germany
GoTaq® DNA Polymerase	Promega, Madison, USA
HindIII-HF®	New England Biolabs, Frankfurt a. M., Germany
MluI-HF®	New England Biolabs, Frankfurt a. M., Germany
NcoI-HF®	New England Biolabs, Frankfurt a. M., Germany
NEBuffer™ 3.1	New England Biolabs, Frankfurt a. M., Germany
NheI-HF®	New England Biolabs, Frankfurt a. M., Germany
NotI-HF®	New England Biolabs, Frankfurt a. M., Germany
Phusion® High Fidelity DNA Polymerase	Thermo Scientific, Dreieich, Germany
Precision Plus Protein™ All Blue Prestained Standard	Bio-Rad, München, Germany
Precision Plus Protein™ Unstained Standard	Bio-Rad, München, Germany

Proteinase K	Sigma Aldrich, Neu-Ulm, Germany
T4 DNA Ligase (HC)	Promega, Madison, USA
T4 DNA Ligase Buffer	Promega, Madison, USA
Trypsin	Carl Roth, Karlsruhe, Germany

2.1.9 Antibodies

Antibodies used for analytics in this project are listed in the following table:

Table 2-8 List of antibodies used for analytics in this project

Antibody	Description	Source
Goat anti-mouse IgG (Fc-specific, polycl-nal), AP conjugate	115-055-071	Dianova, Hamburg, Germany
Goat anti-mouse IgG (Fc-sepcific, polycl-nal), HRP conjugate	A0168	Sigma Aldrich, München, Germany
Mouse anti-c-myc-tag	9E10	AG Duebel, Braunschweig, Germany
Mouse anti-His-tag	DIA-900	Dianova, Hamburg, Germany

2.1.10 Plasmids

Plasmids used for cloning in this project are listed in the following table:

Table 2-9 List of plasmids used in this project

Description	Application
pCSE2.6-mIgG2c-Fc-XP	Expression vector for productionof scFv-Fc (murine Fc) in HEK cells
pCSE2.5-Fab-h-HIS-XP	Expression vector for production of Fab heavy chain in HEK cells
pCSE2.5-Fab-k-HIS-XP	Expression vector for production of Fab kappa light chain in HEK cells
pHAL30	Phagemid vector for antibody library generation

2.1.11 Oligonucleotides (primer)

Oligonucleotides used in this project as primers for PCR experiments are purchased from Biolegio B.V. (Nijmegen, Netherlands) and listed in the following table:

Table 2-10 List of oligonucleotides used in this project

Description	Oligonucleotide sequence	Application
JoJ48C11_VH_BssHII_f	TCCACAGGCGCGCACTCCG AGGTCCAGCTGCAACAATCT	Fab cloning
JoJ48C11_VH_NheI_b	TGGGCCCTTGGTGCTAGCTG AGGAGACTGTGAGAGTGGT	Fab cloning
JoJ48C11_VLK_BssHII_f	TCCACAGGCGCGCACTCCG ATATTGTGCTAACTCAGTCT	Fab cloning
JoJ48C11_VLK_BsiWI_b	TGGTGCAGCCACCGTACGT TTCAGCTCCAGCTTGGTCCC	Fab cloning
JoJ48C11-VH-D105A-f	GGTACTGCCTACTGGGGCC AAGGCAC	Point mutation
JoJ48C11-VH-D105A-b	CCAGTAGGCAGTACCCAGG GGCCATAG	Point mutation
JoJ48C11-VH-E59A-f	GGTTATACTGCATACAATC AGAAGTTCAAGGAC	Point mutation
JoJ48C11-VH-E59A-b	CTGATTGTATGCAGTATAA CCAGTGCTAGG	Point mutation
JoJ48C11-VH-H35A-f	CTACTGGATGGCCTGGGT AAAACAGAGGCCTG	Point mutation
JoJ48C11-VH-H35A-b	GTTTTACCCAGGCCATCCA GTAGCTAGTAAAG	Point mutation
JoJ48C11-VH-S31A-f	CTTTACTGCCTACTGGATG CACTGGG	Point mutation

JoJ48C11-VH-S31A-b	CCAGTAGGCAGTAAAGGTGTAGCCAG	Point mutation
JoJ48C11-VH-W33A-f	CTAGCTACGCAATGCACTGGGTAAAACAGAGG	Point mutation
JoJ48C11-VH-W33A-b	CAGTGCATTGCGTAGCTAGTAAAGGTGTAGCC	Point mutation
JoJ48C11-VH-W47A-f	GGTCTGGAAGCAATTGGATACATTAATCC	Point mutation
JoJ48C11-VH-W47A-b	GTATCCAATTGCTTCCAGACCCTGTCCAG	Point mutation
JoJ48C11-VH-W100A-f	CCCCTAGCACCCCTGGGTACTGAC	Point mutation
JoJ48C11-VH-W100A-b	CAGGGGTGCTAGGGGTGCACAGTAATAG	Point mutation
JoJ48C11-VH-Y27A-f	CTTCTGGCGCAACCTTTACTAGCTACTGGATG	Point mutation
JoJ48C11-VH-Y27A-b	GTAAAGGTTGCGCCAGAAGCCTTGCAGG	Point mutation
JoJ48C11-VH-Y50A-f	GATTGGAGCAATTAATCCTAGCACTGG	Point mutation
JoJ48C11-VH-Y50A-b	GATTAATTGCTCCAATCCATTCCAGACCC	Point mutation
JoJ48C11-VH-Y57A-f	CACTGGTGCAACTGAGTACAATCAGAAG	Point mutation

JoJ48C11-VH-Y57A-b	CTCAGTTGCACCAGTGCTAGGATTAATG	Point mutation
JoJ48C11-VL-D49A-f	GGATTTATGCCACATCCAAACTGGC	Point mutation
JoJ48C11-VL-D49A-b	GGATGTGGCATAAATCCATCTTTTGG	Point mutation
JoJ48C11-VL-K52A-f	CACATCCGCACTGGCTTCTGGAGTCC	Point mutation
JoJ48C11-VL-K52A-b	GAAGCCAGTGCGGATGTGTCATAAATCC	Point mutation
JoJ48C11-VL-N93A-f	GGAGTAGTGCACCACCCACGTTCGGTG	Point mutation
JoJ48C11-VL-N93A-b	GTGGGTGGTGCACTACTCCACTGCTGG	Point mutation
JoJ48C11-VL-S55A-f	CTGGCTGCAGGAGTCCCTGCTCG	Point mutation
JoJ48C11-VL-S55A-b	GACTCCTGCAGCCAGTTTGGATGTG	Point mutation
JoJ48C11-VL-W90A-f	GCCAGCAGGCAAGTAGTAACCCACCCACG	Point mutation
JoJ48C11-VL-W90A-b	GTTACTACTTGCCTGCTGGC#AGTAATAAGTGG	Point mutation
MHC.F	GGCCAGTGGATAGTCAGATGGGGGTGTCGTTTTGGC	Library construction

MHC.F.Hind	GGCCAGTGGATAAAGCTTT GGGGGTGTCGTTTTGGC	Library construction
MhgIII_r	CTAAAGTTTTGTCGTCTTT CC	Colony PCR and Sequencing
MHLacZ-Pro_f	GGCTCGTATGTTGTGTGG	Colony PCR
MHV.B1	GATGTGAAGCTTCAGGAG TC	Library construction
MHV.B1.Nco	GAATAGGCCATGGCGGAT GTGAAGCTTCAGGAGTC	Library construction
MHV.B2	CAGGTGCAGCTGAAGGA GTC	Library construction
MHV.B2.Nco	GAATAGGCCATGGCGCAG GTGCAGCTGAAGGAGTC	Library construction
MHV.B3	CAGGTGCAGCTGAAGCAG TC	Library construction
MHV.B3.Nco	GAATAGGCCATGGCGCAG GTGCAGCTGAAGCAGTC	Library construction
MHV.B4	AGGTTACTCTGAAAGAGTC	Library construction
MHV.B4.Nco	GAATAGGCCATGGCGCAG GTTACTCTGAAAGAGTC	Library construction
MHV.B5	GAGGTCCAGCTGCAACAA TCT	Library construction
MHV.B5.Nco	GAATAGGCCATGGCGGAG GTCCAGCTGCAACAATCT	Library construction

MHV.B6	GAGGTCCAGCTGCAGCAG TC	Library construction
MHV.B6.Nco	GAATAGGCCATGGCGGAG GTCCAGCTGCAGCAGTC	Library construction
MHV.B7	GAGGTGAAGCTGGTGGAG TC	Library construction
MHV.B7.Nco	GAATAGACCATGGCGCAG GTCCAACTGCAGCAGCCT	Library construction
MHV.B8	GAGGTGAAGCTGGTGGA GTC	Library construction
MHV.B8.Nco	GAATAGGCCATGGCGGAG GTGAAGCTGGTGGAGTC	Library construction
MHV.B9	GAGGTGAAGCTGGTGGA ATC	Library construction
MHV.B9.Nco	GAATAGGCCATGGCGGAG GTGAAGCTGGTGGAATC	Library construction
MHV.B10	GATGTGAACTTGGAAGTG TC	Library construction
MHV.B10.Nco	GAATAGGCCATGGCGGAT GTGAACTTGGAAGTGTC	Library construction
MHV.B12	GAGGTGCAGCTGGAGGA GTC	Library construction
MHV.B12.Nco	GAATAGGCCATGGCGGAG GTGCAGCTGGAGGAGTC	Library construction

MKC.F	GGATACAGTTGGTGCAGCATC	Library construction
MKC.F.Not	TGACAAGCTTGCGGCCGCGGATACAGTTGGTGCAGCATC	Library construction
MKV.B1	GATGTTTTGATGACCCAAACT	Library construction
MKV.B1.Mlu	TACAGGATCCACGCGTAGATGTTTTGATGACCCAAACT	Library construction
MKV.B2	GATATTGTGATGACGCAGGCT	Library construction
MKV.B2.Mlu	TACAGGATCCACGCGTAGATATTGTGATGACGCAGGCT	Library construction
MKV.B3	GATATTGTGATAACCCAG	Library construction
MKV.B3.Mlu	TACAGGATCCACGCGTAGATATTGTGATAACCCAG	Library construction
MKV.B4	GACATTGTGCTGACCCAATCT	Library construction
MKV.B4.Mlu	TACAGGATCCACGCGTAGACATTGTGCTGACCCAATCT	Library construction
MKV.B5	GACATTGTGATGACCCAGTCT	Library construction
MKV.B5.Mlu	TACAGGATCCACGCGTAGACATTGTGATGACCCAGTCT	Library construction

MKV.B6	GATATTGTGCTAACTCAGT CT	Library construction
MKV.B6.Mlu	TACAGGATCCACGCGTAG ATATTGTGCTAACTCAGTCT	Library construction
MKV.B7	GATATCCAGATGACACAGA CT	Library construction
MKV.B7.Mlu	TACAGGATCCACGCGTAGA TATCCAGATGACACAGACT	Library construction
MKV.B8	GACATCCAGCTGACTCAGT CT	Library construction
MKV.B8.Mlu	TACAGGATCCACGCGTAGA CATCCAGCTGACTCAGTCT	Library construction
MKV.B9	CAAATTGTTCTCACCCAG TCT	Library construction
MKV.B9.Mlu	TACAGGATCCACGCGTACA AATTGTTCTCACCCAGTCT	Library construction
MKV.B10	GACATTCTGATGACCCAGT CT	Library construction
MKV.B10.Mlu	TACAGGATCCACGCGTAGA CATTCTGATGACCCAGTCT	Library construction
MLC.F	GGTGAGTGTGGGAGTGGA CTTGGGCTG	Library construction

MLC.F.Not	TGACAAGCTTGCGGCCGCG GTGAGTGTGGGAGTGGACT TGGGCTG	Library construction
MLV.B	CAGGCTGTTGTGACTCAG GAA	Library construction
MLV.B.Mlu	TACAGGATCCACGCGTACA GGCTGTTGTGACTCAGGAA	Library construction
Tor-pCMV-mIgG01-FC-seq-f	CACTTTGCCTTTCTCTCC	Colony PCR
Tor-pCMV-mIgG01-FC-seq-r	CAGATGGCTGGCAACTAG	Colony PCR
ToR-pCMV-Seq-f	TGGTAGCAACAGCTACAG	Sequencing

2.1.12 *E. coli* strains, bacteriophage, mammalian cell line and mice

Organisms used in this project are listed in the following table:

Table 2-11 List of organisms used in this project

Description	Genotype or properties	Source
BALB/c mice	Inbred mouse strain, female, 7 weeks old	TU Braunschweig, Braunschweig, Germany

E. coli XL1-Blue MRF'	Δ(*mcrA*)183, Δ(*mcr*CB-*hsd*SMR-*mrr*)173, *end*A1, *sup*E44, thi-1, *rec*A1, *gyr*A96, *rel*A1, *lac* [F' proAB, *lacIq*ZΔM15, Tn10 (Tetr)]	Stratagene, La Jolla, USA
E. cloni® 10G Surpreme	F- *mcrA* Δ(*mrr-hsd*RMS-*mcr*BC) *end*A1 *rec*A1 Φ80*dlac*ZΔM15 Δ*lac*X74 *ara*D139 Δ(*ara,leu*)7697 *gal*U *gal*K *rps*L *nup*G λ- *ton*A (StrR)	Lucigen, Middle-ton,USA
ER2738	[F'*proA+B+ lacIq Δ(lacZ)M15 zzf::Tn10* (Tetr)] *fhuA2 glnVΔ(lac-proAB) thi-1Δ(hsdS-mcrB)5*	Lucigen, Middle-ton,USA
EXPI293-F™	Human embryonic kid-neycells, suspension cell line	Thermo Scientific, Dreieich, Germany
HEK293-6E	Human embryonic kid-ney cells, suspension cell line	NRC Biotechnology Research Institute, Montreal, Canada
Hyperphage	M13K07 Helper phage with deletion of pIII	Progen Biotechnik GmbH, Heidelberg, Germany
M13K07	Helper phage	J. Vieira and J. Messing [50]

2.1.13 Software and databases

Software and databases used for this project are listed in the following table:

Table 2-12 List of Software and databases used for this project

Description	Source/Manufacturer	Application
CCP4MG 2.10.6	University of New York, New York, USA	Structure data visualization
Gen5 2.08	BioTek Instruments, Winooski, USA	ELISA plate documentation
Geneious 4.8.5	Biomatters Ltd, Auckland, New Zealand	Sequence data analysis and processing
IMGT/V-QUEST	http://www.imgt.org	Antibody sequence analysis
Intas GDS	Intas, Göttingen, Germany	Agarose gel documentation
Liquid Handling Control 2.17	BioTek Instruments, Winooski, USA	Controlling of liquid handling system EL 406
Mendeley Desktop	Mendeley Ltd, London, UK	Literature database and citation

Microsoft Office 2010	Microsoft, Redmond, USA	Text, Calculation and Drawing
NanoDrop ND-1000	Coleman Technologies, Orlando, USA	DNA and protein concentration analysis
NCBI	http://www.ncbi.nlm.nih.gov/	Literature research
Scopus	https://www.scopus.com/home.uri	Literature research
Sigma Plot 12.3	Systat Software, Erkrath, Germany	Calculation and data presentation
UNICORN	GE Healthcare, München, Germany	Controlling of ÄKTApurifier
VBASE2	http://www.vbase2.org	Antibody sequence analysis

2.2 Methods

2.2.1 Sterilization

Sterilization of liquids and unsterile consumables as well as inactivation of biological material were done by autoclaving each separately for at least 20 minutes at 121 °C with 1 bar

overpressure. Heat sensitive substances were filtered by a 0.2 µm filter into sterile vessels under sterile conditions.

2.2.2 Molecular biological methods

The following molecular biological methods were used in this project.

2.2.2.1 Preparation of DNA

Plasmid DNA from *E. coli* cultures was isolated with commercial plasmid DNA preparation kits according to their manuals. PCR-products and DNA-fragments were purified either from the reaction mix or from agarose gels with a commercial PCR clean up and gel extraction kits. The purified DNA was solubilized in water and stored at -20 °C.

2.2.2.2 Determination of DNA concentrations by spectrophotometry

The concentration of DNA preparations was determined by measuring the absorbance at λ = 260 nm with a spectrophotometer and were calculated by the correlation A_{260} = 1 ≙ 1 ng μL^{-1}.

2.2.2.3 Fragmentation of DNA with endonucleases

Insert isolation and vector linearization for cloning were performed by treatment with commercial endonucleases. In general, 1 µg of DNA was fragmented with one or a

combination of two commercial endonucleases (1 µL each) in 50 µL of the recommended buffer. After incubation the enzymes were inactivated for 20 minutes at 80 °C.

2.2.2.4 Dephosphorylation of linearized vector DNA

The ligation of linearized vector DNA with itself was prevented by adding 1 µL (5 U) of calve intestinal phosphatase (CIP) to the endonuclease reaction mix during incubation.

2.2.2.5 Ligation of vector DNA with insert DNA

The construction of functional plasmids from linearized vector DNA and insert DNA was performed by ligation with commercial T4 DNA Ligase. Therefore, 50 ng of the linearized vector DNA was mixed with insert DNA in a molar ratio of one to three in 20 µL of T4 ligation buffer. 0.5 µL of T4 DNA ligase was added and the reaction mix was incubated for 30 minutes at 20 °C (room temperature) or overnight at 16 °C. If necessary the ligase was heat inactivated by incubation at 70 °C for 10 minutes.

2.2.2.6 Polymerase chain reaction (PCR)

The DNA amplification by PCR were performed to control for correct plasmid construction or to introduce changes in DNA sequences.

Colony PCR

Insert rates and correct insert size after cloning and transformation were controlled via colony PCR with primers flanking the cloning sites of the vectors. A small amount of *E. coli* cells, either a colony from an agar plate or less than 1 µL from a liquid culture, were added to 10 µL of the reaction mix. The mixture was incubated in a thermocycler with the appropriate temperature program. The reaction mix was used for agarose gel electrophoresis after PCR.

Table 2-13 Reaction mix for colony PCR

Stock solution	Volumes [µL] per 10 µL reaction mix
5x Green GoTag® Reaction Buffer	2.0
25 mM $MgCl_2$	0.8
10 mM dNTP mix	0.2
10 mM forward primer	0.5
10 mM reverse primer	0.5
5 U μL^{-1} GoTag® DNA Polymerase	0.05
Water	5.95

Table 2-14 Temperature profile for colony PCR

Step	Profile	Repeats
1. Initial denaturation	95 °C for 2 minutes	x1
2. Denaturation	94 °C for 15 seconds	x25
3. Annealing	56 °C for 20 seconds	
4. Elongation	72 °C for 30 seconds per kbp insert	
5. Final Elongation	72° C for 3 Minutes	x1
6. Store	16 °C forever	

PCR for Fab construction

Separation of the VH and VL sequence segments from pHAL30-JoJ48C11 and introduction of new endonuclease recognition sites were performed by PCR. The amplificated segments were isolated by agarose gel electrophoresis and used for cloning after gel extraction.

Table 2-15 PCR reaction mix for Fab construction

Stock solution	Volumes [µL] per 100 µL reaction mix
5 ng μL^{-1} pHAL30-JoJ48C11	1.0
5x Green GoTag® Reaction Buffer	20.0
25 mM $MgCl_2$	6.0
10 mM dNTP mix	2.0
10 mM forward primer	2.0
10 mM reverse primer	2.0
5 U μL^{-1} GoTag® DNA Polymerase	0.5
Water	66.0

Table 2-16 PCR temperature profile for Fab construction

Step	Profile	Repeats
1. Initial denaturation	95 °C for 2 min	x1
2. Denaturation	95 °C for 15 s	x25
3. Annealing	56 °C for 20 s	
4. Elongation	72 °C for 2.5 min	
5. Final Elongation	72° C for 3 min	x1
6. Store	16 °C forever	

Quick change PCR

The exchange of codons in antibody sequences was performed via quick change PCR. Therefore, the whole plasmid carrying the antibody sequence was amplified with 3'-overlapping primers which have the new codon integrated on the desired position.[56] After PCR the methylated template was erased by addition of 1 µL of the endonuclease DpnI to the reaction and incubation for 1 hour at 37 °C. 10 µL of the reaction mix was directly used for heat shock transformation. The linear PCR product had overlapping 3'-overhangs which resulted to stabile circularization. The nicked plasmid was repaired inside the *E. coli* cells by homologous recombination.

Table 2-17 Reaction mix for quickchange PCR

Stock solution	Volumes [µL] per 25 µL reaction mix
0.5 ng μL^{-1} pCSE2.6-mIgG2c-Fc-JoJ48C11	1.0
5x Phusion® HF Reaction Buffer	5.0
10 mM dNTP mix	0.5
10 mM forward primer	1.25
10 mM reverse primer	1.25
5 U μL^{-1} Phusion® High Fidelity DNA Polymerase	0.25
Water	15.75

Table 2-18 Temperature profile for quick change PCR

Step	Profile	Repeats
1. Initial denaturation	98 °C for 30 s	x1
2. Denaturation	98 °C for 10 s	x5
3. Annealing (part I)	72 °C for 2 s	
4. Annealing (part II)	Ramp of 1 °C s^{-1} to 64 °C	
5. Annealing (part III)	64 °C for 10 s	
6. Elongation	72 °C for 2 min	
7. Denaturation	98 °C for 10 s	x20
8. Annealing & Elongation	72 °C for 2 min	
9. Final Elongation	72° C for 5 min	x1
10. Store	16 °C forever	

2.2.2.7 Agarose gel electrophoresis

Samples were filled into wells of an agarose gel that was inside of electrophoresis chamber filled with TAE buffer. The separation of DNA fragments was done by electrophoresis for 25 – 30 minutes with a constant voltage of 120 V. The result of separation was documented by UV radiation of the agarose gel.

2.2.2.8 DNA sequencing

DNA sequencing was performed by the Sanger sequencing service from Seqlab Sequence Laboratories GmbH (Göttingen, Germany) after providing purified plasmid DNA.

2.2.3 Biochemical methods

The following biochemical methods were used in this project.

2.2.3.1 Determination of protein concentrations by spectrophotometry

The concentration of purified proteins was determined by measuring the absorbance at λ = 280 nm with a spectrophotometer. With their respective molecular weight and molar absorption coefficient the concentration was calculated via the lambert beer law.

2.2.3.2 Determination of protein concentrations with Lowry protein assay

The protein concentration in aqueous glucan solutions was determined spectro-photometrical with the Lowry protein assay [57]. 100 µL of the sample was mixed with 1 mL of freshly prepared Lowry reagent E (100 vol. Lowry reagent A, 1 vol. Lowry reagent B and 1 vol. Lowry reagent C) and incubated for 5 minutes at room temperature in the dark. 100 µL

of fresh prepared 50 % (v/v) Folin & Ciocalteu's phenol reagent was added and the solution was instantly mixed. After an additional incubation for 30 minutes in the dark, the absorption of the mixture was measured with a photometer (λ = 660 nm). Water was used as blind and 50 mg L^{-1}, 100 mg L^{-1}, 150 mg L^{-1}, 200 mg L^{-1} and 250 mg L^{-1} solutions of bovine serum for calibration.

2.2.3.3 Determination of glucan concentrations by 2-propanol precipitation

The gravimetric determination of the glucans was carried out by precipitation with 2-propanol. 5 mL of aqueous glucan solution was mixed with 15 mL of cold 2-propanol and stored overnight at 4 °C. The solution with the precipitated glucan was transferred into a pre-weighed metallic centrifuge tube and centrifuged for 15 minutes with 13,000 xg at 4°C. The supernatant was discarded and the glucan pellet was dried for 48 hours at 50 °C in a vacuum oven. After cooling down to room temperature in a desiccator, the tube was weighed and the glucan concentration was calculated from the mass difference.

2.2.3.4 Determination of glucose concentration with dinitrosalicylic acid (DNS)

The glucose concentration in aqueous glucan solutions was determined spectro-photometrical with DNS. Therefore, 1 mL of glucan solution was mixed with 1 mL water and 2 mL of DNS reagent. The mixture was incubated in a water bath at 95°C for 15 minutes and instantly transferred to an ice bath. After 5 minutes of cooling down, the mixture was stored for 10 minutes at room temperature before its absorption was measured (λ = 660 nm). Water was used as blind and 0.1 g L^{-1}, 0.2 g L^{-1}, 0.3 g L^{-1}, 0.4 g L^{-1}, 0.6 g L^{-1}, 0.8 g L^{-1} and 1.0 g L^{-1} solutions of D-glucose for calibration.

2.2.3.5 Determination of Schizophyllan concentration via Glucatell® kit

The determination of Schizophyllan concentration was carried out with the β-(1,3)-D-glucan sensitive Glucatell® kit from Asocciates of Cape Cod, Inc. (Mörfelden-Walldorf, Germany). It is based on *Limulus* amebocyte lysate (LAL) from horseshoe crabs which reacts with β-(1,3)-D-glucans by activation of a clotting enzyme that cleaves a chromogenic peptide. The analysis was performed according to the end-point assay manual but with bisected volumes of used reagents

and samples. The absorption of the freed and diazotized chromogen was measured at 540 nm.

2.2.3.6 Sodium dodecyl sulfate polyacrylamide gel electrophoresis (SDS-PAGE)

Analysis of proteins for purity and correct molecular weight was performed by SDS-PAGE. Therefore, the discontinuous SDS-PAGE was applied as described by Laemmli [58] with a separation gel overlaid with a stacking gel. Samples were prepared by heating 20 µL for 5 minutes at 95 °C with 5 µL reducing 5x Laemmli buffer or 65 °C with 5 µL of non-reducing 5x Laemmli buffer. The samples were loaded into the wells of the stacking gel and the proteins were separated by electrophoresis in SDS-PAGE running buffer for 45 - 50 minutes with a constant voltage of 200 V. After the electrophoresis the gel was stained or used for immunoblot.

Table 2-19 Composition of the stacking gel

Stock solution	Volume per 4% gel
Water	1.0 mL
30 % (w/v) Acrylamide/Bis	260 µL
1 M Tris-HCl, pH 6.8	200 µL
10 % (w/v) SDS	15 µL
10 % Ammonium persulfate	15 µL
N,*N*,*N*',*N*'-Tetramethylethane-1,2-diamine	2 µL

Table 2-20 Composition of the separation gels

Stock solution	Volume per 12% gel	Volume per 15% gel
Water	1.3 mL	900 µL
30 % (w/v) Acrylamide/Bis	1.6 mL	2.0 mL
1.5 M Tris-HCl, pH 8.8	1.0 mL	1.0 mL
10 % (w/v) SDS	40 µL	40 µL
10 % Ammonium persulfate	40 µL	40 µL
N,*N*,*N*′,*N*′-Tetramethylethane -1,2-diamine	2 µL	2 µL

2.2.3.7 Coomassie staining of polyacrylamide gels

The polyacrylamide gel from the SDS-PAGE was submerged in Coomassie staining solution and heated in a microwave oven until the gel was completely stained. In the next step the gel was destained by heating and incubation in aqueous 10 % (v/v) acetic acid until the gel was destained and protein bands were clearly visible.

2.2.3.8 Immunoblot

Immunoblot was performed for the detection of specific proteins inside of a sample. Therefore, the proteins of a sample were separated by SDS-PAGE. A PVDF membrane was activated by submerging in ethanol and was rinsed with

blotting buffer. The membrane was placed onto a filter paper that was soaked with running buffer. Onto the membrane the gel was overlaid and this was covered with another soaked filter paper. The proteins in the gel were blotted onto the PVDF membrane with a blotting device (20 V, 35 minutes). The membrane was blocked with 10 mL MPBST for 1 hour at room temperature. The primary antibody 9E10 (1:500 in 10 mL MPBST) was added to the membrane. After 1 hour it was washed two times with 20 mL PBST and the secondary antibody 115-055-071 (AP conjugate, 1:30,000 in 10 mL MPBST) was added for another hour of incubation. It was washed again two times with 20 mL PBST. The developer solution (100 µL NBT and 100 µL BCIP in 10 mL AP substrate buffer) was added to the membrane. The blot was developed without rocking until clear bands from the protein of interest became visible. Afterwards the membrane was washed extensively with water and was dried with paper towels.

2.2.3.9 Immobilization of Schizophyllan at hydroxyl functionalized magnetic beads

The methodic approach was nearly the same as described by Sun *et al.* [59]. 0.5 mL of epoxy-coated magnetic beads (Dynabeads® M-270 Epoxy; 15 mg mL^{-1} in DMF) was washed

three times with 0.5 mL 100 %(v/v) ethanol. The surface was functionalized with hydroxy-groups attached by incubation in 0.5 mL 20 mM 4-Hydroxybenzhydrazide in anhydrous N,N-Dimethylformamide for 10 h under gentle shaking at 37 °C. The modified beads were washed three times with 0.5 mL 100 %(v/v) ethanol and were stored in 0.5 mL 100 %(v/v) ethanol at 4°C. For immobilization a respective amount of modified bead suspension was washed three times with 0.2 mM sodium acetate buffer (pH 5.4) and was incubated overnight in 0.2 mM sodium acetate buffer with glucan at 37 °C over night. Glucan which did not bind to the beads was removed by washing three times with 0.2 mM sodium acetate buffer. The glucan conjugated beads were stored in PBS containing 0.2 g L^{-1} NaN_3 until use. Prior to usage the glucan conjugated beads were washed three times with water.

2.2.3.10 Immobilization of Schizophyllan at hydrazide functionalized magnetic beads

The methodic approach was nearly the same as described by Park *et al.* [60]. 0.25 mL of amine-coated magnetic beads (Dynabeads® M-270 Amine; 30 mg mL^{-1} in N,N-Dimethylformamide) was washed three times with 0.5 mL N,N-Dimethylformamide (DMF) and resuspended in 3 % (w/v) succinic anhydride (in DMF). After 3 h incubation at room temperature

under gentle shaking, the beads were washed again three times with 0.5 mL N,N-dimethylformamide (DMF). The next steps involved: 3 h incubation in 0.5 mL 3 % (w/v) N-hydroxy-succinimide + 3 % (v/v) diisopropylcarbodiimide (in DMF) at room temperature; three times washing with 0.5 mL DMF; 3 h incubation in 0.5 mL 3 % (v/v) 4,7,10-trioxa-1,3-tridecan-diamin (in DMF) at RT; three times washing with 0.5 mL DMF; 3 h incubation in 0.5 mL 3 % (w/v) succinic anhydride (in DMF) at RT; three times washing with 0.5 mL DMF; 3 h incubation in 0.5 mL 3 % (w/v) N-hydroxysuccinimide + 3 % (v/v) diisopropylcarbodiimide (in DMF) at room temperature; 3 times washing with DMF; and 3 h incubation in 0.5 mL 3 % (v/v) hydrazine monohydrate at room temperature. After additional washing with 0.5 mL DMF, the beads were stored in 0.5 mL DMF at 4 °C. For immobilization a respective amount of modified bead suspension was washed three times with PBS (pH adjusted to 5.0) and was incubated overnight in PBS (pH 5.0) with glucan and 30 % (v/v) glycerol at 50 °C. Glucan which did not bind to the beads was removed by washing three times PBS (pH 7.4). The glucan conjugated beads were stored in PBS containing 0.2 g L^{-1} NaN_3 until use. Prior to usage the glucan conjugated beads were washed three times with water.

2.2.3.11 Coating of Carbo-BIND™ 96-Well plates

For the antibody selection and ELISA experiments, Schizophyllan was immobilized to Carbo-BIND™ multiwell plates. The wells were filled with 100 µL of 10 µg mL^{-1} SCH-PK in 10 mM acetate buffer (pH 5.4) and the sealed plates were incubated at 37 °C overnight. The following day the wells were washed 10 times with water and filled for storage with 300 µL PBS containing 0.2 g L^{-1} NaN_3 until use.

2.2.3.12 Enzyme-linked immunosorbent assay (ELISA)

Analytics of the recombinant antibodies for their binding properties were generally performed by ELISA experiments.

Titration ELISA

The half maximal effective concentration (EC50) values of the produced rAbs was determined by titration ELISA using serial dilutions of the antibodies. The SCH-PK loaded Carbo-BIND™ plate was blocked with MPBST for 1 hour at room temperature. The blocking solution was discarded and 100 µL of the rAbs (dilution series in blocking solution) were filled into the wells. After 1 hour incubation, the plate was washed for 3 times with PBST or 0.05% (w/v) Tween20. Afterwards, 100 µL $well^{-1}$ peroxidase-conjugated goat anti-murine Fc antibody (1:40,000 in MPBST) was added and

incubated for an additional hour. The plate was then washed again for 3 times. The color reaction was obtained by adding 100 µL well^{-1} freshly mixed TMB (20 volume TMB A and 1 volume TMB B). The reaction was stopped after 10-15 min by addition of 100 µL well^{-1} of 0.5 mol L^{-1} H_2SO_4. The resulting absorption was measured at 450 nm (reference wavelength 620 nm).

For antibodies in the Fab format, an additional incubation step with 100 µL well^{-1} of an anti-His-tag murine antibody (40 ng mL^{-1}) was necessary before the peroxidase conjugated antibody was added.

The EC50 was derived from a regression of absorbance signal against the logarithm of antibody concentration by a sigmoidal function with 3 parameters.

Competitive ELISA

Antigen specificity was evaluated via competition of scFv-Fc binding to immobilized SCH-PK by various soluble saccharides. Each scFv-Fc was used in the concentration that resulted in 40 % of the saturation signal in the titration ELISA. They were preincubated with serial dilutions of competitors solved in MPBST for 1 h before transfer to the SCH-PK loaded Carbo-BIND™ plate. The further procedure and the analytics of the results were executed as described for titration ELISA.

2.2.4 Microbiological methods

The following microbiological methods were used frequently in this project.

2.2.4.1 Cultivation of Escherichia coli (E. coli) on plates

E. coli suspension from transformation or phage infection was plated with a spatula onto 2xYT-GA agar in a petri dish. The plate was incubated overnight at 37 °C.

2.2.4.2 Cultivation of E. coli in liquid cultures

Cultivation of *E. coli* for phage infection or plasmid amplification was performed in suspension culture. Therefore, the required volume of 2xYT medium with the respective supplements was inoculated with *E. coli* cells from a cryo conserved culture, with a colony from a plate or with cell suspension of a pre-culture. The suspension was incubated in a shake incubator at 37 °C and 250 rpm overnight or until the desired cell density was reached. The cell density of the culture was measured as optical density (OD) in a photometer with λ = 600 nm.

2.2.4.3 Cryo conservation of E. coli

Long time storage of *E. coli* cells was performed by supplementing liquid culture with 30 % (w/v) glycerol and keeping the culture at -80 °C.

2.2.4.4 Preparing chemically competent E. coli cells

Chemically competent *E. coli* cells for heat shock transformation were prepared from a liquid culture of *E. coli* XL1-blue MRF' in the exponential growth phase (OD_{600} = 0.5). 100 mL culture was centrifuged for 10 minutes with 3,220 xg at 4 °C. The cell pellet was suspended in 15 mL cold TFB1 an incubated for 90 minutes on ice. Afterwards it was centrifuged a second time, the cells were suspended in 4 mL cold TFB2 and stored at -80 °C as 50 µL aliquots.

2.2.4.5 Heat shock transformation of E. coli with Plasmid-DNA

Transport of plasmid DNA into *E. coli* cells was performed by heat shock transformation. Therefore, an aliquot of chemically competent *E. coli* cells was thawed carefully on ice. 20 µL of the cells were mixed with 1 µL of purified plasmid DNA or with 10 µL reaction mix from ligation. After 20 minutes storage on ice the cells were incubated at 42 °C for 45 seconds and afterwards for 2 minutes on ice. 100 µL of pre-warmed SOC medium was added to the cells. The transformed cells were plated directly on an 2xYT-GA agar plate.

2.2.4.6 Titration of phage particles

The concentration of a phage preparation was determined by infection of *E. coli* with different phage dilutions. A culture of *E. coli* XL1-blue MRF' was prepared and cultivated until an OD_{600} of 0.5 was reached. 10 µL of diluted phage particles in PBS were added to 50 µL of the *E. coli* culture and incubated for 30 minutes at 37 °C. The culture was plated onto a 2xYT-GA agar plate. The plates were incubated overnight at 37 °C and the particle concentration was calculated from the number of grown colonies.

2.2.5 Cell culture methods

The following cell culture methods were used in this project.

2.2.5.1 Cultivation of human embryonic kidney cells (HEK-cells)

HEK-cells were cultivated and used for the production of rAbs. Therefore, an aliquot of cryo conserved cells was carefully thawed in 12 mL of culture medium. The suspension was centrifuged with 500 xg for 5 minutes and the cell pellet was suspended in 13 mL of fresh culture medium. The cell suspension was cultivated in an Erlenmeyer flask at 37 °C, with 110 rpm and 5 % CO_2 content in the air. The cell concentration and vitality of the culture was observed by mixing a sample with trypan blue solution and counting of cells in a

Neubauer chamber. After 2-3 days the cells were passaged by inoculation of fresh culture media with cultured cells to a concentration of 0.2 x10^5 cells mL^{-1}. The HEK cell culture was maintained for approx. 25 passages and discarded afterwards.

2.2.5.2 Transfection of HEK-cells for protein production

HEK cells were transiently transfected with polyethylenimine (PEI) as transfection reagent. The transfection was prepared by suspending of 25 µg of expression vector in 1.25 mL transfection media and mixing it with 62.5 µL 0.1 % (w/v) PEI in 1.25 mL transfection media. For production of antibodies in the Fab format, a mixture of 12.5 µg of heavy chain expression vector and 12.5 µg of light chain expression vector was used. After incubation for 20 minutes at room temperature, the mixture was added to 25 mL culture which has been grown to a cell concentration of 1.5*10^6 cells mL^{-1}. The culture was cultivated in an Erlenmeyer flask at 37 °C, with 110 rpm and 5 % CO_2 content in the air and was fed after 48 hours with 25 mL of feed media. The production was stopped 96 hours after feeding and the culture was centrifuged for 10 minutes with 1,000 xg at 4 °C. The supernatant with the produced antibodies was directly used for purification or stored at -20 °C.

Transfection for small scale productions was performed by mixing 5 µg expression vector DNA in 250 µL transfection media with 25 µg PEI in 250 µL transfection media and transferring to 5 mL culture after incubation. Cultivation was performed as described for normal production and 5 mL of feed medium was used for feeding.

2.2.6 Purification methods

The following purification methods for glucans and antibodies were used in this project.

2.2.6.1 Purification of glucans

The glucans were derived as cell free production supernatant stabilized with formic acid and were purified as described.

Diafiltration

The glucans were diafiltrated to remove contaminants of the production media and the formic acid. The production supernatants were diluted to 1.0 g L^{-1} glucan in 100 mL with water and were adjusted to pH 7.5 with NaOH. In the next step the supernatants were diluted further to 1 L with water and were reduced to 200 mL with a cross flow filtration cassette (100,000 Da cut off). The supernatants were refilled to 1 L with water and again reduced to 200 mL. This procedure

was repeated until the conductance of the retentate dropped to 0 µS cm^{-1}. The glucan solution was thereafter reduced to 100 mL and sterilized.

Proteinase K treatment

SCH and Scleroglucan (*S. rolfsii*) were additionally treated with proteinase K. The production supernatant was diluted to 1.0 g L^{-1} glucan in 100 mL with water and was adjusted to pH 7.5 with NaOH. 2 mL Proteinase K buffer and 1 mL of 10 % (w/v) sodium dodecyl sulfate were added and the solution was incubated at 80 °C for 4 hours. After cooling down to 40 °C, 10 mg of Proteinase K was solved in the solution and incubated for 24 h at 40°C under slight shaking. The proteinase K treatment was stopped by incubation at 80 °C for 4 hours. The solution was diluted to 1 L with water, cleared by centrifugation with 13,000 xg for 1 h at 16 °C and was diafiltrated as described above.

2.2.6.2 Purification of recombinant antibodies

The produced antibodies were purified with the following methods.

Affinity purification via Fc domain recognition by protein A

Recombinant antibodies produced in the scFv-Fc format were purified by affinity purification with protein A.

Therefore, an automated protein purification system or a manually operated purification system was used.

The automated system was used for supernatants from the normal production in HEK cells. 5 mL of 5x protein A binding buffer was added to 45 mL of cell free production supernatant. This was filtrated and degassed by vacuum filtration with a 0.45 µm filter. In the Profinia™ system the supernatant was loaded onto a 1 mL protein A column with a flow rate of 1 ml min^{-1}. After washing with 30 mL of protein A binding buffer, the antibodies were eluted with 4 mL protein A elution buffer. The eluate was instantly transferred to a 10 mL desalting column in which the protein A elution buffer was exchanged against PBS.

The manually operated system was used for supernatants from small scale productions. 9.5 ml of cell free supernatant was filled into one well of a 24 deep well vacuum filtration plate with 500 µL of protein A purification matrix. After 5 minutes incubation the supernatant was removed. The loaded protein A matrix was washed once with 5 mL PBS and additional two times with 2.5 mL PBS. 500 µL of protein A elution buffer was added to the matrix and this was incubated for 5 minutes. The buffer with the eluted rAbs was directly transferred to 220 µL of 1 M Tris. The protein A matrix was washed two times with 750 µL elution buffer, which was

removed and added to the eluate. Afterwards the buffer of the eluate was exchanged against PBS by centrifugation with 1,000 xg for 2 minutes through desalt spin columns.
The purified antibodies were stored at -80 °C

Affinity purification via His-tag by complexation with nickel ions

The produced antibodies in the Fab format were purified via their His-tag by nickel complexation. Therefore 2 mL chelating sepharose was loaded with nickel ions by incubation with 2 mL of 0.1 M $NiSO_4$ for 5 minutes. After removal of the residual $NiSO_4$ solution by centrifugation for 5 minutes with 500 xg, the Ni-sepharose was washed two times with 20 ml water. The cell free production supernatant was supplemented with 0.5 M NaCl and was incubated with the Ni-sepharose for 45 minutes with smooth rocking at room temperature. The mixture was transferred to an empty chromatography column and the supernatant was removed by gravitation. The loaded Ni-sepharose was washed with 25 mL His-tag binding buffer. Elution of the protein was performed in two steps by incubation of the loaded Ni-sepharose with á 1 mL His-tag elution buffer for 5 minutes. The eluate was used directly or after storage overnight at 4 °C for size exclusion chromatography

Preparative size exclusion chromatography

Since the antibody for the x-ray crystallography had to be free of agglomerates and to be solved in gel filtration buffer, size exclusion chromatography was performed. Therefore, an automated chromatography system with fraction collector was used. The eluate from the His-tag affinity purification was loaded onto a Superdex™ 75 HiLoad™ 16/60 column with 0.75 mL min^{-1}, gel filtration buffer was used as running solution. After 30 mL, the flow through was collected in fractions of 1 mL.

The fractions with the agglomerate free Fab were pooled and concentrated with a dialyze spin column (30 kD cut off) to a concentration of 10 mg mL^{-1}. The protein solution was kept on ice and was used directly for the crystallography experiments.

2.2.7 Construction of an antibody phage library

The construction of the antibody phage library from immunized mice was performed as described by L. Toleikis and A. Frenzel. [61] Two sub-libraries for antibodies with V_L-kappa and V_L-lambda domain were derived from each mouse.

2.2.7.1 Immunization of mice

Three mice were immunized with SCH-PK by intraperitoneal injection. Three injections were applied in two-week intervals. Each injection consisted of 25 µg of SCH-PK and 50 µL of the adjuvant Magic™-Mouse (Creative Biomart, New York, USA). Four weeks after the third injection, three additional injections with 50 µg of SCH-PK and 100 µL of PBS were applied over a period of three days to boost the B cell proliferation. Two days later, the mice were sacrificed. Their spleens were isolated and homogenized in TRIzol® LS Reagent.

Ethics statement

The experimental protocols were carried out in accordance with the Directive 2010/63/EU of the European Parliament and the Council of the European Union of 22 September 2010 and all procedures were approved by guidelines from the Animal Committee on Ethics in the Care and Use of Laboratory Animals of TU Braunschweig, Germany (Az §5 (02.05) TschB TU BS Az:33.42502-14-005/08).

2.2.7.2 RNA isolation and cDNA synthesis

From the spleen homogenate of each mouse a volume equal to 1 x10^7 of homogenized leucocytes was used to isolate the total RNA with the Directzol™ MiniPrep kit. The RNA was

solubilized in water and directly used for cDNA synthesis with SuperScript™ IV cDNA synthesis kit. The cDNA synthesis was performed with the enclosed random hexamer primer according the kits instructions.

2.2.7.3 Cloning of V_L and V_H into pHAL30

The cDNA preparation was used for the isolation of the V_H and V_L domain sequences. Therefore, PCR experiments with primer sets that are designed to frame V_H, V_L-kappa and V_L-lambda sequences were performed.

Table 2-21 Primer sets for V_H, V_L-kappa and V_L-lambda sequence isolation

Primer set	Forward primer	Reverse primers
V_H	MHC.F	MHV.B1, MHV.B2, MHV.B3, MHV.B4, MHV.B5, MHV.B6, MHV.B7, MHV.B8, MHV.B9, MHV.B10, MHV.B12
V_L-kappa	MKC.F	MKV.B1, MKV.B2, MKV.B3, MKV.B4, MKV.B5, MKV.B6, MKV.B7, MKV.B8, MKV.B9, MKV.B10
V_L-lambda	MLC.F	MLV.B

Table 2-22 PCR mix for V_H, V_L-kappa and V_L-lambda sequence isolation

Stock solution	Volumes [µL] per 50 µL reaction mix
cDNA	1.44
5x Green GoTag® Reaction Buffer	10.0
25 mM $MgCl_2$	3.0
10 mM dNTP mix	1.0
10 mM forward primer	2.0
10 mM reverse primer	2.0
5 U μL^{-1} GoTag® DNA Polymerase	0.25
water	30.31

Table 2-23 Temperature profile for V_H, V_L-kappa and V_L-lambda sequence isolation

Step	Profile	Repeats
1. Initial denaturation	95 °C for 2 minutes	x1
2. Denaturation	95 °C for 45 seconds	x30
3. Annealing	56 °C for 45 seconds	
4. Elongation	72 °C for 1.5 minutes	
5. Final Elongation	72° C for 5 minutes	x1
6. Store	16 °C forever	

The desired PCR products had a size of around 380 bp. They were isolated by agarose gel electrophoresis followed by a

gel extraction. The products for isolation of V_H and V_L-kappa were each pooled.

The isolated sequences were equipped with endonuclease cleavage sites for cloning by additional PCR experiments. The respective primers were used for each product of the previous PCR experiments.

Table 2-24 Primer sets for addition of endonuclease sites to V_H, V_L-kappa and V_L-lambda sequences

Primer set	Forward primer	Reverse primers
V_{H-}Nco/Hind	MHC.F.Hind	MHV.B1.Nco, MHV.B2.Nco, MHV.B3.Nco, MHV.B4.Nco, MHV.B5.Nco, MHV.B6.Nco, MHV.B7.Nco, MHV.B8.Nco, MHV.B9.Nco, MHV.B10.Nco, MHV.B12.Nco
V_L-kappa-Mlu/Not	MKC.F.Not	MKV.B1.Mlu, MKV.B2.Mlu, MKV.B3.Mlu, MKV.B4.Mlu, MKV.B5.Mlu, MKV.B6.Mlu, MKV.B7.Mlu, MKV.B8.Mlu, MKV.B9.Mlu, MKV.B10.Mlu
V_L-lambda-Mlu/Not	MLC.F.Not	MLV.B.Mlu

Table 2-25 PCR mix for addition of endonuclease sites to V_H, V_L-kappa and V_L-lambda sequences

Stock solution	Volumes [µL] per 100 µL reaction mix
90 ng $µL^{-1}$ PCR product	1.0
5x Green GoTag® Reaction Buffer	10.0
25 mM $MgCl_2$	6.0
10 mM dNTP mix	2.0
10 mM forward primer	2.0
10 mM reverse primer	2.0
5 U $µL^{-1}$ GoTag® DNA Polymerase	0.5
water	76.5

Table 2-26 Temperature profile for addition of endonuclease sites to VH, VL-kappa and VL-lambda sequences

Step	Profile	Repeats
1. Initial denaturation	95 °C for 2 minutes	x1
2. Denaturation	95 °C for 45 seconds	x20
3. Annealing	56 °C for 45 seconds	
4. Elongation	72 °C for 1.5 minutes	
5. Final Elongation	72° C for 5 minutes	x1
6. Store	16 °C forever	

The expected size of the product was 400 bp and was isolated by agarose gel electrophoresis. After gel extraction, the products of V_H and V_L-kappa were pooled each.

The V_H and V_L sequences were subsequently cloned into the vector pHAL30. First the V_L-kappa and V_L-lambda sequences were cloned into the vector separately. Therefore, each V_L preparation and the vector pHAL30 were treated with the endonucleases NotI and MluI. The linearized vector was additionally dephosphorylated with CIP. After heat inactivation of the endonucleases, the inserts and the vector were purified with a PCR clean up kit and used for ligation. 300 ng of each insert preparation was ligated with 1 µg of linearized vector pHAL30. The ligated products were purified with centrifugal dialyzes tubes (30 kDa cut off) by centrifugation for 20 minutes with 14,000 xg and refilling with water for three times. Afterwards the ligation mixtures were concentrated to 60 µL. 20 µL of one ligation were mixed with 12.5 µL of freshly thawed electro competent *E. coli* cells (E. cloni® 10G Supreme) and 12.5 µL cold water, incubated on ice for 1 minute and transferred into a cold electroporation cuvette. The DNA was transformed into the cells with an electrical pulse of 1.7 kV and 1 mL of warm recovery medium was added. The cell suspensions were incubated for 1 hour at 37 °C in a thermomixer with 600 rpm before they were

plated onto a 2xYT-GA agar plate. After overnight incubation at 37 °C, single colonies of each transformation were checked for correct insert size by colony PCR. The cells from each plate were suspended in 25 mL 2xYT medium and the plasmid DNA was prepared from those.

With a second cloning step the V_H sequences were added to the vectors containing the V_L sequences. 7.5 µg of the V_H preparation, 10 µg of pHAL30 with V_L-kappa and of pHAL30 with V_L-lambda were treated with the endonuclease NcoI. The preparations were purified with a PCR clean up kit and were additionally treated with the second endonuclease HindIII. The linearized vector preparations were dephosphorylated with CIP. After purification, 1 µg of each vector preparation was ligated with 300 ng of the V_H preparation. The ligations were purified with a centrifugal dialyzes tube as described in the first cloning step. 20 µL of one ligation were mixed with 25 µL of freshly thawed electro competent *E. coli* cells (ER2738), incubated for 1 minute on ice and transformed into the cells with a 1.7 kV pulse. The cell suspension was incubated for 1 hour at 37 °C with 600 rpm, plated onto a 2xYT-GA agar plate and incubated overnight at 37 °C. Single colonies of each transformation were checked for correct insert size by colony PCR. The cells from each

plate were suspended in 25 mL 2xYT medium and cryo conserved in 1 mL aliquots.

2.2.7.4 Packing of library into scFv phage particles

The generated sub-libraries were packed into scFv phage particles for the antibody selection. Therefore, one aliquot of a sub-library was thawed and used to inoculate 200 mL 2xYT-GA media. Starting with an OD_{600} of 0.07, the culture was incubated at 37 °C with 250 rpm until the OD_{600} reached 0.5. 20 mL of the culture were infected with 2.5 $x10^{11}$ cfu of hyperphage. After 30 minutes incubation at 37 °C without shaking and 30 minutes incubation at 37°C with 250 rpm, the culture was centrifuged for 10 minutes with 3,220 xg and the cell pellet was resuspended in 400 mL of 2xYT-KA media. The scFv phage particles were produced during overnight incubation of the culture at 30 °C with 250 rpm. For purification of the scFv-phage, the culture was centrifuged for 30 minutes with 10,000 xg at 4 °C. 100 mL of phage precipitation solution was added to 350 mL of the supernatant and stored overnight at 4°C. The precipitated phage particles were isolated by centrifugation (1 h, 10,000 xg, 4 °C) and resuspended in 20 mL of phage dilution buffer. This solution was filtered with a 0.45 µm sterile filter and mixed with 5 mL of phage precipitation solution for a second overnight

precipitation at 4 °C. The precipitate was resuspended in 2 mL of phage dilution buffer after centrifugation (30 min, 20,000 xg, 4°C). The phage particle titer was determined and the scFv phage were stored at 4 °C.

2.2.8 Selection of glucan binding antibodies (Panning)

Recombinant antibodies against SCH were selected by amplification of scFv phage particle that were isolated through binding to immobilized SCH. As source for the antibodies the naive human antibody library with the sub-libraries HAL9 and HAL10 (kindly provided from Prof. Dr. Stefan Dübel & Prof. Dr. Michael Hust, Department of Biotechnology, Technische Universität Braunschweig, Braunschweig, Germany), as well as generated immune library with its pooled sub-libraries for V_L-kappa and V_L-lambda were used.

Each round of selection 8 SCH-PK loaded wells and 8 blank wells of a Carbo-BIND™ plate were blocked with 300 µL MPBST for 1 hour. 3 $x10^{10}$ cfu of each sub-library was suspended in 200 µL MPBST and added to two of the blank wells (100 µL per well). After 1 hour at room temperature, the supernatants were transferred to the SCH-PK loaded wells and were incubated for an additional hour. In the first round of selection the SCH-PK loaded wells with the bound phage particles were washed 10 times with 300 µL PBST. The bound

scFv phage particles were eluted by incubation with 200 µL 10 mg mL^{-1} trypsin (in PBS) for 30 min at 37 °C. The eluted phage of one sub-library were used to infect 10 mL culture of *E. coli* XL1 Blue MRF' in 2xYT-T media which was grown to an OD_{600} of 0.5. After 30 minutes incubation at 37 °C and 30 minutes incubation at 37 °C with 250 rpm, the cells were separated (2500 xg, 10 minutes, 25°C) and plated on a 2xYT-GA agar plate. The plates were incubated overnight at 37 °C. The grown colonies were suspended in 5 mL 2xYT media and used to inoculate 20 mL 2xYT-GA media with an OD_{600} = 0.01. For the production of new scFv phage particles 5 mL of this culture was infected with M13K07 helper phage after it reached an OD_{600} = 0.5. During infection the culture was incubated 30 minutes at 37 °C followed by 30 minutes at 37 °C with 250 rpm. The infected cells were separated by centrifugation (2,500 xg, 10 minutes, 25 °C), suspended in 5 mL 2xYT-AK media and cultivated overnight at 30 °C with 500 rpm in a 24 deep well plate. The culture was centrifuged with 3,220 xg for 20 min at 4 °C and 100 µL of the supernatant with the produced antibody phage particles was used for an additional round of selection. Three rounds of selection were done. In the second round 20 washing steps and in the third round 30 washing steps were carried out after incubation of the antibody phage in the SCH-PK loaded wells.

10 µL of the eluted phage in the third round were used to prepare different dilutions in PBS, 50 µL of *E. coli* XL1 Blue MRF' cells (OD_{600} of 0.5) were infected with 10 µL of diluted phage and plated on 2xYT-GA agar plates. The plates were incubated at 37°C and 92 grown colonies were transferred to 130 µL 2xYT-GA each in a polypropylene multiwell plate (u-shape bottom) and cultivated for 6 hours at 37 °C with 800 rpm. 60 µL 80 % (v/v) sterile glycerol was added to the cultures and the plate was stored as master plate at -80 °C.
An antigen ELISA with soluble scFv was performed to identify the SCH binding antibodies. For production of soluble scFv, a micro well plate was filled with 150 µL 2x YT-GA and inoculated with 1 µL form the 92 isolated *E. coli* clones stored in the master plate. 2 of the 4 residual wells were inoculated with an *E. coli* clone which contains the information for an anti-lysozyme scFv as positive control and the other 2 wells were used as negative control (no inoculation). After 2 hours incubation at 37 °C and 800 rpm, the plate was centrifuged (2,000 xg, 10 minutes, 30 °C). The media was exchanged for 2xYT-AI and the plate was incubated at 30°C and 800 rpm overnight. A Carbo-BIND™ plate was loaded with SCZ-PK besides 2 wells which were coated with lysozyme (100 µL $well^{-1}$, 0.5 µg mL^{-1} lysozyme in PBS). As additional control for unspecific antibodies a second Carbo-BIND™ plate was coated

with BSA (100 µL well^{-1}, 0.5 µg mL^{-1} BSA in PBS). The loaded plates were blocked with MPBST (300 µL well^{-1}) and washed three times with PBST (300 µL per well). 50 µL of MPBST were added to the wells of the scFv production plate, which was thereafter centrifuged with the 3220 xg for 20 min at 4 °C. 100 µL of the supernatants were transferred to the Carbo-BIND™ plate and to the control plate. The plates were incubated for 1 hour at room temperature and washed 3 times with PBST, filled with 100 µL well^{-1} of monoclonal anti-c-myc tag mouse antibody 9E10 (1:50 in MPBST) and incubated for 1 hour again. The plates were washed 3 times with PBST and incubated for 1 h with the 100 µL well^{-1} peroxidase-conjugated goat anti-murine Fc antibody A0168 (1:10,000 MPBST). For the visualization of the ELISA the washed wells of the plates were filled with 100 µL freshly mixed TMB (20 vol. TMB A and 1 volume TMB B). The color reaction was stopped after 10-15 minutes development by adding 100 µL 0.5 M H_2SO_4. The absorbance was measured at 450 nm (reference wavelength: 620 nm). The *E. coli* clones which hold a positive tested rAb were used for inoculation of overnight cultures (2xYT-GA, 37 °C, 250 rpm). Plasmid preparations were derived from each culture and were sequenced.

3 Results

3.1 Construction of an immune library

The antibody generation was planned to be performed by selection from phage displayed libraries of recombinant antibodies. Therefore, an immune library was constructed from three mice which had been immunized with SCH-PK. The immunization experiments were kindly performed by Sabine Buchmeier (Institute for Physical and Theoretical Chemistry, Technische Universität Braunschweig, Braunschweig, Germany). For immunization three injections of SCH-PK were applied in two-week intervals. Four weeks after the third injection, three additional injections were applied over a period of three days to boost the B cell proliferation. Two days later, the mice were sacrificed and total RNA was derived from their spleens. After reverse transcription to cDNA, the sequences of V_H and V_L domains were isolated by PCR with sets of respective primers. Subsequently, the V_H and V_L sequences were cloned into the library vector pHAL30. The sub-libraries (mouse 1 lambda, mouse 1 kappa, mouse 2 lambda, etc.) were packed into antibody phage particles with the helper phage hyperphage or M13K07. The analysis for the number of vectors with successful insertion

of V_H and V_L showed insert rates of 69 % in the sub libraries mouse 1 lambda and mouse 1 kappa, 63 % in mouse 2 kappa, mouse 3 lambda and mouse 3 kappa and 31 % in mouse 2 lambda (Table 3-1). The titers of the hyperphage packed sub-libraries ranged from 0.9×10^{12} cfu mL^{-1} to 1.7×10^{12} cfu mL^{-1} and for the M13K07 packed sub-libraries from 0.8×10^{13} cfu mL^{-1} to 2.5×10^{13} cfu mL^{-1}. Presentation of scFv-p3 fusions in the packed sub-library preparations were checked via immunoblot by using the antibody 9E10 which is directed against the myc-tag in the peptide linker between scFv and p3. The blot showed stained bands at an apparent

Table 3-1 Generated immune library with insertion rates and titers of the antibody phage packed sub-libraries

Mouse	Light chain class	Insertion rate	Titer hyper-phage packed sub-library	Titer M13K07 packed sub-library
1	lambda	69 %	0.9×10^{12} cfu mL^{-1}	1.1×10^{13} cfu mL^{-1}
	kappa	69 %	1.4×10^{12} cfu mL^{-1}	2.3×10^{13} cfu mL^{-1}
2	lambda	31 %	1.7×10^{12} cfu mL^{-1}	1.2×10^{13} cfu mL^{-1}
	kappa	63 %	1.0×10^{12} cfu mL^{-1}	2.5×10^{13} cfu mL^{-1}
6				
3	lambda	63 %	1.7×10^{12} cfu mL^{-1}	1.4×10^{13} cfu mL^{-1}
	kappa	63 %	1.0×10^{12} cfu mL^{-1}	0.8×10^{13} cfu mL^{-1}

molecular weight of ~70 kDa. This band was observed also in the positive control (naive library HAL10) and correlates with the sum of the molecular weights of scFv (≈25-30 kDa) and p3 (43.2 kDa). The hyperphage packed sub-libraries as well as the M13K07 packed sub-libraries were each pooled for lambda-V_L and kappa-V_L.

3.2 Establishment of an immobilization method for Schizophyllan

Before selection of recombinant antibodies from the antibody libraries, an immobilization method for SCH had to be established. Freund showed that immobilization of β-D-glucan via adsorption onto common multiwell plate materials is not stable which leads to a loss of antigen during selection and consequently to a loss of potential SCH binding antibodies [62]. Therefore, three methods for immobilization of polysaccharides via covalent binding were compared. The first method was immobilization onto magnetic beads which were functionalized with hydroxyl-groups, the second method was immobilization onto magnetic beads which were functionalized with hydrazide-groups, and the third method was immobilization onto Carbo-BIND™ multiwell plates (Corning, New York, USA) which were functionalized

with hydrazide-groups [59, 60]. Analyses was performed qualitatively with the ß-D-Glucan sensitive Glucatell® kit. 22.5 ng SCH-PK were used to coat 31.5 µg Beads and one cavity of a Carbo-BIND plate (50 µL well^{-1}). After 10 times washing with 100 µL glucan-free water (component of the kit), 25 µL glucan-free water was added to each. All methods showed a positive result for SCH immobilization (Figure 3-1).

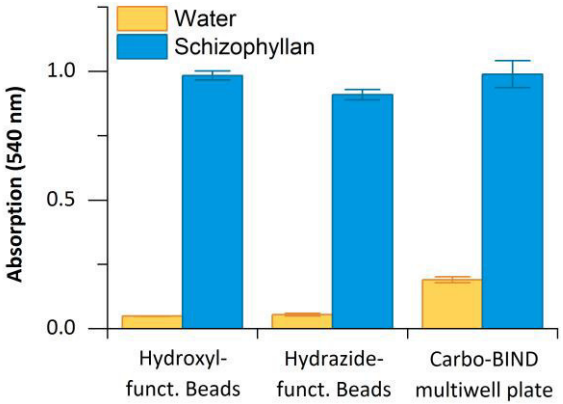

Figure 3-1 Analysis of immobilization methods for SCH via Glucatell® kit. Here, the result of SCH immobilization onto hydroxyl-functionalized magnetic beads, hydrazide-functionalized magnetic beads and a Carbo-BIND multiwell plate is shown. After coating and removal of unbound glucan the carrier matrices were checked for bound SCH with Glucatell® kit (blue) and compared with matrices which were analogous treated with water (yellow). Analysis was performed in duplets.

Due to minor experimental effort the SCH binding onto Carbo-BIND multiwell plates was chosen as immobilization method for antibody selection.

3.3 Generation of anti-Schizophyllan antibodies

Anti-Schizophyllan antibodies were selected from the phage displayed libraries by panning for binding of immobilized SCH-PK. Three rounds of panning were performed with each of the pooled libraries and additionally with the human based naive antibody libraries HAL9 and HAL10 (kindly provided from Prof. Dr. Stefan Dübel & Prof. Dr. Michael Hust, Department of Biotechnology, Technische UniversitätBraunschweig, Braunschweig, Germany). Single clones were isolated and tested for unspecific binding to BSA by antigen ELISA (Figure 3-2). Overall 205 of 644 isolated clones where tested positive for SCH-PK binding and for sufficient specificity (signal ratio BSA:SCH-PK < 5 %). No positive clone was isolated from the panning with the naive library HAL10.

Randomly, 35 of the clones which showed reproducible specificity and production as soluble scFv were chosen for sequence analysis. The sequences were compared with the respective germline sequences via the online sequence analysis tools IMGT/V-QUEST from the International ImMunoGeneTics information system® (IMGT®, http://www.imgt.org)

and VBASE2 (http://www.vbase2.org) [63–65]. Analysis of the sequences identified 15 individual rAbs, 4 rAbs of the mouse immune library and 11 rAbs of the human naive library.

All 4 rAbs of the immune library contain V_H domains of the subfamily VH1 and V_L-domains of the kappa sub family VK4. Noticeable, three rAbs were selected from the lambda V_L pool despite having V_L domains of the kappa type which could be explained by cross contamination of the pools. The 11 rAbs from the naive library contain mainly V_H domains of gene subfamily VH1 except for JoJ58C5 which has a V_H domain of gene subfamily VH5. Their V_L domains are all of the lambda type and show different gene subfamilies: VL1 (mainly), VL2 (JoJ58B9), VL3 (JoJ58B10 & JoJ61G1) and VL6 (JoJ58C10). A detailed overview of the gene combinations for the V_H (V, D and J genes) and for the V_L domain (V and J genes) of each rAb is listed in Table 3-2.

For further analysis, the 15 rAbs were converted into the scFv-Fc format consisting of the scFv fused to a murine IgG2c Fc part. The scFv-Fc format is a bivalent antibody comparable to a full-length IgG. Therefore, the scFv sequence of each rAb was cloned into the expression vector pCSE2.6-mIgG2c-Fc-XP and transiently transfected into HEK293-6E cells.

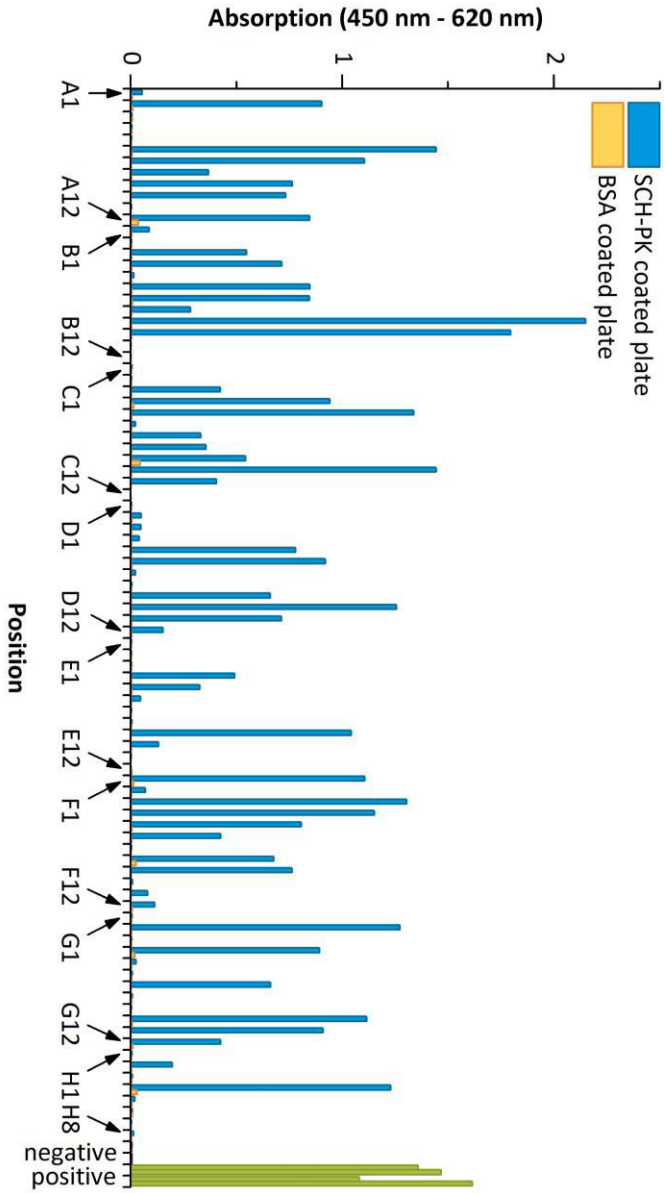
Absorption (450 nm - 620 nm)
0
1
2
SCH-PK coated plate
BSA coated plate
Position
A1
A12
B1
B12
C1
C12
D1
D12
E1
E12
F1
F12
G1
G12
H1
H8
negative
positive

Figure 3-2 Antigen ELISA for identification of SCH specific antibodies. This example shows the result for isolated clones in master plate JoJ48. The production supernatants of the selected clones were transferred into Carbo-BIND™ plates which were coated with SCH-PK (blue) and BSA (yellow). As positive control supernatant containing scFv of the antibody D1.3 (anti–Lysozyme) were used for the cavities H11 and H12 (coated with lysozyme, green) of each plate. ScFv-free culture media was used as negative control in the cavities H9 and H10 (violet).

5 days after transfection, the secreted scFv-Fc were purified from the cultivation supernatant by protein A affinity chromatography and transferred into PBS. The purity of the scFv-Fc was analyzed by SDS-PAGE and coomassie staining. A scFv-Fc consists of a homodimer with a molecular weight of approx. 110 kDa and is stabilized by disulfide bonds under reducing conditions it dissociates into two monomers of approx. 55 kDa. In the SDS-PAGE each of the produced scFv-Fc showed bands for the expected molecular weight of about 55 kDa.

3.4 Binding specificity of the generated antibodies

The first analyzed characteristic was the binding strength of each rAb in form of the half maximal effective concentration (EC50). Therefore, serial dilutions (approx. 0.95 pM - approx. 950 nM) of the rAb were applied on SCH-PK loaded and blank Carbo-BIND™ multiwell plates and were analyzed by

Table 3-2 Comparison of the antibody sequences with the respective germline sequences

rAb	Source	VH sequence			VL sequence	
		V gene	D gene	J gene	V gene	J gene
JoJ48C11	Mouse	IGHV1-7*01	IGHD1-1*02	IGHJ2*01	IGKV4-59*01	IGKJ5*01
JoJ48D6	Mouse	IGHV1S135*01	no result	IGHJ4*01	IGKV4-74*01	IGKJ1*01
JoJ48F1	Mouse	IGHV1-7*01	IGHD1-1*02	IGHJ2*01	IGKV4-59*01	IGKJ2*07
JoJ48D10	Mouse	IGHV1-7*01	IGHD1-1*02	IGHJ2*01	IGKV4-59*01	IGKJ5*01
JoJ58A2	Human	IGHV1-69*12	IGHD5-24*01	IGHJ6*02	IGLV1-44*01	IGLJ1*01
JoJ58B9	Human	IGHV3-48*02	IGHD1-7*01	IGHJ4*02	IGLV2-8*01	IGLJ3*02
JoJ58B10	Human	IGHV1-69*01	IGHD3-9*01	IGHJ4*02	IGLV3-21*02	IGLJ2*01 or IGLJ3*01
JoJ58C5	Human	IGHV5-51*01	IGHD2-2*01	IGHJ3*02	IGLV1-51*01	IGLJ2*01 or IGLJ3*01
JoJ58C10	Human	IGHV1-69*01 or IGHV1-69D*01	IGHD4-17*01	IGHJ4*02	IGLV6-57*01	IGLJ2*01 or IGLJ3*01

JoJ58C5	Human	IGHV5-51*01	IGHD2-2*01	IGHJ3*02	IGLV1-51*01	IGLJ2*01 or IGLJ3*01
JoJ58C10	Human	IGHV1-69*01 or IGHV1-69D*01	IGHD4-17*01	IGHJ4*02	IGLV6-57*01	IGLJ2*01 or IGLJ3*01
JoJ58E9	Human	IGHV1-69*01 or IGHV1-69D*01	IGHD6-19*01	IGHJ1*01	IGLV1-47*02	IGLJ2*01 or IGLJ3*01
JoJ58G2	Human	IGHV1-69*12	IGHD5-12*01	IGHJ3*02	IGLV1-36*01	IGLJ2*01 or IGLJ3*01
Jo60A11	Human	IGHV1-69*01 or IGHV1-69D*01	IGHD2-15*01	IGHJ4*02	IGLV1-44*01	IGLJ3*02
JoJ60E9	Human	IGHV1-69*12	IGHD2-2*01	IGHJ6*02	IGLV1-44*01	IGLJ3*03
JoJ60E12	Human	IGHV1-69*01 or IGHV1-69D*01	IGHD2-2*01	IGHJ6*02	IGLV1-44*01	IGLJ3*03
JoJ61G1	Human	IGHV1-69*01 or IGHV1-69D*01	IGHD5-18*01	IGHJ4*02	IGLV3-21*02	IGLJ2*01 or IGLJ3*01

titration ELISA. The absorbance signal on the SCH-PK loaded plates showed a sigmoidal increase of the absorbance signal with increasing scFv-Fc concentration in a half-logarithm plot (Figure 3-3). The EC50 values were derived from the regression of absorbance signal against the logarithm of antibody concentration by a sigmoidal function (3 parameters). JoJ48C11 showed the highest binding strength with an EC50 value of 0.16 nM. The EC50 values of the other rAb ranged from 0.19 nM to 6.6 nM (Table 3-3).

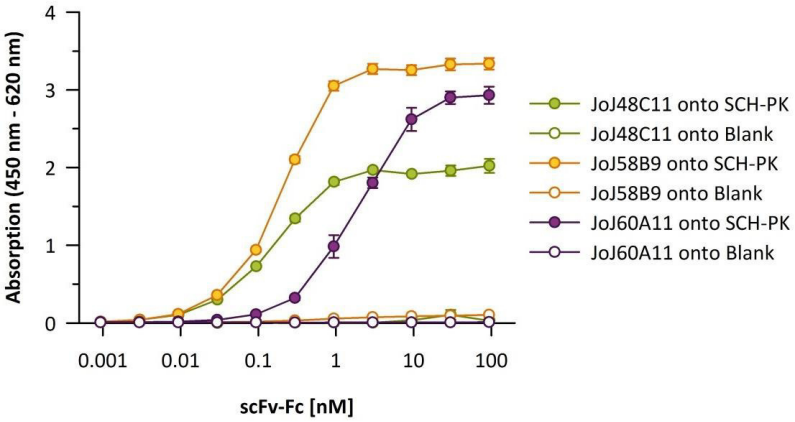

Figure 3-3 Titration ELISA of the rAb for EC50 calculation. This example shows the half logarithmic plotted absorbance signals from the titration ELISA of JoJ48C11, JoJ58B9 & JoJ60A11. Serial dilutions ranging from approx. 0.95 pM to approx. 95 nM of each rAb in the scFv-Fc format were applied on SCH-PK loaded and blank Carbo-BIND™ multiwell plates. Analysis was performed in triplets.

Table 3-3 Estimated EC50 values for the scFv-Fc of the derived rAb

rAb	EC50 [nM]	rAb	EC50 [nM]
JoJ48C11	0.16 ± 0.005	JoJ58C10	0.19 ± 0.02
JoJ48D6	1.33 ± 0.30	JoJ58E9	1.25 ± 0.51
JoJ48F1	0.21 ± 0.007	JoJ58G2	3.55 ± 1.11
JoJ49D10	0.19 ± 0.01	JoJ60A11	1.91 ± 0.24
JoJ58A2	6.61 ± 2.59	JoJ60E9	0.99 ± 0.15
JoJ58B9	0.19 ± 0.003	JoJ60E12	0.37 ± 0.01
JoJ58B10	0.63 ± 0.03	JoJ61G1	0.87 ± 0.03
JoJ58C5	0.28 ± 0.001		

The next analyzed characteristic was the antigen specificity of the rAb. It was analyzed in a competitive approach with different saccharides and yeast extract as competitors. Each rAb was used in a concentration that showed 40 % of the saturation signal in the titration ELISA and was incubated with different concentrations of competitor. After incuba ion the mixtures were applied on SCH-PK loaded Carbo-BIND™ multiwell plates and the amount of unbound rAb was analyzed. Thus, with increasing concentration of a competitor which is interacting with the rAb, the absorbance signal should decrease.

A first experiment (Figure 3-4) was performed with SCH-PK as competing substance in concentrations from 0.32 µg mL^{-1} to 316 µg mL^{-1}. JoJ48C11, JoJ48D6, JoJ48F1, JoJ49D10 and JoJ58B9 were the only rAbs which showed the expected decrease of absorbance signal in this experiment.

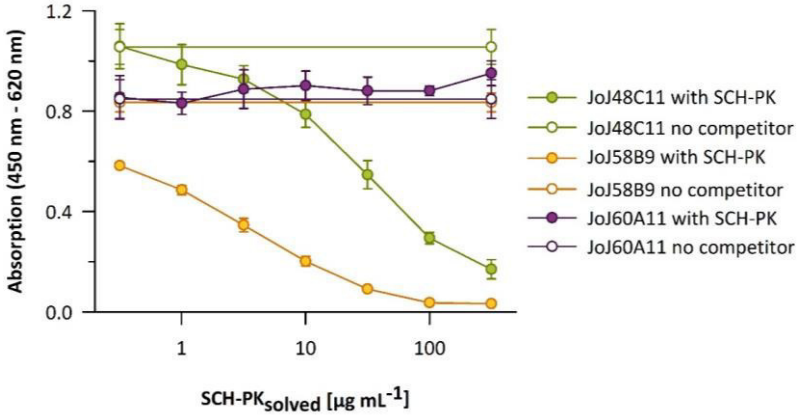

Figure 3-4 Competitive ELISA of rAb with SCH-PK as competitor. This example shows the half logarithmic plotted absorbance signals from the competitive ELISA with JoJ48C11, JoJ58B9 & JoJ60A11 (all as scFv-Fc). Serial dilutions ranging from 0.32 µg mL^{-1} to 316 µg mL^{-1} of SCH-PK were incubated with each rAb in the scFv-Fc format before application on SCH-PK loaded Carbo-BIND™ multiwell plates. The rAbs were also incubated without competitor as negative control and mark of maximal signal. Analysis was performed in triplets.

The experiment was repeated with more competitors in a concentration range from 3.12 ng mL^{-1} to 1 mg mL^{-1} (Figure 3-5).

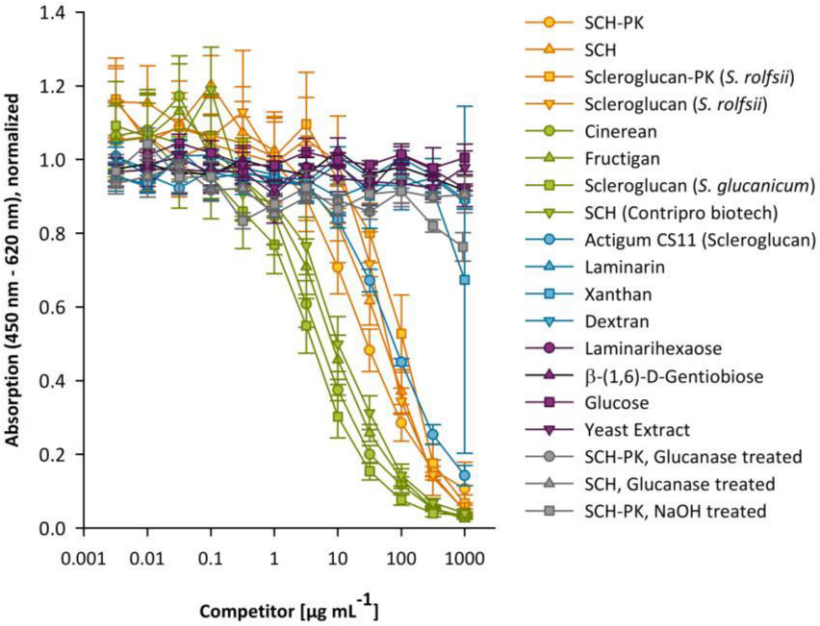

Figure 3-5 Competitive ELISA of antibody JoJ48C11 for the characterisation of antigen specificity. JoJ49D10 (scFv-Fc) was preincubated in dilutions of different carbohydrates or yeast extract ranging from 3.12 ng mL^{-1} to 1 mg mL^{-1} before being added to SCH-PK loaded Carbo-BIND™ multiwell plates. The absorbance signals were normalized by division with the absorbance of respective samples without competitor. Analysis was performed in triplets.

In this experiment only the rAbs JoJ48C11, JoJ48F1, JoJ49D10 and JoJ58B9 were analyzed. The other rAbs except for JoJ48D6 were dismissed due to the lack of interaction with SCH-PK in its solved form. JoJ48D6 was not further analyzed since it is scarcely producible while showing low binding strength.

The following substances were used as competitors: SCH-PK, SCH, scleroglucan (*S. rolfsii*), scleroglucan (*S. rolfsii*) treated with proteinase K, Cinerean, Fructigan, Scleroglucan of *S. glucanicum*, SCH from Contipro Biotech, Actigum™ CS 11 (scleroglucan), Laminarin, Dextran, Xanthan, Laminarihexaose, β-(1,6)-D-gentiobiose, yeast extract (Ohly, Hamburg, Germany) and glucose. Furthermore, NaOH treated SCH-PK was used, due to its changed secondary structure (triplex denatured to single chains, partial formation of cyclic structures). It was derived by adding NaOH until a pH of 13.8 had been reached and was neutralized with HCl before use. Solutions of degraded SCH-PK and SCH were also used. Both were prepared by overnight incubation of SCH-PK and SCH with endoglucanase from *Penicillium funicolosum* (kindly provided by Erbslöh, Geisenheim, Germany) at 50 °C. The endoglucanase was inactivated by heating up to 80 °C for 20 minutes.

The fungal β-(1,6)-branched β-(1,3)-D-glucan preparations of SCH, Scleroglucan, Cinerean and Fructigan exhibited clear interactions with each of the four antibodies. In contrast, an interaction for the non-fungal glucans Xanthan and Dextran as well as for degraded (glucanase treated) SCH, the linear hexamer of β-(1,3)-linked D-glucose Laminarihexaose, the dimer of β-(1,6)-linked D-glucose gentiobiose, monomeric D-glucose could not be observed. This hinting towards the recognition of intact β-(1,6)-branched β-(1,3)-D-glucan molecules. The media component yeast extract did not interact as well, excluding the recognition of possible non-glucan. Interestingly, NaOH treated SCH-PK just slightly interacted with all four rAbs but it was not quantitative determinable. Additionally, Laminarin seemed to be slightly bound by JoJ48D10. 1 mg mL^{-1} Xanthan showed also influence in binding for JoJ48C11 and JoJ48F1 at the highest concentration. But this interaction was most likely based on to the high viscosity of the Xanthan solution.

The interaction strengths of the strong competitors were determined as EC50 value similar as described for the binding strength of the antibodies (Table 3-4). Scleroglucan of *S. glucanicum* showed the highest interaction strength for the rAbs JoJ48C11, JoJ48F1 and JoJ49D10 with EC50 values of 3.1 µg mL^{-1}, 1.7 µg mL^{-1} and 4 µg mL^{-1}. The highest inter-

action with JoJ58B9 was observed for SCH-PK with an EC50 value of 1.7 µg mL^{-1}.

Table 3-4 EC50 values of competitors which are recognized by the recombinant antibodies

Competitors	EC50 values [µg mL^{-1}]			
	JoJ48C11	JoJ48F1	JoJ49D10	JoJ58B9
SCH-PK	25.1 ± 1.8	24.9 ± 3.7	7.8 ± 1.0	1.5 ± 0.4
SCH	36.2 ± 4.6	29.4 ± 6.4	9.1 ± 0.6	3.9 ± 0.5
Scleroglucan-PK (*S. rolfsii*)	54.4 ± 2.0	52.3 ± 5.3	19.9 ± 2.8	6.9 ± 1.2
Scleroglucan (*S. rolfsii*)	83.1 ± 5.1	54.5 ± 13.2	34.0 ± 1.2	2.6 ± 0.3
Cinerean	4.2 ± 0.2	4.7 ± 0.7	0.5 ± 0.1	6.7 ± 0.9
Fructigan	6.8 ± 0.4	8.8 ± 1.8	1.0 ± 0.2	6.1 ± 0.3
Scleroglucan (*S. glucanicum*)	3.1 ± 0.2	1.7 ± 0.5	0.4 ± 0.1	1.9 ± 0.6
SCH (Contipro biotech)	8.2 ± 1.2	7.0 ± 1.2	1.1 ± 0.2	2.0 ± 0.3
Actigum CS11 (Scleroglucan)	88.5 ± 5.0	74.2 ± 14.4	31.7 ± 1.5	2.3 ± 0.1

The results indicate the specificity of the rAb for the polysaccharide structure of SCH and for other fungal β-(1,6)-

branched β-(1,3)-D-glucans with similar structure. This specificity is limited to full length glucans with their native triple helical conformation in water.

3.5 Complex structure model of JoJ48C11 with SCH

Identification of the binding epitope for the rAb was approached by structure analysis via X-ray crystallography. The analysis was performed with JoJ48C11, since it exhibits the highest binding strength and shows high sequence similarity with the other two rAb JoJ48F1 and JoJ49D10 from the immune library. For the crystallization experiments JoJ48C11 was produced in the Fab format. Therefore, its VH and VL domain sequence were cloned into the expression vectors pCSE2.5-Fab-h-HIS-XP and pCSE2.5-Fab-k-HIS-XP, which were co-transfected into HEK293-6E cells for production. The produced Fab was isolated via HIS-tag affinity purification and ran through size exclusion chromatography to derive a monodisperse protein solution. The purity of the Fab was validated by SDS-PAGE with coomassie staining. A Fab consists of a heterodimer with a molecular weight of approx. 50 kDa and is stabilized by a disulfide bond. Under reducing conditions, it dissociates into two monomers of approx. 25 kDa. In the SDS-PAGE the produced Fab showed a band for the expected molecular weight of about 25 kDa. After

concentration of the solution for the crystallization experiment, the activity of JoJ48C11 in the Fab format was validated by ELISA (Figure 3-6) by using solutions ranging from 20.33 µM to 0.64 pM and application onto SCH-PK coated Carbo-BIND™ plates. The calculated EC50 value was 123.4 ± 11.4 nM.

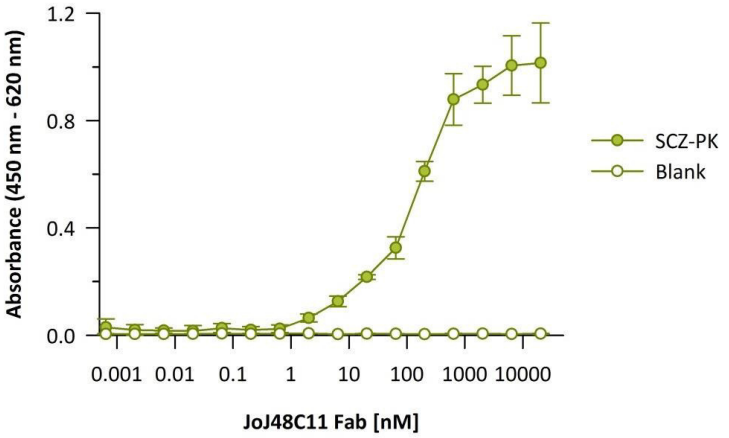

Figure 3-6 Titration ELISA of JoJ48C11 in the Fab format. Half logarithmic plot of absorbance signals from the titration ELISA of JoJ48C11 in the Fab format. Serial dilutions ranging from approx. 0.6 pM to approx. 20.3 µM of each rAb in the scFv-Fc format were applied on SCH-PK loaded and blank Carbo-BIND™ multiwell plates. Analysis was performed in triplets.

The crystallization and X-ray diffraction experiments as well as the structure modelling were performed by Dr. Kwang

Hoon Sung (working group “Structure and Function of Proteins”, Helmholtz Centre for Infection Research, Braunschweig). Protein crystals were grown in 200 nL Fab solution and an equal volume of reservoir solution in a 96-well sitting-drop Intelli-plates (Hampton Research, Aliso Viejo, USA) at 20 °C. The first crystals were obtained with a precipitant containing 0.1 M Tris (pH 8.5), 0.2 M lithium sulfate and 30 % (w/v) polyethylene glycol (avg. 4,000 kDa). After washing with cryoprotectant [0.1 M Tris (pH 8.5), 0.2 M lithium sulfate and 30 % (w/v) polyethylene glycol (avg. 4,000 kDa) and 20 % (w/v) glycerol] and flash-cooling in liquid nitrogen, a single needle of the needle-shaped multicrystals was isolated and a data set with 3 Å resolution was collected. Diffraction data were processed and scaled using autoPROC with XDS, pointless and aimless [66–70]. The structure of JoJ48C11 was solved (PDB entry 6EV1) with the automated molecular replacement pipeline BALBES and the Fab fragment of a chimeric antibody against CD25 (PDB entry 1MIM7) as search model. An initial atomic model was manually improved using COOT and refined with PHENIX and REFMAC by standard protocols [71, 72]. Furthermore, the co-crystallization of JoJ48C11 with native SCH and Laminarihexaose was pursued. While the generation of a co-crystal with SCH failed, it was possible to generate a 2.4 Å data set

of JoJ48C11 in complex with Laminarihexaose (PDB entry 6EV2). Therefore, new crystals were grown with optimized precipitant [0.1 M HEPES (pH 7.5), 0.1 M sodium acetate, 0.2 M lithium sulfate, 25 % (w/v) polyethylene glycol (avg. 4,000 kDa)] using the existing crystals as macroseed (600 nL precipitant and 100 nL macroseed crystal and 500 nL Fab solution). The JoJ48C11-Laminarihexaose complex was derived by adding 50 mM Laminarihexaose to the crystal drop and incubation for one week with subsequent flash freezing. The structure of the complex was solved by molecular replacement with PHASER as included in the PHENIX software suite using the apo-structure of JoJ48C11 Fab as search model [73, 74]. Details about the data collection and refinement statistics can be seen in Table 11-1 (chapter: supplemental information).

The derived structure of JoJ48C11 (Figure 3-7) adopts the expected dimer of heavy and light chain which both consist of two Ig domains (constant and variable domain). The Ig domains show the typical immunoglobulin fold characterized by two anti-parallel β-sheets packed against each other [75]. With the solved structure of the JoJ48C11-Laminarihexaose complex a binding site was identified which is probably involved in binding of SCH (Figure 3-8, A). The 2.4 Å-structure

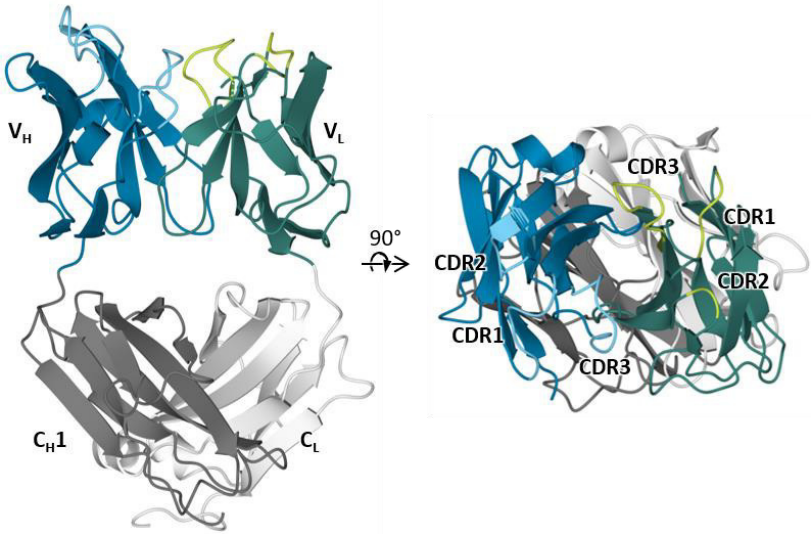

Figure 3-7 Solved overall structure of JoJ48C11 in the Fab format (PDB entry 6EV1). The model shows the solved structure of JoJ48C11, consisting of the variable and the constant domains from the heavy chain (V_H in blue and C_H1 in grey) and the light chain (V_L in green and C_L in white). The domains show the typical immunoglobulin beta barrel structure with three loop structures in the variable domains forming the CDRs (light blue in V_H and light green in V_L).

showed that the glucose of the non-reducing end of Laminarihexaose is bound to a cavity-like structure at the margin of the antigen binding area. The structure is formed by CDR3 of the heavy chain and CDR2 of the light chain. In the cavity-like structure, the residue Asp105 in CDR3 of the heavy chain ($Asp105_H$) binds the O4- and O6-atoms of the non-reducing

end of Laminarihexaose via hydrogen bonds in a bidentate fashion. A second possible binding site was found by calculation of molecular docking models with SwissDock using the RU of SCH (CID:24777, PubChem Compound Database) as ligand and the results were visualized with the UCSF Chimera package [76–79]. 256 models in 44 clusters were generated and then inspected to select the most likely models for further experimental analysis. Two similar poses were identified that show docking of the monomeric unit inside of the typical antigen binding area by location of the β-(1-6)-linked glucose inside of a second cavity structure. (Figure 3-8, B) The second cavity is located in the typical area of antigen binding and formed by CDR2 and CDR3 of the heavy chain as well as CDR3 of the light chain.

The generation of a model for the complex of JoJ48C11 and SCH was performed with the information gained from the X-ray structure and computational analysis. A model of triple helical SCH for the simulation of binding was computed from the solved structure of triple helical curdlan as described by Kony *et al.* [8, 80]. A conspicuous characteristic of the antibody was the distance of approx. 18 Å between both identified binding sites which correlates with the minimal distance between two β-(1,6)-linked glucose residues of SCH with the

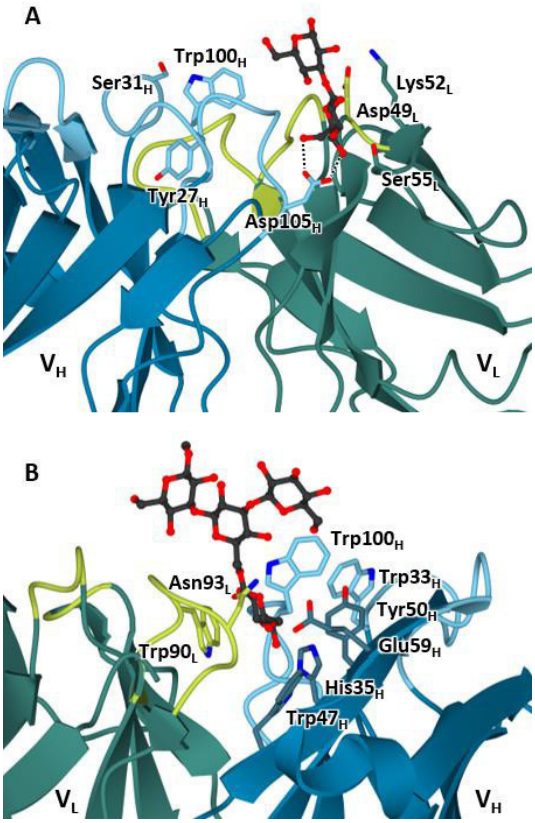

Figure 3-8 Identification of possible SCH binding sites in JoJ48C11. (A) Cavity structured binding site identified by the structure of the JoJ48C11 Fab/Laminarihexaose complex (PDB entry 6EV2; carbohydrate in black, V_H in blue; V_L in green). The glucose residue of the reducing end is bound by $Asp105_H$ via hydrogen bonds (dashed lines) in a bidentate fashion. (B) Cavity-like structured binding side identified by computational modeling with monomeric unit of SCH as ligand. The β-(1,6)-linked glucose is located inside of the cavity.

same spatial direction (Figure 3-9, A) [81]. Under assumption that the binding site for the reducing end of Laminarihexaose normally binds a β-(1,6)-linked glucose of SCH, a binding model was generated by fitting the SCH model onto the antibody structure with positioning β-(1-6)-linked glucose residues of SCH chain 1 the identified cavity-shaped binding sites. After energy minimization with the YASARA Energy Minimization Server, the final model shows that the triple helix fits very well into the binding area of the antibody with each of the binding sites accommodating a β-(1,6)-linked glucose (Figure 3-9, B) [82].

The validation of the binding model was performed by binding studies with point mutants of JoJ48C11. The mutants where generated by exchange of codons for specific amino acid residues for an alanine codon via quick change PCR. The exchanged amino acid residues were the respective ones identified by the X-ray structure analysis and computational analysis ($Trp33_H$, $His35_H$, $Trp47_H$, $Tyr50_H$, $Glu59_H$, $Trp100_H$, $Asp105_H$, $Trp90_L$ and $Asn93_L$). Additionally, mutants were used with residues exchanged located close to the SCH binding sites in the binding model ($Tyr27_H$, $Ser31_H$, $Tyr57_H$, $Asp49_L$, $Lys52_L$ and $Ser55_H$). The mutants were produced as scFv-Fc in EXPI293-F cells and were purified via protein A affinity purification. Purity of the produced point mutants

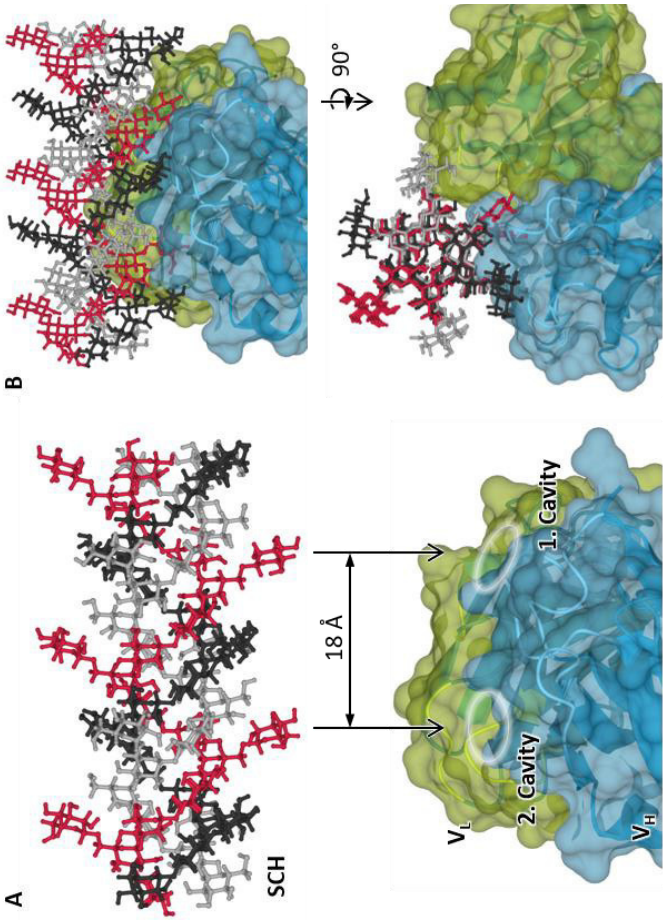

Figure 3-9 Binding model of JoJ48C11 with SCH. (A) Conformity of the 18 Å distance between two β-(1,6)-linked glucose residues of SCH protruding to the same direction and between the two identified cavity-shaped binding sites (SCH chain 1 in red; SCH chain 2 in black; SCH chain 3 in grey; V_H in blue; V_L in green). (B) The generated structure model of the JoJ48C1-SCH complex.

were checked by SDS-PAGE with coomassie staining. The influence of the point mutations on JoJ48C11 was analyzed via titration ELISA. Therefore, the mutants were applied on SCH-PK coated Carbo-BIND™ plates in a concentration range from 3 fM to 950 nM (Figure 3-10).

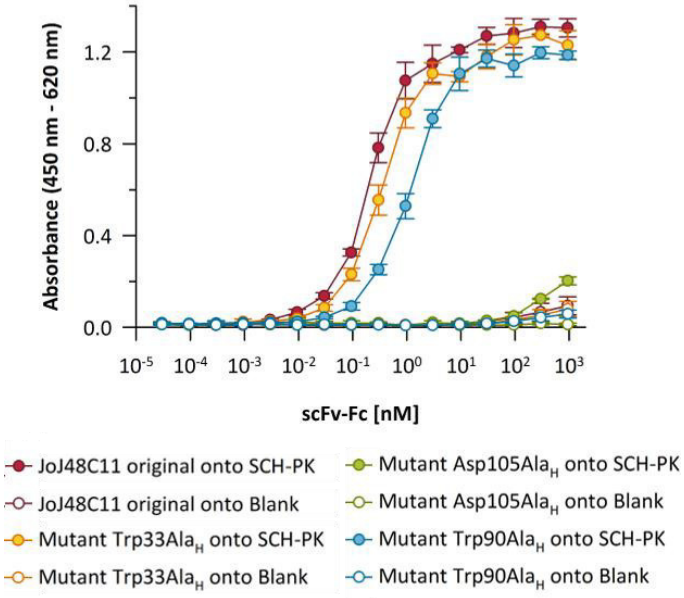

Figure 3-10 Titration ELISA with point mutants of JoJ48C11. This example shows the half logarithmic plotted absorbance signals from the titration ELISA of JoJ48C11 in the scFv-Fc format and its point mutants Trp33Ala$_H$, Asp105Ala$_H$ as well as Trp90Ala$_L$. Serial dilutions ranging from 3 fM to 950 nM of each mutant were applied on SCH-PK loaded and blank Carbo-BIND™ multiwell plates. Analysis was performed in triplets.

The calculated EC50 values were compared (Table 3-5). With an EC50 value of 0.6 nM (approx. 3 times the value of JoJ48C11) and higher, significant decrease of the binding strength was observed for the exchange of the nine residues $Tyr27_H$, $His35_H$, $Trp47_H$, $Trp100_H$, $Asp105_H$, $Asp49_L$, $Lys52_L$ and $Trp90_L$. The strongest decrease of binding was observed for the exchange of $Asp105_H$ with an EC50 value not quantifiable in our experiments (>> 200 nM), showing the importance of this residue. The alanine mutant for $Asp49_L$ showed the second highest EC50 value of roughly 163.2 nM. The values of the alanine mutants for the residues $Tyr27_H$, $His35_H$, $Trp47_H$, $Trp100_H$, $Lys52_L$ and $Trp90_L$ ranged from 0.9 nM to 10.9 nM and verified the significance of those residues for the binding of SCH as well.

Table 3-5 EC50 values from point mutants of JoJ48C11

scFv-Fc	EC50 [nM]	scFv-Fc	EC50 [nM]
JoJ48C11 original	0.22 ± 0.01	Mutant $Glu59Ala_H$	0.52 ± 0.03
Mutant $Trp27Ala_H$	0.86 ± 0.11	Mutant $Trp100Ala_H$	10.94 ± 1.15
Mutant $Ser31Ala_H$	0.22 ± 0.04	Mutant $Asp105Ala_H$	>> 1000
Mutant $Trp33Ala_H$	0.36 ± 0.08	Mutant $Asp49Ala_L$	163.2 ± 9.5
Mutant $His35Ala_H$	2.28 ± 0.17	Mutant $Lys52Ala_L$	4.78 ± 0.26
Mutant $Trp47Ala_H$	6.40 ± 1.17	Mutant $Ser55Ala_L$	0.30 ± 0.06
Mutant $Tyr50Ala_H$	0.30 ± 0.05	Mutant $Trp90Ala_L$	1.07 ± 0.09
Mutant $Tyr57Ala_H$	0.22 ± 0.02	Mutant $Asn93Ala_L$	0.23 ± 0.02

The significant role of Asp105$_H$, that was identified by the JoJ48C11 Fab Laminarihexaose complex was verified. The decrease of binding strength observed by exchange of

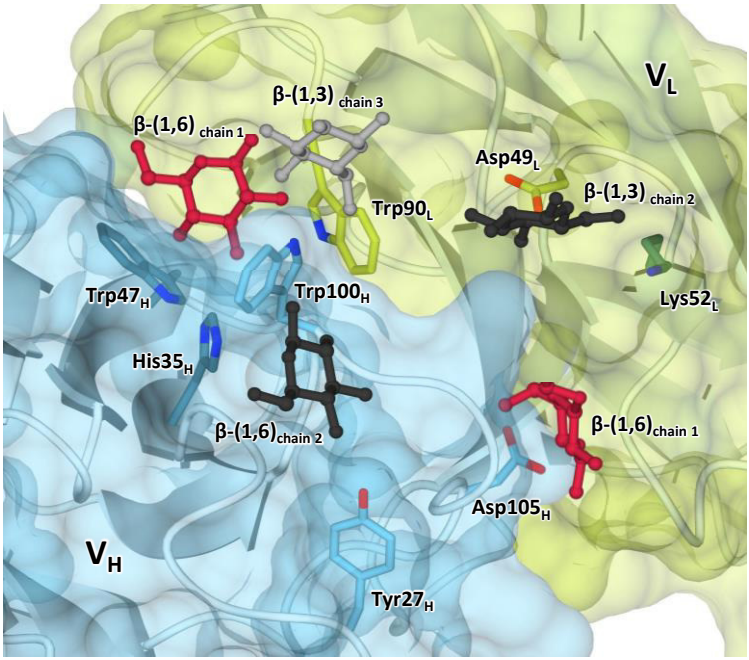

Figure 3-11 Paratope of the rAb JoJ48C11. A view from above on the antibody paratope. The amino acid residues, which showed influence in binding of SCH are displayed and named (V_H in blue; V_L in green). Additionally, the two β-(1,6)-linked glucose moieties of SCH chain 1 (red); the β-(1,6)-linked glucose moiety and β-(1,3)-linked glucose moiety of SCH chain 2 (black) and the β-(1,3)-linked glucose moiety of SCH chain 3 (grey) which are possibly involved in the interaction are plotted.

$His35_H$, $Trp47_H$, $Trp100_H$ and $Trp90_L$ validated the second cavity structure identified by computational docking with the RU of SCH. $Trp27_H$, $Asp49_L$ and $Lys52_L$ are located between both cavity-shaped binding sites and showed further points of interaction with the triple helical SCH.

Next to the two β-(1,6)-linked glucose moieties of SCH chain 1 which fit into the cavity-shaped binding sites, the complex model suggests additional interacting glucose moieties of the SCH triplex. One β-(1,6)-linked glucose moiety and one β-(1,3)-linked glucose moiety of SCH chain 2 interact with V_H and V_L in the area between the two binding cavities, and one β-(1-3)-linked moiety of SCH chain 3 interacts with V_L near the second cavity-shaped binding site (Figure 3-11).

4 Discussion

The first part of this study involved the construction of an immune library and the antibody generation. The immune library originated from three mice which were immunized with proteinase K treated Schizophyllan (SCH-PK). SCH-PK was applied to avoid maturation of IgG antibodies against possible protein contaminants associated with SCH. From the mice, the genetic information of the IgG V_L domains and V_H domains were isolated and subsequently cloned into the library vector pHAL30. Two sub-libraries containing V_L

domains of the kappa or lambda type, were generated for each mouse. Nearly all sub-libraries showed over 60 % insertion content of complete V_H and V_L pairs, except for the V_L lambda sub-library of mouse 2 with 30 % insertion content. Due to the boosted expansion of the respective B-lymphocytes before the sacrifice of the mice, the mRNA of anti-SCH IgG in the isolated mouse spleens should have been prevalent. Therefore, the generated libraries are assumed to contain predominantly phagemids with inserts of anti-SCH IgG even at a low insertion content like 30 %. Consequently, the insertion contents were accepted and not further improved. Immune libraries represent the IgG V_L domain and V_H domain variants of the donor after immunization with the antigen of interest. Those libraries show a higher potential to generate antibodies with high affinity for a specific antigen since they are based on IgG antibodies which have been matured *in vivo* for binding to the antigen of interest [83].

Next to the immune library the naive libraries HAL9 and HAL10 were used for antibody generation as well. Those libraries are based on IgM antibodies from 98 human donors with HAL9 containing rAbs with V_L domains of the lambda type and HAL10 containing rAbs with V_L domains of the kappa type [48]. IgM antibodies represent naive antibody variants before affinity maturation and show more diversity

compared to the IgG antibody variants. In a previous study, the naive libraries HAL7 and HAL8 (the antibody genes of HAL7 were included in HAL9 and HAL10 [48]) were used unsuccessfully for generation of β-(1,3)-D-glucan binding antibodies. An investigation unraveled that adsorption of β-(1,3)-D-glucans to common multiwell plate materials was unstable and led to a loss of glucan and therefore β-(1,3)-D-glucan binding antibodies during panning. The only antibody isolated is directed against proteins associated with the glucans [62]. Here, the antibody generation from the naive libraries was repeated with proteinase K treated SCH as antigen immobilized in Carbo-BIND® multiwell plates was successfully established. The Carbo-BIND® multiwell plates from Corning (New York, USA) are functionalized with hydrazide-groups which react selectively with the anomeric carbon of the reducing end in carbohydrates, forming a covalent bond. This allowed the site-specific and covalent immobilization of chemically unmodified SCH [84]. Besides, two more methods based on magnetic beads which are functionalized with hydroxyl- or hydrazide groups for covalent immobilization were established successfully. But those methods were not applied further due to the multiwell plate-based protocol of the antibody isolation procedure.

By panning, screening and sequencing, 4 individual rAbs from the immune library and 11 rAbs from the naive library HAL9 were isolated. Interestingly, from the immune library only rAbs with V_L domains of the kappa type were obtained and from the naive libraries only with V_L domains of the lambda type (HAL9). This observation can be concluded back to the natural proportion of V_L domain types in human and mice. The lambda type is predominant in human antibody variants (65 %) while it is the opposite in mice (5 %) [27]. Therefore, the likeliness to isolate antibodies with lambda type V_L domains from the naive library and with kappa type V_L domains from the immune library was foreseeable, even with the bias from preferred production of the lambda type scFv-Fc by *E. coli* [48].

The characterization of the isolated rAb composed the second part of this study. It involved the analysis of binding strength and binding specificity. Therefore, the antibodies were cloned from the monovalent scFv into the bivalent scFv-Fc format with the Fc part of mouse IgG (isotype 2c). The format enhances the binding strength of the antibodies due to the avidity effect with the second scFv and the Fc part allows the direct use of established anti-mouse-Fc antibody conjugates for detection in the other experiments.

With the titration ELISA on SCH-PK the half maximal effective concentration (EC50) of the rAbs was calculated, which allows the comparison of binding strength. This value was used for comparison of the antibodies instead of the dissociation constant (K_D), representing the binding affinity of the antibody paratope for its epitope. The reason lies in the inhomogeneity of the SCH molecule size and the highly repetitive structure that displays a multivalent antigen. Therefore, affinity measurements would just result in apparent affinities since the avidity effects cannot be clearly defined. However, the EC50 values range from 0.16 nM for JoJ48C11 to 6.61 nM of JoJ58A2, indicating that JoJ48C11 is the antibody with the highest binding strength by showing the lowest EC50 value.

Binding specificities of the rAbs were tested via competition ELISA with solved competitors and immobilized SCH-PK. The advantage of this method was the independency of immobilization efficiency of the single competitors and the possibility to observe the binding in solution. For comparison, the EC50 values of the competitors were calculated.

In a first experiment with SCH-PK as competitor, only 5 of the 15 isolated rAbs showed the expected signal decrease with rising concentration of solved SCH-PK. The other rAbs were probably directed against the linker-region between

SCH and Carbo-BIND plate. From the 5 positive tested rAbs, the rAb JoJ48D6 was omitted due to its scarcely production and low binding strength. The 4 residual rAbs JoJ48C11, JoJ48F1, JoJ49D10 and JoJ58B9 were used for a more detailed investigation. Interestingly, next to the same origin, JoJ48C11, JoJ48F1 and JoJ49D10 share a high identity.

The second more detailed competition ELISA showed that all of the tested rAbs binds to different SCH preparations (SCH-PK, non-treated SCH, SCH from Contipro Biotech) and preparations of other β-(1,6)-branched β-(1,3)-D-glucans (Scleroglucan, Cinerean, Fructigan). The Scleroglucans (non- and PK-treated Scleroglucan of *S. rolfsii*, Scleroglucan of *S. glucanicum*, Actigum™ CS 11) and Cinerean consist of the same primary molecular structure as SCH and show a triple helical conformation as well [85, 86]. Fructigan is slightly different with the position of the β-(1,6)-bound D-glucose varying at every second or third glucose moiety of the β-(1,3)-chain [87, 88]. Its secondary structure is considered to be a triplex as well.

Binding was not observed for the polysaccharides Xanthan and Dextran, demonstrating that there are any unspecific interactions of the rAbs with high molecular polysaccharides of different glycosidic linkages. Xanthan has a β-(1,4)-D-glucan backbone with β-(1,3)-linked β-D-mannose-(1,4)-β-D-

glucoronic acid-(1,2)-α-D-mannose side chain at every second glucose and forms a double helix in aqueous solution [89]. Dextran is an α-(1,6)-D-glucan with around 5 % α-(1,3)-branches to a single glucose or a dimer of glucose [90]. Furthermore, there was not an interaction with D-glucose, Laminarihexaose (linear hexamer of β-(1,3)-bound D-glucose) and β-(1,6)-D-gentiobiose (dimer of β-(1,6) bound D-glucose), indicating that D-glucose and the β-(1,6)- or β-(1,3)-linkage of D-glucose are not alone sufficient for recognition. Yeast extract and glucanase-treated SCH does not show binding as well, assuring that there was not an interaction of the rAbs with impurities from culture media or degraded saccharides and other SCH associated components. These results suggest that the rAbs interact with the high molecular structure of the β-(1,6)-branched β-(1,3)-D-glucans and, therefore, they are specific for SCH and glucans with the same structural properties.

Further investigation for identification of the possible antigen epitope structure was intended with NaOH treated SCH-PK and Laminarin. A slight signal decrease at higher concentrations of NaOH treated SCH-PK was observed for each rAb. This indicates that the native triple helical structure is an important factor for the recognition of the β-(1,6)-branched β-(1,3)-D-glucan molecule by the selected antibodies, since

the primary structure is not changed but the secondary structure. The residual interaction could be explained by occasional formation of triple helical stretches inside the predominant random coils and small amounts of renatured SCH triplex [10, 91, 92]. JoJ48F1 showed a slight interaction with the oligosaccharide Laminarin. It is produced by the algae *Laminaria digitata* and consists of a β-(1,3)-D-glucan main chain with an occasional β-(1,6)-bound D-glucose. While it exists predominantly as linear molecule, approximately 5 % occur as a triplex [93]. A similar interaction of Laminarin with JoJ48C11 cannot be fully excluded, since it was once observed in the mentioned previous experiment (Supplemental Figure 11-1).

Therefore, the results showed that the triple helical structure of the glucans is the essential factor for antibody recognition, which implies that the antibodies bind to the interchain region. It is also assumed that at least one β-(1,6)-linked D-glucose residue is part of the antigen epitope, since it could not be fully excluded with the experiments. Furthermore, paratope structures of antibodies have a diameter of roughly 30 Å [94]. A triple helical SCH stretch of this size presents 9 β-(1,6)-linked glucose residues protruding to the outside in every direction, rather unlikely that none of those residues are involved in the interaction with the antibodies.

Fructigan possesses a higher degree of branching points compared to the other β-(1,6)-branched β-(1,3)-D-glucans but does not increase the reactivity of the antibodies, possibly indicating an optimal branching degree of ca 33 % due to steric effects of the antibody. Laminarin shows not only a low occurrence of triplex structure but additional a lower degree of branching which could explain the weak antibody binding. Eventually, this leads to the additional conclusion that besides the triplex the β-(1,6)-branching degree also influences antibody reactivity.

EC50 values could be determined just for the β-(1,6)-branched β-(1,3)-D-glucans (except for NaOH treated SCH). In dependence of the rAb, the EC50 values differ for each glucan preparation. For JoJ48C11, JoJ48F1 and JoJ49D10 a similar trend was observed with Scleroglucan from *S. glucanicum* showing the highest interaction. For JoJ58B9 the highest interaction was observed with SCH-PK as competitor and the diversity of the EC50 values between each glucan was smaller (1.5 to 6.9 µg mL^{-1}) compared to the other rAbs (0.4 to 88.5 µg mL^{-1}). The difference of EC50 values by JoJ48C11, JoJ48F1 and JoJ49D10 between the glucans can be explained by different molecular size distribution, additional macro molecular structures depending on the production strains and downstream processing. For example, SCH and

SCH-PK showed similar EC50 values because both derived from the same batch production and were identically purified except proteinase K treatment. The commercial SCH purchased by Contipro Biotech, produced and purified in unknown procedures, showed lower EC50 data. JoJ58B9 seems to be less sensitive to the macro molecular differences indicating different molecular interactions.

However, with the investigation of the binding specificity false positive anti-SCH rAbs and a more general specificity for β-(1,6)-branched β-(1,3)-D-glucan of the positive anti-SCH rAbs were identified. Also, a hypothesis about the antigen recognition could be concluded, which proposes a conformational epitope requiring an intact triple helical secondary structure of β-(1,6)-branched β-(1,3)-D-glucans with an optimal branching degree of one β-(1,6)-bound D-glucose attached to approximately every three glucose units of the main chain.

The third part of this study was performed in cooperation with Prof. Dr. Wulf Blankenfeldt and Dr. Kwang Hoon Sung from the working group “Structure and Functions of Proteins” (Helmholtz-Centre for Infection Research in Braunschweig). In this part, the main subject of interest was the validation of the stated hypothesis about the binding epitope of SCH for the isolated antibodies. The strategy was

the structure analysis of the antibody paratope via X-ray crystallography from which the antigen epitope could be concluded.

For the structure analysis, the rAb JoJ48C11 was produced as chimeric Fab fragment with human constant domains (C_L-kappa and C_H1). The Fab format is a commonly used antibody format for crystallographic experiments. It still consists the antigen binding ability but misses the hinge region in the scFv-Fc format which could hinder the formation of suitable crystals [95]. JoJ48C11 was the only rAb used from the immune library for these experiments since it shares high identity with JoJ48F1 and JoJ49D10. JoJ58B9 from the naive library was considered for the structure analysis as well but was not further pursued due to missing productivity as Fab.

The structure of JoJ48C11 Fab was successfully solved and refined to a resolution of 3 Å (PDB entry 6EV1). *In silico* docking studies with the repeating unit of SCH on this apo structure identified a possible cavity-shaped binding site for a β-(1,3)-bound D-glucose residue of SCH. Furthermore, a successful co-crystallization with Laminarihexaose (hexamer of β-(1,3)-bound D-glucose) was possible by soaking of the protein crystal with the respective solution. The complex structure was solved and refined with 2.4 Å resolution (PDB entry 6EV2). In that complex structure, the electron densities of

two glucose residues from Laminarihexaose were observed. One of those glucose residues was located in another cavity structure of the paratope and therefore identified a second binding site. The gathered information from the crystallography and *in silico* docking studies revealed a paratope structure with two distinct cavity shaped binding sites which are approximately 18 Å apart and connected by a shallow groove.

For the paratope structure of anti-carbohydrate antibodies, principle characteristics were early defined by studies of anti-Dextran binding antibodies. They propose, that respective antibodies consist of a cavity shaped paratope for accommodation of terminal saccharide residues or a groove structure for up to seven internal saccharide residues of a linear polysaccharide chain [96, 97]. Up to today, the structures of only a few anti-carbohydrate antibodies have been solved by X-ray crystallography. They show the predicted cavity or groove structures of their paratope and some even consist of a combined structure of both types [98]. To name one example that is particular interesting for this study, the monoclonal antibody F22-4, which is directed against the O-antigen (lipopolysaccharide) from serotype 2a *Shigella flexneri*, consist of a groove shaped paratope with two small cavities integrated. Somewhat resembling the suggested

JoJ48C11 paratope structure. Co-crystallization of F22-4 with a synthetic fragment (decasaccharide) of the O-antigen clearly showed the binding-orientation of the helical bowed fragment along the groove with two branches of single glucose residues fitting into the small cavities [99].

Like for F22-4, the generation of a complex structure with the full antigen epitope was tried by using native SCH. Despite extensive attempts, it was not possible to generate a co-crystal with SCH. But parallel experiments with the available saccharide Laminarihexaose resulted in the JoJ48C11 Fab/Laminarihexaose complex structure as mentioned. Interestingly, JoJ48C11 does not show no binding to Laminarihexaose in the competitive ELISA assay. Assumably, the restricted movement inside the crystal led to a stable arrangement of the molecule on the paratope, caused by interactions partly involved in binding of SCH. This in mind, the parallel experiments with the carbohydrates representing SCH primary structure features was conducted. Davies *et al.* used a similar approach to generate an antagonist for an receptor based on the information from co-crystals with low affinity fragments [100].

However, without a complex structure from crystallography studies with SCH, the JoJ48C11 Fab/SCH complex structure was modeled *in silico*. Therefore, the structure of triple

helical SCH was modeled from experimental literature data and posed onto the paratope structure of the JoJ48C11. Positioning was carried out by fitting protruding β-(1,6)-bound D-glucose moieties into the cavity shaped binding site, as observed for the antibody F22-4 [99]. This arrangement was supported by the distance of the two binding sites of 18 Å which corresponds strikingly well with the helical pitch distance of the SCH chains in the triple helical conformation. Although the generated model was quite reasonable, further experimental validation was achieved by antigen ELISA experiments with alanine mutants of JoJ48C11. The model suggested 15 amino acid residues of JoJ48C11 to be involved in SCH binding which were replaced by alanine to confirm their importance. The residues $Tyr27_H$, $His35_H$, $Trp47_H$, $Trp100_H$, $Asp105_H$, $Asp49_L$, $Lys52_L$ and $Trp90_L$ could be validated.

In the following their involvement in binding is discussed:

$Asp105_H$ was identified to be a critical residue of JoJ48C11 due to complete abrogation of binding by its mutation. The acidic residue is a part of the binding cavity detected in the resolved complex structure of JoJ48C11 Fab with Laminarihexaose. There, it was shown to engage in bidentate hydrogen bonds with the glucose of the non-reducing end of Laminarihexaose. The complex model with SCH suggests a

similar interaction for binding one of the β-(1-6)-linked moiety from SCH chain 1. Those interactions are an important motif in protein/carbohydrate complexes [101].

$His35_H$, $Trp47_H$, $Trp100_H$ and $Trp90_L$ are part of the second binding cavity which was identified by *in silico* docking with the SCH RU. They act as walls of the cavity and based on their nature are suggested to bind the second β-(1-6)-linked moiety from SCH chain 1 through aromatic interactions [101]. These types of residues are often found in carbohydrate binding sites and their interactions with saccharides are known to determine the specificity of carbohydrate binding proteins. In contrast to this, their contribution to the stability of such complexes is rather modest, which is in line with the observation that mutation of these residues lead to a smaller affinity decrease than in the case of $Asp105_H$ [102, 103]. The function of $Trp47_H$ and $Trp100_H$ probably even extends beyond establishing aromatic contacts. $Trp47_H$ seems to be an important structural element, as conserved residue in frame work 2 of the VH domain. Herold *et al*. reported that substitution of $Trp47_H$ in the antibodies MAK33 (mouse IgG, anti-creatine kinase-M) and 2A2 rheumatoid factor (human IgM, anti-human IgG Fc, named 1HEZ in reference) results in the destabilization of the V_H domain structure as well as the V_H/V_L association [104]. $Trp100_H$ is assumed to form a

hydrogen bond between the indole group and a β-(1,3)-glucose moiety of SCH chain 2, according to the generated model. Similar interaction was observed by Cygler *et al*. for an antibody against polysaccharide O-antigen of pathogenic Salmonella of serogroup B [105].

$Tyr27_H$, $Asp49_L$ and $Lys52_L$ were only discovered through the JoJ48C11/triple-helical SCH complex model to be potentially involved in SCH recognition. $Tyr27_L$ is proposed to interact with a β-(1,6)-bound glucose of SCH chain 3, while $Asp49_L$ and $Lys52_L$ engage in hydrogen bonds with one β-(1,3)-bound glucose unit of the same SCH chain. Especially $Asp49_L$ seems to be important since mutation to alanine largely decreases the binding affinity of JoJ48C11.

The identification of residues involved in SCH recognition along the paratope validate the *in silico* generated JoJ48C11 Fab/SCH complex structure. Additionally, the results of the mutant binding studies allow an assumption of binding mechanism. Binding of SCH is probably induced by the strong interaction with $Asp105_H$ of the first binding cavity and $Asp49_L$ due to hydrogen bonds, while the residues of the second binding site contribute to the specificity of the antibody by further stabilization of the binding complex, as mentioned before.

Of course, the roles of the individual residues may just be suggestions, since the mutations could have led to unfavorable alterations of the paratope structure which were not further investigated. But anyway, the modeled complex is validated due to confirmation of the involvement of the two binding cavities for β-(1,6)-linked glucose residues. The first cavity with $Asp105_H$ was approved directly by structural analysis with complex structure of Laminarihexaose and alanine mutation. The second binding site detected by *in silico* studies showed clearly space for one glucose residue and alanine mutations led to reduced binding strength, because of either structural changes in this binding site hindering the incorporation of the β-(1,6)-linked glucose residue or missing interacting amino acid residues.

Overall, in this study the 3 highly similar rAbs JoJ48C11, JoJ48F1 and JoJ49D10 from an immune antibody library and the rAb JoJ58B9 from a naive antibody library were isolated. Reports about generation of other antibodies against SCH do exist. In 1990, a polyclonal antiserum from immunized rabbits was described by Tabata *et al.* [106]. Later on, Hirata *et al.* reported the isolation of a monoclonal antibody which was identified by binding to BSA coupled SCH [107]. In contrary to this study, they describe the generation of a

polyclonal antiserum from rabbits and a monoclonal antibody via hybridoma technology. Thus, here, the first generation of recombinant anti-SCH antibodies by phage display technology from immune- and naive antibody libraries is described.

Via ELISA-based binding studies with different carbohydrates and modified SCH preparations, the rAbs were identified to recognize SCH and other high molecular β-(1,6)-branched β-(1,3)-D-glucans by their triple helical structure with the protruding β-(1,6)-linked glucose residues. Other studies about hybridoma antibodies generated for β-(1,3)-D-glucans report a similar binding specificity to more than one glucan as well [108–113]. Worth mentioning is the isolation of two antibodies against the extracellular β-glucan of *Pleurotus ostreatus* by Semedo *et al.*. The molecular structure of this glucan is similar to SCH. It is assumed that these antibodies recognize and bind to a common conformational epitope, like the rAbs of this study. In difference to their investigations, here, it was proven that the triple helical arrangement is an essential element for the recognition by binding studies with proteinase and endoglucanase treated SCH as well as with denatured SCH.

For the rAb JoJ48C11, its structure was solved by X-ray crystallography. Even further insight into SCH binding was

obtained, by modeling of a JoJ48C11 Fab/SCH complex based on the results from structure analysis of a JoJ48C11 Fab/Laminarihexaose complex and *in silico* docking of SCH RU onto the JoJ48C11 Fab structure. The generated model is consistent with experimental data and supports our hypothesis that the β-(1,6)-bound D-glucose residues in conjunction with the triple-helical structure constitute the binding epitope for the antibody JoJ48C11. Therefore, this study provides first insight into the structural principles that govern the binding of triple-helical SCH to a SCH-specific antibody and represents an additional example of an anti-carbohydrate antibody structure in complex with its antigen.

5 Prospective

This study describes the successful generation of monoclonal recombinant antibodies from mouse and human sources against the β-D-glucan Schizophyllan via phage display. The investigations showed that the antibodies recognize the macromolecular structure of the triple helical conformation with protruding glucose residues. For the antibody JoJ48C11 this was directly confirmed by modeling of a Fab/SCH complex based on X-ray crystallography analysis and computational docking simulation.

Due to the high versatility of applications for SCH the generated antibodies can be used as tool for analytical investigations of respective preparations. They are suited for the determination of content of SCH or of other glucans with the same macromolecular structure in respective preparations. The conformational specificity of the antibodies may also be used for the quality control of SCH preparation by determination of changes in their conformation. Furthermore, the rAbs could support studies investigating the biological activity of SCH in mammals and also in studies for understanding the biosynthesis of SCH which are both not completely understood until now.

But there is room for further investigations of the rAbs as well. For example, the successful structure generation of JoJ58B9 would be informative. Despite of JoJ48F1 and JoJ49D10 which share a high identity with JoJ48C11 and therefore are likely to have nearly the same structure, JoJ58B9 consist of a different primary sequence especially in the CDRs. The insight into the structure of JoJ58B9 may offer an alternative binding complex and give another example of SCH recognition. Another point could be an investigation, if the biological activity of SCH can be further improved by the rAbs themselves or by rAb conjugates with other biological active compounds using SCH as carrier. Further

development to higher binding strength or higher specificity for one glucan may be also possible by additional *in vitro* maturation of the antibodies. It may also be possible to use *in vitro* maturation for the development of catalytical active antibodies which allow the directed modification or hydrolysis of SCH based on the generated rAbs.

6 Summary

Schizophyllan is a β-(1,6)-branched β-(1,3)-D-glucan that can be used for a variety of applications due to its physical properties and bioactivity. It is produced by the basidiomycete *Schizophyllum commune* as an extracellular homopolysaccharide. Aqueous solutions consist of a pseudo plastic flow behavior, due to its rod-like macromolecular structure which is stable at temperatures up to 135 °C and at pH values up to pH 12. This makes it interesting for the food, cosmetic and oil industry. The bioactivities, like antitumoral and immunomodulating effects which are interesting for the pharmaceutical industry are based on enhancement of cell-mediated immune response. Due to these various applications of SCH the generation of antibodies would be of great value because they could be used as tool for quantitative analysis and for the investigation of glucan bioactivity.

In this study the successful generation of four recombinant monoclonal antibodies (rAb) which bind to SCH is described. The rAbs JoJ48C11, JoJ48F1 and JoJ49D10 were generated from a constructed immune library and JoJ58B9 from the naive library HAL9 via phage display technology. Immunochemical ELISA experiments for characterization of the rAbs specificity showed that the antibodies are not directed solely against SCH but also against other β-glucans consistent of a β-(1,3)-D-glucan backbone with protruding β-(1,6)-linked glucose residues at every third β-(1,3)-D-glucose moiety forming a triplex structure, like Scleroglucan, Cinerean and Fructigan. Additionally, the molecular structure of JoJ48C11 as Fab and a complex structure with Laminarihexaose were solved using X-ray crystallography. From the gained structural data and computational docking models a respective binding complex was modeled and validated by mutagenesis studies. With this the assumed combination of the β-(1,6)-bound glucose residues and the triple helical structure as conformational antigen epitope could be proved for JoJ48C11.

Taken together this study describes the first successful generation of monoclonal antibodies via phage display from a human naive and mouse immune antibody library, which recognize a structural epitope of β-(1,6)-branched β-(1,3)-D-

glucans like SCH. Additionally, it shows the first structural description of such an anti-β-D-glucan antibody complex which was further validated by mutagenesis studies.

7 Acknowledgements

First of all, my deepest gratitude goes to Prof. Dr. Udo Rau, my mentor and first examiner of this thesis, who allowed me to work at his working group and made it possible for me to produce this thesis. He supported me the last years with his scientific guidance and gave me the freedom to develop my professional carrier as scientist independently.

I am also very thankful to Prof. Dr. Stefan Dübel, for being the second examiner of this thesis, for the scientific feedback and for the possibility to perform most of my work at his laboratories.

My gratitude also goes to Prof. Dr. Michael Hust who was so kind to be head of the thesis committee and to Dr. André Frenzel. Both supported me in my experimental work and professional writing with their scientific knowledge and technical advice.

I am also much obliged to our cooperation partners Ms. Sabine Buchmeier and Prof. Dr. Philip Tinnefeld as well as to Dr. Kwang Hoon Sung and Prof. Dr Wulf Blankenfeldt. Without their expertise and crucial experimental contribution, the

study would have not been possible in this successfully extend.

I want to thank all my colleagues of the biotechnology department for the great work environment which helped to overcome frustrating episodes. In particular I want to thank Wolfgang Graßl and Doris Meier for their excellent technical support and continuous effort to keep the facilities working. Also, I want to name my fellow PhD attendants Lars Freund, Viola Fühner, Wieland Fahr, Giullio Russo and Esther Wenzel for their help and for the daily discussions in the office and laboratory.

Last but not least, I want to thank my friends and family for the continuous support und understanding.

This thesis is dedicated to Johannes, who walked with me through the highs and downs during my time as PhD student.

8 List of Figures

9 List of Tables

10 References

1. S. Kikumoto, T. Miyajima, K. Kimura, S. Okubo, and N. Komatsu: “Polysaccharide produced by schizophyllum commune. Part II. Chemical structure of an extracellular polysaccharide.” *J. Agric. Chem. Soc. Japan*. vol. 45, pp. 162–168, 1971.
2. U. Rau, R. Müller, K. Cordes, and J. Klein: “Process and molecular data of branched 1,3-β-D-glucans in comparison with xanthan.” *Bioprocess Eng.* vol. 5, pp. 89–93, 1990.
3. T. Norisuye, T. Yanaki, and H. Fujita: “Triple helix of a Schizophyllum commune polysaccharide in aqueous solution.” *J. Polym. Sci. Polym. Phys. Ed.* vol. 18, no. 3, pp. 547–558, 1980.
4. S. Kikumoto, T. Miyajima, S. Yoshizumi, S. Fujimoto, and K. Kimura: “Polysaccharide produced by Schizophyllum commune. Part I. Formation and some properties of an extracellular polysaccharide.” *J. Agric. Chem. Soc. Japan*. vol. 44, pp. 337–342, 1970.
5. T. Sato, T. Norisuye, and H. Fujita: “Triple helix of Schizophyllum commune polysaccharide in dilute solution. 5. Light scattering and refractometry in mixtures of water and dimethyl sulfoxide.” *Macromolecules*. vol. 16, no. 2, pp. 185–189, 1983.
6. T. Yanaki, T. Norisuye, and H. Fujita: “Triple helix of Schizophyllum commune polysaccharide in dilute solution. 3. Hydrodynamic properties in water.” *Macromolecules*. vol. 13, no. 6, pp. 1462–1466, 1980.

7. Y. Kashiwagi, T. Norisuye, and H. Fujita: “Triple helix of Schizophyllum commune polysaccharide in dilute solution. 4. light scattering and viscosity in dilute aqueous sodium hydroxide.” *Macromolecules*. vol. 14, no. 5, pp. 1220–1225, 1981.
8. D.B. Kony, W. Damm, S. Stoll, W.F. van Gunsteren, and P.H. Hünenberger: “Explicit-solvent molecular dynamics simulations of the polysaccharide schizophyllan in water.” *Biophys. J.* vol. 93, no. 2, pp. 442–455, 2007.
9. T. Yanaki, K. Tabata, and T. Kojima: “Melting behaviour of a triple helical polysaccharide schizophyllan in aqueous solution.” *Carbohydr. Polym.* vol. 5, pp. 275–283, 1985.
10. B.T. Stokke, A. Elgsaeter, D.A. Brant, T. Kuge, and S. Kitamura: “Macromolecular cyclization of (1 → 6)-branched-(1 → 3)-β-D-glucans observed after denaturation–renaturation of the triple-helical structure.” *Biopolymers*. vol. 33, pp. 193–198, 1993.
11. U. Rau and F. Wagner: “Non-newtonian flow behaviour of colloid-disperse glucan solutions.” *Biotechnol. Lett.* vol. 9, no. 2, pp. 95–100, 1987.
12. U. Rau, A. Haarstrick, and F. Wagner: “Eignung von Schizophyllan-Lösungen zum Polymerfluten von Erdöl-Lagerstätten mit hoher Temperatur und Salinität.” *Chemie Ing. Tech.* vol. 64, no. 6, pp. 576–577, 1992.
13. B. Leonhardt, M. Santa, A. Steigerwald, and T. Kaeppler: “Polymer flooding with the polysaccharide Schizophyllan - First field trial results.” From Fundamental Science to Deployment: 17th European Symposium on Improved Oil Recovery, IOR 2013. , Saint Petersburg, Russia (2013).

14. X. Meng, H. Liang, and L. Luo: “Antitumor polysaccharides from mushrooms: a review on the structural characteristics, antitumor mechanisms and immunomodulating activities.” *Carbohydr. Res.* vol. 424, pp. 30–41, 2016.
15. N. Komatsu, S. Okubo, S. Kikumoto, K. Kimura, G. Saito, and S. Sakai: “Host-mediated antitumor action of schizophyllan, a glucan produced by Schizophyllum commune.” *Japanese J. Cancer Res.* vol. 60, no. 2, pp. 137–144, 1969.
16. A. Mansour, A. Daba, N. Baddour, M. El-Saadani, and E. Aleem: “Schizophyllan inhibits the development of mammary and hepatic carcinomas induced by 7,12 dimethylbenz(α)anthracene and decreases cell proliferation: comparison with tamoxifen.” *J. Cancer Res. Clin. Oncol.* vol. 138, no. 9, pp. 1579–1596, 2012.
17. Y. Kimura, H. Tojima, S. Fukase, and K. Takeda: “Clinical evaluation of sizofilan as assistant immunotherapy in treatment of head and neck cancer.” *Acta Otolaryngol.* vol. 114:sup511, pp. 192–195, 1994.
18. K. Miyazaki, H. Mizutani, H. Katabuchi, K. Fukuma, S. Fujisaki, and H. Okamura: “Activated (HLA-DR+) T-lymphocyte subsets in cervical carcinoma and effects of radiotherapy and immunotherapy with sizofiran on cell-mediated immunity and survival.” *Gynecol. Oncol.* vol. 56, no. 3, pp. 412–20, 1995.
19. K. Okamura, Y. Hamazaki, A. Yajima, and K. Noda: “Adjuvant immunotherapy: two randomized controlled studies of patients with cervical cancer.” *Biomed. Pharmacother.* vol. 43, no. 3, pp. 177–181, 1989.
20. V.E.C. Ooi and F. Liu: “Immunomodulation and Anti-Cancer Activity of Polysaccharide- Protein Complexes.” *Curr. Med. Chem.* vol. 7, pp. 715–729, 2000.

21. M. Suzuki, T. Arika, K. Amemiya, and M. Fujiwara: “Cooperative role of T lymphocytes and macrophages in anti-tumor activity of mice pretreated with schizophyllan (SPG).” *Jpn. J. Exp. Med.* vol. 52, no. 2, pp. 59–65, 1982.
22. I. Sugawara, K.C. Lee, and M. Wong: “Schizophyllan (SPG)-treated macrophages and anti-tumor activities against syngeneic and allogeneic tumor cells. I. Characteristics of SPG-treated macrophages.” *Cancer Immunolgy Immunother.* vol. 16, pp. 137–144, 1984.
23. Y. Tsuchiya, M. Igarashi, M. Inoue, and K. Kumagai: “Cytokine-related immunomodulating activities of an anti-tumor glucan, sizofiran (SPG).” *J. Pharmacobiodyn.* vol. 12, no. 10, pp. 616–625, 1989.
24. L. Kubala, J. Ruzickova, K. Nickova, J. Sandula, M. Ciz, and A. Lojek: “The effect of (1→3)-β-d-glucans, carboxymethylglucan and schizophyllan on human leukocytes in vitro.” *Carbohydr. Res.* vol. 338, no. 24, pp. 2835–2840, 2003.
25. J. Nemoto, N. Ohno, K. Saito, Y. Adachi, and T. Yadomae: “Expression of interleukin 1 family mRNAs by a highly branched, OL-2.” *Biol. Pharm. Bull.* vol. 16, no. 10, pp. 1046–1050, 1993.
26. A. Fagraeus: “The plasma cellular reaction and its relation to the formation of antibodies in vitro.” *J. Immunol.* vol. 58, no. 1, pp. 1–13, 1948.
27. K. Murphy, P. Travers, and M. Walport: “Janeway’s Immunobiology.” *Taylor & Francis Ltd.* , 2008.
28. R.R. Porter: “Structural studies of Immunoglobulins.” *Science (80-.).* vol. 180, no. 4087, pp. 713–716, 1973.
29. G.M. Edelman: “Antibody Structure and Molecular Immunology.” *Science (80-.).* vol. 180, no. 4088, pp. 830–840, 1973.

30. R.E. Bird, K.D. Hardman, J.W. Jacobson, S. Johnson, B.M. Kaufman, S.M. Lee, T. Lee, S.H. Pope, G.S. Riordan, and M. Whitlow: “Single-Chain Antigen-Binding Proteins.” *Science (80-.).* vol. 242, no. 4877, pp. 423–426, 1988.
31. J.S. Huston, D. Levinson, M. Mudgett-Hunter, M.S. Tai, J. Novotný, M.N. Margolies, R.J. Ridge, R.E. Bruccoleri, E. Haber, R. Crea, and H. Oppermann: “Protein engineering of antibody binding sites: recovery of specific activity in an anti-digoxin single-chain Fv analogue produced in Escherichia coli.” *Proc. Natl. Acad. Sci. U. S. A.* vol. 85, no. 16, pp. 5879–83, 1988.
32. D.B. Powers, P. Amersdorfer, M. Poul, U.B. Nielsen, M.R. Shalaby, G.P. Adams, L.M. Weiner, and J.D. Marks: “Expression of single-chain Fv-Fc fusions in Pichia pastoris.” *J. Immunol. Methods*. vol. 251, no. 1–2, pp. 123–135, 2001.
33. G. Köhler and C. Milstein: “Continuous cultures of fused cells secreting antibody of predefined specificity.” *Nature*. vol. 256, pp. 495–497, 1975.
34. R. Orlandi, D.H. Güssow, P.T. Jones, and G. Winter: “Cloning immunoglobulin variable domains for expression by the polymerase chain reaction.” *Proc. Natl. Acad. Sci. U. S. A.* vol. 86, no. 10, pp. 3833–3837, 1989.
35. W. Huse, L. Sastry, S. Iverson, A. Kang, M. Alting-Mees, D. Burton, S. Benkovic, and R. Lerner: “Generation of a large combinatorial library of the immunoglobulin repertoire in phage lambda.” *Science (80-.).* vol. 246, no. 4935, pp. 1275–1281, 1989.
36. J.D. Marks, H.R. Hoogenboom, T.P. Bonnert, J. McCafferty, A.D. Griffiths, and G. Winter: “By-passing immunization: Human antibodies from V-gene libraries displayed on phage.” *J. Mol. Biol.* vol. 222, no. 3, pp. 581–597, 1991.

37. A. Knappik, L. Ge, A. Honegger, P. Pack, M. Fischer, G. Wellnhofer, A. Hoess, J. Wölle, A. Plückthun, and B. Virnekäs: “Fully synthetic human combinatorial antibody libraries (HuCAL) based on modular consensus frameworks and CDRs randomized with trinucleotides.” *J. Mol. Biol.* vol. 296, no. 1, pp. 57–86, 2000.
38. H.R. Hoogenboom and G. Winter: “By-passing immunisation: Human antibodies from synthetic repertoires of germline VH gene segments rearranged in vitro.” *J. Mol. Biol.* vol. 227, no. 2, pp. 381–388, 1992.
39. J. Hanes and A. Plückthun: “In vitro selection and evolution of functional proteins by using ribosome display.” *Proc. Natl. Acad. Sci. U. S. A.* vol. 94, no. 10, pp. 4937–4942, 1997.
40. J. McCafferty, A.D. Griffiths, G. Winter, and D.J. Chiswell: “Phage antibodies: filamentous phage displaying antibody variable domains.” *Nature*. vol. 348, pp. 552–554, 1990.
41. E.T. Boder and K.D. Wittrup: “Yeast surface display for screening combinatorial polypeptide libraries.” *Nat. Biotechnol.* vol. 15, pp. 553–557, 1997.
42. M. Russel, H.B. Lowman, and T. Clackson: “Introduction to phage biology and phage display.” In: Clackson, T. and Lowman, H.B. (eds.) Phage display: A practical approach. pp. 1–26. *Oxford University Press Inc.*, Oxford (2004).
43. S.S. Sidhu: “Engineering M13 for phage display.” *Biomol. Eng.* vol. 18, no. 2, pp. 57–63, 2001.
44. L.J. Holt, C. Herring, L.S. Jespers, B.P. Woolven, and I.M. Tomlinson: “Domain antibodies: Proteins for therapy.” *Trends Biotechnol.* vol. 21, no. 11, pp. 484–490, 2003.

45. R.M. Hoet, E.H. Cohen, R.B. Kent, K. Rookey, S. Schoonbroodt, S. Hogan, L. Rem, N. Frans, M. Daukandt, H. Pieters, R. Van Hegelsom, N. Coolen-Van Neer, H.G. Nastri, I.J. Rondon, J.A. Leeds, S.E. Hufton, L. Huang, I. Kashin, M. Devlin, G. Kuang, M. Steukers, M. Viswanathan, A.E. Nixon, D.J. Sexton, H.R. Hoogenboom, and R.C. Ladner: "Generation of high-affinity human antibodies by combining donor-derived and synthetic complementarity-determining-region diversity." *Nat. Biotechnol.* vol. 23, no. 3, pp. 344–348, 2005.
46. M. Hust, E. Maiss, H.J. Jacobsen, and T. Reinard: "The production of a genus-specific recombinant antibody (scFv) using a recombinant potyvirus protease." *J. Virol. Methods*. vol. 106, no. 2, pp. 225–233, 2002.
47. F. Breitling, S. Dübel, T. Seehaus, I. Klewinghaus, and M. Little: "A surface expression vector for antibody screening." *Gene*. vol. 104, no. 2, pp. 147–53, 1991.
48. J. Kügler, S. Wilke, D. Meier, F. Tomszak, A. Frenzel, T. Schirrmann, S. Dübel, H. Garritsen, B. Hock, L. Toleikis, M. Schütte, and M. Hust: "Generation and analysis of the improved human HAL9/10 antibody phage display libraries." *BioMed Cent. Biotechnol.* vol. 15:10, 2015.
49. L. Chasteen, J. Ayriss, P. Pavlik, and A.R.M. Bradbury: "Eliminating helper phage from phage display." *Nucleic Acids Res.* vol. 34, no. 21, pp. 1–11, 2006.
50. J. Vieira and J. Messing: "Production of single-stranded plasmid DNA." *Methods Enzymol.* vol. 153, pp. 3–11, 1987.
51. S. Rondot, J. Koch, F. Breitling, and S. Dübel: "A helper phage to improve single-chain antibody presentation in phage display." *Nat. Biotechnol.* vol. 19, no. 1, pp. 75–78, 2001.

52. S.F. Parmley and G.P. Smith: “Antibody-selectable filamentous fd phage vectors: affinity purification of target genes.” *Gene*. vol. 73, pp. 305–318, 1988.
53. M. Hust, T. Meyer, B. Voedisch, T. Rülker, H. Thie, A. El-Ghezal, M.I. Kirsch, M. Schütte, S. Helmsing, D. Meier, T. Schirrmann, and S. Dübel: “A human scFv antibody generation pipeline for proteome research.” *J. Biotechnol.* vol. 152, no. 4, pp. 159–170, 2011.
54. F. Breitling and S. Dübel: “Rekombinante Antikörper.” *Spektrum Akademischer Verlag* , 1997.
55. M. Kirsch, M. Zaman, D. Meier, S. Dübel, and M. Hust: “Parameters affecting the display of antibodies on phage.” *J. Immunol. Methods*. vol. 301, no. 1–2, pp. 173–185, 2005.
56. L. Zheng: “An efficient one-step site-directed and site-saturation mutagenesis protocol.” *Nucleic Acids Res.* vol. 32, no. 14, pp. e115–e115, 2004.
57. O.H. Lowry, N.J. Rosebrough, A.L. Farr, and R.J. Randall: “Protein measurement with the folin phenol reagent.” *Readings*. vol. 193, no. 1, pp. 265–275, 1951.
58. U.K. Laemmli: “Cleavage of structural proteins during the assembly of the head of bacteriophage T4.” *Nature*. vol. 227, pp. 680–685, 1970.
59. X. Sun, G. Yang, S. Sun, R. Quan, W. Dai, B. Li, C. Chen, and Z. Li: “The hydroxyl-functionalized magnetic particles for purification of glycan-binding proteins.” *Curr. Pharm. Biotechnol.* vol. 10, no. 8, pp. 753–760, 2009.
60. S. Park, M.R. Lee, and I. Shin: “Construction of carbohydrate microarrays by using one-step, direct immobilizations of diverse unmodified glycans on solid surfaces.” *Bioconjug. Chem.* vol. 20, no. 1, pp. 155–162, 2009.

61. L. Toleikis and A. Frenzel: “Cloning single-chain antibody fragments (ScFv) from hyrbidoma cells.” *Methods Mol. Biol.* vol. 907, pp. 59–71, 2012.
62. L.-R. Freund: “Untersuchungen zu rekombinaten ß-Glucan-spezifischen Antikörpern,” (2012).
63. V. Giudicelli, X. Brochet, and M.-P. Lefranc: “IMGT/V-QUEST: IMGT standardized analysis of the immunoglobulin (IG) and T cell receptor (TR) nucleotide sequences.” *Cold Spring Harb. Protoc.* vol. 2011, no. 6, pp. 695–715, 2011.
64. X. Brochet, M.-P. Lefranc, and V. Giudicelli: “IMGT/V-QUEST: the highly customized and integrated system for IG and TR standardized V-J and V-D-J sequence analysis.” *Nucleic Acids Res.* vol. 36, pp. W503–W508, 2008.
65. I. Retter, H.H. Althaus, R. Münch, and W. Müller: “VBASE2, an integrative V gene database.” *Nucleic Acids Res.* vol. 33, no. DATABASE ISS., pp. 671–674, 2005.
66. C. Vonrhein, C. Flensburg, P. Keller, A. Sharff, O. Smart, W. Paciorek, T. Womack, and G. Bricogne: “Data processing and analysis with the autoPROC toolbox.” *Acta Crystallogr. Sect. D Biol. Crystallogr.* vol. 67, no. 4, 2011.
67. W. Kabsch: “XDS.” *Acta Crystallogr. Sect. D Biol. Crystallogr.* vol. 66, no. 2, 2010.
68. P. Evans: “Scaling and assessment of data quality.” *Acta Crystallogr. Sect. D Biol. Crystallogr.* vol. 62, no. 1, 2006.
69. P.R. Evans: “An introduction to data reduction: Space-group determination, scaling and intensity statistics.” *Acta Crystallogr. Sect. D Biol. Crystallogr.* vol. 67, no. 4, 2011.
70. P.R. Evans and G.N. Murshudov: “How good are my data and what is the resolution?” *Acta Crystallogr. Sect. D Biol. Crystallogr.* vol. 69, no. 7, 2013.

71. P. Emsley and K. Cowtan: “Coot: Model-building tools for molecular graphics.” *Acta Crystallogr. Sect. D Biol. Crystallogr.* vol. 60, no. 12 I, 2004.
72. G.N. Murshudov, P. Skubák, A.A. Lebedev, N.S. Pannu, R.A. Steiner, R.A. Nicholls, M.D. Winn, F. Long, and A.A. Vagin: “REFMAC5 for the refinement of macromolecular crystal structures.” *Acta Crystallogr. Sect. D Biol. Crystallogr.* vol. 67, no. 4, 2011.
73. A.J. McCoy, R.W. Grosse-Kunstleve, P.D. Adams, M.D. Winn, L.C. Storoni, and R.J. Read: “Phaser crystallographic software.” *J. Appl. Crystallogr.* vol. 40, no. 4, 2007.
74. P.D. Adams, P.V. Afonine, G. Bunkóczi, V.B. Chen, I.W. Davis, N. Echols, J.J. Headd, L.-W. Hung, G.J. Kapral, R.W. Grosse-Kunstleve, A.J. McCoy, N.W. Moriarty, R. Oeffner, R.J. Read, D.C. Richardson, J.S. Richardson, T.C. Terwilliger, and P.H. Zwart: “PHENIX: A comprehensive Python-based system for macromolecular structure solution.” *Acta Crystallogr. Sect. D Biol. Crystallogr.* vol. 66, no. 2, 2010.
75. P. Bork, L. Holm, and C. Sander: “The immunoglobulin fold: Structural classification, sequence patterns and common core.” *J. Mol. Biol.* vol. 242, no. 4, 1994.
76. A. Grosdidier, V. Zoete, and O. Michielin: “SwissDock, a protein-small molecule docking web service based on EADock DSS.” *Nucleic Acids Res.* vol. 39, no. SUPPL. 2, 2011.
77. A. Grosdidier, V. Zoete, and O. Michielin: “Fast docking using the CHARMM force field with EADock DSS.” *J. Comput. Chem.* vol. 32, no. 10, 2011.
78. S. Kim, P.A. Thiessen, E.E. Bolton, J. Chen, G. Fu, A. Gindulyte, L. Han, J. He, S. He, B.A. Shoemaker, J. Wang, B. Yu, J. Zhang, and S.H. Bryant: “PubChem substance and compound databases.” *Nucleic Acids Res.* vol. 44, no. D1, 2016.

79. E.F. Pettersen, T.D. Goddard, C.C. Huang, G.S. Couch, D.M. Greenblatt, E.C. Meng, and T.E. Ferrin: “UCSF Chimera - A visualization system for exploratory research and analysis.” *J. Comput. Chem.* vol. 25, no. 13, 2004.
80. C.T. Chuah, A. Sarko, Y. Deslandest, and R.H. Marchessault: “Triple-helical crystalline structure of curdlan and paramylon hydrates.” *Macromolecules*. vol. 16, no. 8, pp. 1375–1382, 1983.
81. A.-H. Bae, M. Numata, S. Yamada, and S. Shinkai: “New approach to preparing one-dimensional Au nanowires utilizing a helical structure constructed by schizophyllan.” *New J. Chem.* vol. 31, no. 5, pp. 618–622, 2007.
82. E. Krieger, K. Joo, J. Lee, J. Lee, S. Raman, J. Thompson, M. Tyka, D. Baker, and K. Karplus: “Improving physical realism, stereochemistry, and side-chain accuracy in homology modeling: Four approaches that performed well in CASP8.” *Proteins Struct. Funct. Bioinforma.* vol. 77, no. SUPPL. 9, 2009.
83. I. Saggy, Y. Wine, L. Shefet-Carasso, L. Nahary, G. Georgiou, and I. Benhar: “Antibody isolation from immunized animals: Comparison of phage display and antibody discovery via v gene repertoire mining.” *Protein Eng. Des. Sel.* vol. 25, no. 10, pp. 539–549, 2012.
84. M.R. Lee and I. Shin: “Facile preparation of carbohydrate microarrays by site-specific, covalent immobilization of unmodified carbohydrates on hydrazide-coated glass slides.” *Org. Lett.* vol. 7, no. 19, pp. 4269–4272, 2005.
85. T.L. Bluhm, Y. Deslandest, and R.H. Marchessault: “Solid-state and solution conformation of scleroglucan.” *Carbohydr. Res.* vol. 100, pp. 117–130, 1982.

86. M. Gawronski, N. Donkai, T. Fukuda, T. Miyamoto, H. Conrad, and T. Springer: “Triple helix of the polysaccharide cinerean in aqueous solution.” *Macromolecules*. vol. 30, no. 97, pp. 6994–6996, 1997.
87. F. Santamaria, F. Reyes, and R. Lahoz: “Extracellular glucan containing (1→3)-β and (1→6)-β linkages isolated from Monilinia fructigena.” *J. Gen. Microbiol.* vol. 109, pp. 287–293, 1978.
88. W.M. Kulicke, A.I. Lettau, and H. Thielking: “Correlation between immunological activity, molar mass, and molecular structure of different (1→3)-β-D-glucans.” *Carbohydr. Res.* vol. 297, no. 2, pp. 135–143, 1997.
89. K. Born, V. Langendorff, and P. Boulenguer: “Xanthan.” In: Vandamme, E.J., De Baets, S., and Steinbüchel, A. (eds.) Biopolymers. pp. 259–291. *Wiley-VCH Verlag GmbH & Co. KGaA*, Weinheim (2003).
90. O. Larm, B. Lindberg, and S. Svensson: “Studies on the length of the side chains of the dextran elaborated by Leuconostoc mesenteroides NRRL B-512.” *Carbohydr. Res.* vol. 20, no. 1, pp. 39–48, 1971.
91. H. Saito, T. Ohki, and T. Sasaki: “A 13C-nuclear magnetic resonance study of polysaccharide gels. Molecular architecture in the gels consisting of fungal, branched (1→3)-β-D-glucans (lentinan and schizophyllan) as manifested by conformational changes induced by sodium hydroxide.” *Carbohydr. Res.* vol. 74, pp. 227–240, 1979.
92. M. Sletmoen, E. Geissler, and B.T. Stokke: “Determination of molecular parameters of linear and circular scleroglucan coexisting in ternary mixtures using light scattering.” *Biomacromolecules*. vol. 7, no. 3, pp. 858–865, 2006.

93. M. Oda, Y. Tanabe, M. Noda, S. Inaba, E. Krayukhina, H. Fukada, and S. Uchiyama: “Structural and binding properties of laminarin revealed by analytical ultracentrifugation and calorimetric analyses.” *Carbohydr. Res.* vol. 431, pp. 33–38, 2016.
94. P.M. Colman: “Structure of Antibody- Antigen Complexes : Implications for Immune Recognition.” *Adv. Immunol.* vol. 43, pp. 99–132, 1988.
95. J. Holcomb, N. Spellmon, Y. Zhang, M. Doughan, C. Li, and Z. Yang: “Protein crystallization: Eluding the bottleneck of X-ray crystallography.” *AIMS Biophys.* vol. 4, no. 4, pp. 557–575, 2017.
96. E.A. Kabat: “Problems in understanding the generation of antibody complementarity.” In: Müftüoğlu, A.Ü. and Barlas, N. (eds.) Recent Advances in Immunology. pp. 1–14. *Springer US*, Boston, MA (1984).
97. E.A. Padlan and E.A. Kabat: “Model-building study of the combining sites of two antibodies to alpha(1→6)dextran.” *Proc Natl Acad Sci U S A*. vol. 85, no. 18, pp. 6885–6889, 1988.
98. O. Haji-Ghassemi, R.J. Blackler, N.M. Young, and S. V. Evans: “Antibody recognition of carbohydrate epitopes.” *Glycobiology*. vol. 25, no. 9, pp. 920–952, 2015.
99. B. Vulliez-Le Normand, F.A. Saul, A. Phalipon, F. Bélot, C. Guerreiro, L.A. Mulard, and G.A. Bentley: “Structures of synthetic O-antigen fragments from serotype 2a Shigella flexneri in complex with a protective monoclonal antibody.” *Proc. Natl. Acad. Sci. U. S. A.* vol. 105, no. 29, pp. 9976–9981, 2008.

100. T.G. Davies, W.E. Wixted, J.E. Coyle, C. Griffiths-Jones, K. Hearn, R. McMenamin, D. Norton, S.J. Rich, C. Richardson, G. Saxty, H.M.G. Willems, A.J.A. Woolford, J.E. Cottom, J.P. Kou, J.G. Yonchuk, H.G. Feldser, Y. Sanchez, J.P. Foley, B.J. Bolognese, G. Logan, P.L. Podolin, H. Yan, J.F. Callahan, T.D. Heightman, and J.K. Kerns: "Monoacidic Inhibitors of the Kelch-like ECH-Associated Protein 1: Nuclear Factor Erythroid 2-Related Factor 2 (KEAP1:NRF2) Protein-Protein Interaction with High Cell Potency Identified by Fragment-Based Discovery." *J. Med. Chem.* vol. 59, no. 8, pp. 3991–4006, 2016.
101. N.K. Vyas: "Atomic features of protein-carbohydrate interactions." *Curr. Opin. Struct. Biol.* vol. 1, no. 5, pp. 732–740, 1991.
102. J.L. Asensio, A. Arda, F.J. Canada, and J. Jimenez-Barbero: "Carbohydrate - Aromatic interactions." *Acc. Chem. Res.* vol. 46, no. 4, pp. 946–954, 2013.
103. K.L. Hudson, G.J. Bartlett, R.C. Diehl, J. Agirre, T. Gallagher, L.L. Kiessling, and D.N. Woolfson: "Carbohydrate-Aromatic Interactions in Proteins." *J. Am. Chem. Soc.* vol. 137, pp. 15152–15160, 2015.
104. E.M. Herold, C. John, B. Weber, S. Kremser, J. Eras, C. Berner, S. Deubler, M. Zacharias, and J. Buchner: "Determinants of the assembly and function of antibody variable domains." *Sci. Rep.* vol. 7, no. 1, pp. 1–17, 2017.
105. M. Cygler, D.R. Rose, and D.R. Bundle: "Recognition of a cell-surface oligosaccharide of pathogenic Salmonella by an antibody Fab fragment." *Science*. vol. 253, no. 5018, pp. 442–445, 1991.
106. K. Tabata, W. Itoh, A. Hirata, I. Sugawara, and S. Mori: "Preparation of polyclonal antibodies to an anti-tumor (1→3)-β-D-glucan, schizophyllan." *Agric. Biol. Chem.* vol. 54, no. 8, pp. 1953–1959, 1990.

107. A. Hirata, W. Itoh, M. Komoda, K. Tabata, S. Itoyama, and I. Sugawara: “Detection of immunoactive schizophyllan by solid-phase enzyme-linked immunosorbent assay.” *Biol. Pharm. Bull.* vol. 16, no. 11, pp. 1091–1093, 1993.
108. A. Hirata, Y. Adachi, W. Itoh, M. Komoda, K. Tabata, and I. Sugawara: “Monoclonal antibody to proteoglycan derived from Grifola frondosa (Maitake).” *Biol. Pharm. Bull.* vol. 17, no. 4, pp. 539–542, 1994.
109. J. Douwes, G. Doekes, R. Montijn, D. Heedrik, and B. Brunekreef: “An immunoassay for the measurement of (1→3)-β-D glucans in the indoor environment.” *Mediators Inflamm.* vol. 6, pp. 257–262, 1997.
110. A. Torosantucci, P. Chiani, C. Bromuro, F. De Bernardis, A.S. Palma, Y. Liu, G. Mignogna, B. Maras, M. Colone, A. Stringaro, S. Zamboni, T. Feizi, and A. Cassone: “Protection by anti-β-glucan antibodies is associated with restricted β-1,3 glucan binding specificity and inhibition of fungal growth and adherence.” *PLoS One*. vol. 4, no. 4, pp. e5392, 2009.
111. I. Sander, C. Fleischer, G. Borowitzki, T. Brüning, and M. Raulf-Heimsoth: “Development of a two-site enzyme immunoassay based on monoclonal antibodies to measure airborne exposure to (1→3)-β-d-glucan.” *J. Immunol. Methods*. vol. 337, no. 1, pp. 55–62, 2008.
112. M.C. Semedo, A. Karmali, S. Martins, and L. Fonseca: “Generation of high-affinity monoclonal antibodies of IgG class against native β-D-glucans from basidiomycete mushrooms.” *Process Biochem.* vol. 51, no. 2, pp. 333–342, 2016.
113. M.C. Semedo, A. Karmali, S. Martins, and L. Fonseca: “Novel polyol-responsive monoclonal antibodies against extracellular β-D-glucans from Pleurotus ostreatus.” *Biotechnol. Prog.* vol. 32, no. 1, pp. 116–125, 2016.

11 Supplemental Information

Table 11-1 Data collection and refinement statistics of structures from X-ray crystallography

	JoJ48C11 Fab	JoJ48C11 Fab + Laminarihexaose
Data collection		
X-ray sources[a]	P11, DESY	P11, DESY
Space group	$P2_1$	$P2_1$
Cell dimensions		
a, b, c (Å)	94.08 112.83 140.82	81.73 131.50 91.03
α, β, γ (°)	90.00, 98.61, 90.00	90.00, 91.50, 90.00
No. of subunits/ASU[b]	6	4
Wavelength (Å)	1.03320	1.03320
Resolution (Å)	3.04 (3.096-3.043)[c]	2.40 (2.445-2.403)[c]
Total number of observation	188636 (9678)	516202 (26154)
Total number unique	55718 (2768)	74793 (3694)
R_{sym} (%)[d]	13.0 (64.7)	9.6 (77.9)
R_{meas} or $R_{r.i.m.}$ (%)[e]	15.5 (76.4)	10.3 (84.0)
R_{pim} (%)[f]	8.3 (40.4)	3.9 (31.2)
Mean(I)/sd(I)	8.9 (2.2)	12.9 (2.2)
Completeness (%)	99.4 (99.3)	100.0 (99.6)
Multiplicity	3.4 (3.5)	6.9 (7.1)
Refinement		
Resolution range (Å)	56.416-3.043	55.787-2.403
Reflections used	55674	74686
R_{work} / R_{free} (%)[g]	18.56 / 23.79	19.35 / 23.29
Number of atoms		
Protein	19269	13102
Ligand		35
Water	9	529

Average *B* factors (Å^2)		
Protein	66.58	57.18
Ligand		97.28
Water	35.30	49.31
RMS deviations		
Bond length (Å)	0.004	0.004
Bond angles (°)	1.003	0.756
Ramachandran outliers (%)	0.08	0.23
PDB ID	6EV1	6EV2

[a]DESY : German Electron Synchrotron, Germany

[b]ASU; Asymmetric Unit

[c]Values in parentheses are for reflections in the highest resolution bin.

[d]$R_{sym} = \Sigma_h\Sigma_i|I_{(h,i)}-\langle I_{(h)}\rangle|/\Sigma_h\Sigma_i\, I_{(h,i)}$, where $I_{(h,i)}$ is the intensity of the i^{th} measurement of reflection h and $\langle I_{(h)}\rangle$ is the corresponding average value for all i measurements.

[e]R_{meas} = $R_{r.i.m.}$ (redundancy-independent merging R-factor) = $\Sigma_h[N/(N-1)]^{1/2}\Sigma_i(|I_{i(h)}-\langle I_{(h)}\rangle|)/\Sigma_h\Sigma_i I_{i(h)}$

[f]$R_{p.i.m.}$ (precision-indicating merging R-factor) = $\Sigma_h[1/(N-1)]^{1/2}\Sigma_i(|I_{i(h)}-\langle I_{(h)}\rangle|)/\Sigma_h\Sigma_i I_{i(h)}$

[g]$R_{work} = \Sigma||F_o|-|F_c||/\Sigma|F_o|$, where R_{free} is calculated for the 5% test set of reflections.

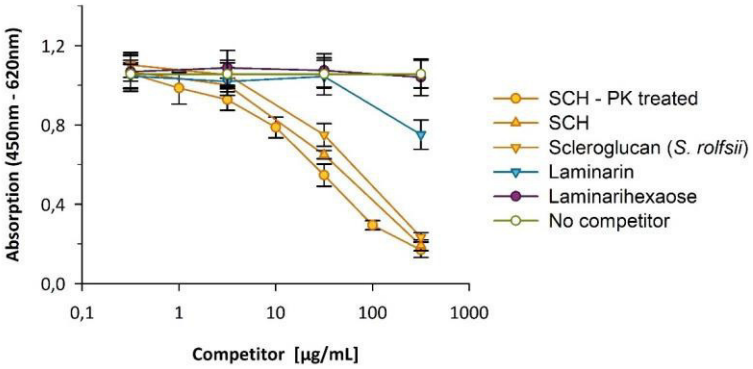

Figure 11-1 Competitive ELISA of rAb JoJ48C11 with different competitors. This example shows the half logarithmic plotted absorbance signals from the competitive ELISA with JoJ48C11 (as scFv-Fc). Serial dilutions ranging from 0.32 µg mL^{-1} to 316 µg mL^{-1} of the competitors were incubated with each rAb in the scFv-Fc format before application on SCH-PK loaded Carbo-BIND™ multiwell plates. The rAbs were also incubated without competitor as negative control and mark of maximal signal.